



Master Thesis

Towards Triphenylamine-based Water-soluble Initiators for Two-Photon-Induced Polymerization

Conducted at the

Institute of Applied Synthetic Chemistry

at the **TU Wien**

under the supervision of

Dipl.-Ing. Dr.techn. **Brigitte Holzer**

and

Univ.Prof. Dipl.-Ing. Dr.techn. **Johannes Fröhlich**

by

Paul Getreuer, BSc.

Matrikelnr.: 01209543

Zeillergasse 6/6, 1170 Wien

Vienna, March, 2020



Die approbierte gedruckte Originalversion dieser Diplomarbeit ist an der TU Wien Bibliothek verfügbar.
The approved original version of this thesis is available in print at TU Wien Bibliothek.



Die approbierte gedruckte Originalversion dieser Diplomarbeit ist an der TU Wien Bibliothek verfügbar.
The approved original version of this thesis is available in print at TU Wien Bibliothek.

Danksagung

An dieser Stelle möchte ich mich bei Univ.Prof. Dr. Johannes Fröhlich für die Ermöglichung dieser Diplomarbeit in seiner Forschungsgruppe, sowie den dabei gewährten Freiraum bedanken.

Im Besonderen bedanke ich mich bei Senior Scientist Dr. Brigitte Holzer für die hervorragende fachliche Betreuung und ihre Leitung durch diese Arbeit.

Senior Lecturer Dr. Ernst Horkel danke ich für die Hilfestellung bei diversen synthetischen Fragestellungen, sowie für administrative Belangen.

Ass.Prof. Christian Hametner danke ich für seine Strukturaufklärungsbemühungen.

DI Dr. Berthold Stöger möchte ich für Kristallstrukturmessungen danken.

Bei Bodo Baumgartner möchte ich mich für sein Mitwirken im Zuge eines Wahlpraktikums bedanken. Auch Luca Klein und Jakob Krall haben meinen Dank für ihr Diplomarbeitsprojekt, dass sie als Teil dieser Arbeit durchgeführt haben.

Meinen Laborkollegen Univ.Ass. Dipl.-Ing. Dorian Bader, Dipl.-Ing. Nikolaus Poremba, Birgit Meindl BSc, Univ.Ass. Dipl.-Ing. Thomas Kader und Dipl.-Ing. Andreas Morawietz, sowie allen anderen Forschungsgruppenmitgliedern danke ich für das hervorragende Arbeitsklima und die allgemeine Hilfsbereitschaft.

Besonders möchte ich mich bei meinen Eltern für die Ermöglichung dieses Studiums, sowie die umfangreiche Unterstützung in den letzten Jahren bedanken.

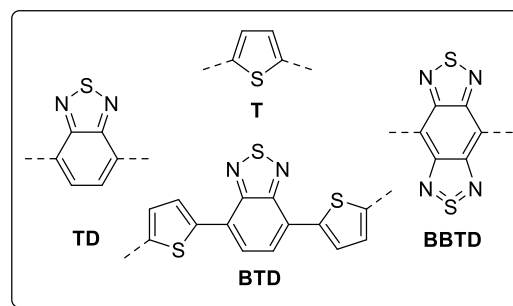
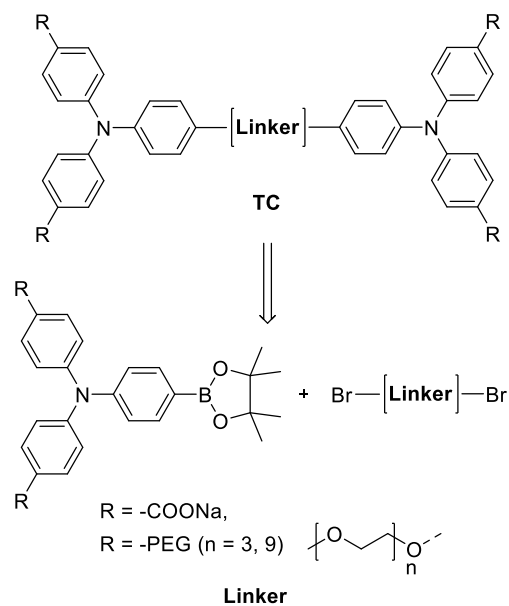


Die approbierte gedruckte Originalversion dieser Diplomarbeit ist an der TU Wien Bibliothek verfügbar.
The approved original version of this thesis is available in print at TU Wien Bibliothek.

Kurzfassung

In den letzten Jahren hat Zwei-Photonen-Absorption, dank seiner möglichen Anwendungen in Materialwissenschaften und biologischer Bildgebung, wie 3D optischem Datenspeicher, lithographischer Mikrofabrikation, optischer Leistungsbegrenzung, Zwei-Photonen-Fluoreszenz-Bildgebung, hoch-konvertiertem Lasern, photodynamischer Therapie und der lokalisierten Abgabe von biologisch aktiven Spezies, viel Aufmerksamkeit erhalten. Obwohl in der Vergangenheit bereits effiziente Zwei-Photonen-Initiatoren (2PIs) hergestellt wurden, stellt das Fehlen von wasserlöslichen 2PIs einen großen Nachteil dieser Technologie dar. Speziell in biologischen Systemen werden wasserlösliche 2PIs für Zwei-Photonen-Polymerisationen (2PP) gebraucht um z.B. Hydrogelstrukturen für Zellkulturanwendungen wie Gewebekonstruktion herzustellen.

Vor kurzem wurden Triphenylamin (TPA)-substituierte Thiophene mit elektronisch verschiedenen Substituenten untersucht, die quadrupolare Donor-Akzeptor-Donor (D-A-D) Systeme (Abbildung, TC) bilden und effiziente 2PIs darstellen. In dieser Arbeit werden unterschiedliche Strategien dargelegt, um diese effizienten Materialien in wasserlösliche 2PIs zu überführen. So werden (i) polare elektronenschiebende (Polyethylenglykol, PEG) oder (ii) -ziehende (Carboxylat) Gruppen an der Triphenylamineinheit eingeführt um die gewünschte Wasserlöslichkeit zu erzielen. Ein weiterer Ansatz dieses Ziel umzusetzen,



Triphenylamin basierte wasserlösliche Zwei-Photonen-Initiatoren.

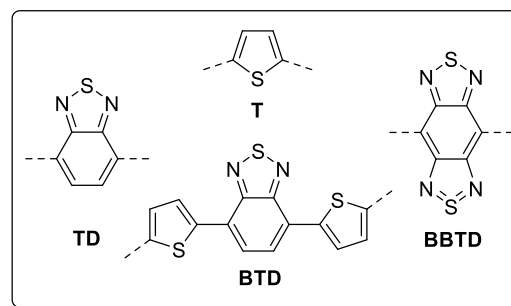
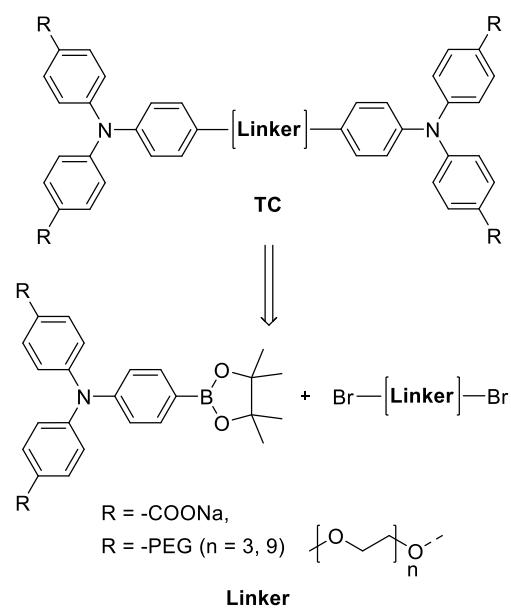
besteht darin (iii) das 2PI Grundgerüst in Cyclodextrin basierten Rotaxanen zu verwenden. Weiters wird die Variation des planaren π -konjugierten Linkers angestrebt, um ein fine-tuning der photophysikalischen Eigenschaften der hergestellten wasserlöslichen D-A-D Systeme zu erzielen.

Die strukturellen Untereinheiten, TPA sowie Linker, wurden mittels Suzuki-Miyaura Kupplung zu den entsprechenden Zielsubstanzen umgesetzt. Die synthetisierten Substanzen wurden photophysikalisch charakterisiert (UV-Vis) und die resultierenden Ergebnisse in dieser Arbeit diskutiert.

Abstract

In recent years, two-photon absorption (2PA) has attracted growing interest due to its potential application in materials science and biological imaging, including 3D optical data storage, lithographic microfabrication, optical power limiting, two-photon fluorescence imaging, up-converted lasing, photodynamic therapy, and the localized release of bio-active species. Although in the past highly efficient two-photon initiators (2PIs) have been developed, the lack of water-soluble 2PIs is still a major drawback of this technology. Especially in biological systems, water-soluble 2PIs are needed for two-photon induced polymerization (2PP) of e.g. hydrogel scaffolds for cell-culture applications, such as tissue engineering.

Recently, triphenylamine (TPA)-substituted thiophenes with various electronically different substituents forming quadrupolar donor-acceptor-donor (D-A-D) systems (Figure, TC) have been developed, which were proven to be efficient new scaffolds for 2PIs. In this contribution, different strategies are outlined to convert these efficient materials into water-soluble 2PIs. Primarily, (i) polar electron-donating (polyethylene glycol, PEG) and (ii) electron-withdrawing (carboxylate) groups will be introduced on the TPA subunit to obtain water solubility. A further approach (iii) to convert the 2PI backbone into cyclodextrin-based materials is pursued within this work.



Triphenylamine-based water-soluble 2PIs.

Secondly, another aim of this contribution is the variation of the planar π -conjugated linker allowing finetuning of the photophysical properties of the synthesized water-soluble D-A-D Systems.

The structural elements, TPA and linkers, were converted to the corresponding target compounds *via* Suzuki-Miyaura coupling. The synthesized compounds were characterized by means of UV-Vis spectroscopy and their photophysical properties are discussed in this contribution.



Die approbierte gedruckte Originalversion dieser Diplomarbeit ist an der TU Wien Bibliothek verfügbar.
The approved original version of this thesis is available in print at TU Wien Bibliothek.

Abbreviations

A	electron-withdrawing component (acceptor)	PE	petroleum ether
ACN	acetonitrile	PEGDA	poly(ethylene glycol) diacrylate
AcOH	acetic acid	Phen	1,10-phenanthroline monohydrate
anh.	anhydrous	PI	photoinitiator
CHCl ₃	chloroform	Pinbop®	2-isopropoxy-4,4,5,5-tetramethyl-1,3,2-dioxaborolan
D	electron-donating component (donor)	PL	photoluminescence
DMF	dimethylformamide	RT	room temperature
DMSO	dimethylsulfoxide	sat.	saturated
PEG	polyethylene glycol	THF	tetrahydrofuran
DCM	dichloromethane	TLC	thin-layer chromatography
EDG	electron-donating group	TMS	trimethylsilyl
EE	ethyl acetate	TPA	triphenylamine
Et ₃ N	triethylamine	VIS	visible light
EtOH	ethanol	UV	ultra-violet
eq.	equivalents	1PA	one-photon absorption
EWG	electron-withdrawing group	1PI	one-photon initiator
GCMS	gas chromatography – mass spectrometry	1PP	one-photon induced polymerization
HV	high vacuum	2PA	two-photon absorption
ICT	intramolecular charge transfer	2PI	two-photon initiator
ⁱ PrOH	iso-propanol	2PP	two-photon induced polymerization
KO ^t Bu	potassium <i>tert</i> -butoxide		
MeOH	methanol		
MEK	methyl ethyl ketone		
NBS	<i>N</i> -bromosuccinimide		
ⁿ BuLi	<i>n</i> -butyllithium		
NIR	near infrared		
NIS	<i>N</i> -iodosuccinimide		
NMR	nuclear magnetic resonance		
OLED	organic light emitting diode		



Die approbierte gedruckte Originalversion dieser Diplomarbeit ist an der TU Wien Bibliothek verfügbar.
The approved original version of this thesis is available in print at TU Wien Bibliothek.

General remarks

Labelling of substances

Identification of substances is achieved by strict sequential numbering. Substances previously reported in literature receive Arabic numerals, whereas substances unknown to literature are labelled in Roman numerals.

References to literature citations

References to literature are given within the text by superscript Arabic numbers in square brackets.

Nomenclature

The nomenclature of chemical compounds not described in literature is based on the rules of Chemical Abstracts. Other compounds, reagents and solvents may be described by simplified terms, trivial or trade names.

Table of Contents

A	Formula Scheme	1
A.1	Synthesis of Cap Systems	2
A.1.1	PEG-substituted Triphenylamine Cap-Systems	2
A.1.1.1	PEG (n = 3)-substituted Triphenylamine Cap-System	2
A.1.1.2	PEG (n = 9)-substituted Triphenylamine Cap-System	2
A.1.1.3	Multiple PEG Approach	3
A.1.2	Carboxylic Acid-substituted Triphenylamine Cap-System	3
A.1.3	Cap Abbreviations	3
A.2	Linker Synthesis	4
A.3	Synthesis of 2PIs	4
A.4	Rotaxane Synthesis	5
B	General Part	6
B.1	Two-Photon Absorption	7
B.1.1	Physical Principles	9
B.1.1.1	Two-Photon Absorption Cross Section δ_{2PA}	10
B.1.2	Molecular Design	11
B.2	Two-Photon Induced Photopolymerization	13
B.2.1	Radical Photopolymerization	13
B.2.2	Photoinitiators	13
B.2.3	Two-Photon Microfabrication	15
B.2.3.1	Two-Photon Initiators for Two-Photon Microfabrication	16
B.2.4	State of the Art Two-Photon Initiators	17
B.2.5	Biological Applications	18
B.3	Goal of this Thesis	20
C	Specific Part	22
C.1	Introduction	23
C.2	Synthesis	24
C.2.1	Synthesis of Cap Systems	24
C.2.1.1	Synthesis of 3PEGTPA	24
C.2.1.2	Synthesis of 9PEGTPA and Multiple PEG-substituted Caps	25
C.2.1.3	Synthesis of CTPA	27

C.2.2	Linker Synthesis.....	28
C.2.2.1	Synthesis of TDZ	28
C.2.2.2	Synthesis of BBTD	29
C.2.2.3	Synthesis of BTD	30
C.2.3	Target Compound Synthesis.....	30
C.2.3.1	Synthesis of Target 2PIs.....	32
	Synthesis of Target Compounds with Electron-Donating Substituents.....	32
	Synthesis of Target Compounds with Electron-Withdrawing Substituents.....	34
C.2.4	Target 2PIs in β -Cyclodextrin-Rotaxanes.....	35
C.2.4.1	Synthesis of Rotaxane Precursors	37
C.2.4.2	Synthesis of β -Cyclodextrin Rotaxanes.....	38
C.3	Solubility of the Target Compounds	41
C.4	Photophysical Characterization of the Target Compounds	41
C.5	Conclusion and Outlook	45
D	Experimental Part	46
D.1	General Remarks	47
D.1.1	Chromatographic Methods	47
D.1.1.1	Thin Layer Chromatography	47
D.1.1.2	Column Chromatography	47
	Preparative MPLC	47
	Preparative HPLC	47
D.2	Analytical Methods.....	47
D.2.1	GCMS Measurements.....	47
D.2.2	NMR-Spectroscopy.....	48
D.2.3	Absorption Spectroscopy	48
D.2.4	Fluorescence Spectroscopy	48
D.3	Synthesis and Characterization of the Compounds.....	48
D.3.1	Synthesis of Cap Systems	48
D.3.1.1	Synthesis of PEG (n=3)-substituted Triphenylamine Cap-System	48
	2-(2-(2-Methoxyethoxy)ethoxy)ethyl 4-methylbenzenesulfonate	48
	1-Iodo-4-(2-(2-(2-methoxyethoxy)ethoxy)ethoxy)benzene	49
	4-Bromo- <i>N,N</i> -bis(4-(2-(2-(2-methoxyethoxy)ethoxy)ethoxy)phenyl)aniline	50
	<i>N,N</i> -Bis(4-(2-(2-(2-methoxyethoxy)ethoxy)ethoxy)phenyl)-4-(4,4,5,5-tetramethyl-1,3,2-dioxaborolan-2-yl)aniline	51
D.3.1.2	Synthesis of PEG (n=9)-substituted Triphenylamine Cap-System	52

3,6,9,12,15,18,21,24,27-Nonaoxaocacosan-1-ol.....	52
3,6,9,12,15,18,21,24,27-Nonaoxaocacos-1-yl 4-methylbenzenesulfonate.....	52
1-Iodo-4-(3,6,9,12,15,18,21,24,27-nonaoxaocacos-1-yl)benzene	53
4-Bromo- <i>N,N</i> -bis(4-methoxyphenyl)aniline	54
4,4'-[(4-Bromophenyl)imino]bisphenol	54
4-Bromo- <i>N,N</i> -bis(4-(3,6,9,12,15,18,21,24,27-nonaoxaocacos-1-yloxy)phenyl)aniline.....	55
<i>N,N</i> -Bis(4-(3,6,9,12,15,18,21,24,27-nonaoxaocacos-1-yloxy)phenyl)-4-(4,4,5,5-tetramethyl-1,3,2-dioxaborolan-2-yl)aniline.....	56
D.3.1.3 Multiple PEG-Approach	57
5-Iodo-1,2,3-trimethoxybenzene	57
5-Iodobenzene-1,2,3-triol.....	57
5-Iodo-1,2,3-tris(2-(2-(2-methoxyethoxy)ethoxy)ethoxy)benzene	58
D.3.1.4 Carboxylic Acid-substituted Triphenylamine Cap-System.....	59
4,4'-(Phenylimino)bisbenzaldehyde	59
4,4'-[(4-Bromophenyl)imino]bisbenzaldehyde.....	60
4,4'-[(4-Bromophenyl)imino]bisbenzoic acid	60
4,4'-[(4-(4,4,5,5-Tetramethyl-1,3,2-dioxaborolan-2-yl)phenyl)imino]bisbenzoic acid	61
D.3.1.5 Linker Synthesis	62
Benzo[<i>c</i>][1,2,5]thiadiazole	62
4,7-Dibromobenzo[<i>c</i>][1,2,5]thiadiazole.....	63
4,7-Di(thiophen-2-yl)benzo[<i>c</i>][1,2,5]thiadiazole	63
4,7-Bis(5-bromothiophen-2-yl)benzo[<i>c</i>][1,2,5]thiadiazole	64
4,7-Dibromo-5,6-dinitrobenzo[<i>c</i>][1,2,5]thiadiazole	65
4,7-Dibromobenzo[<i>c</i>][1,2,5]thiadiazole-5,6-diamine	65
4,8-Dibromobenzo(1,2- <i>c</i> ;4,5- <i>c'</i>)bis(1,2,5)thiadiazole.....	66
D.3.1.6 Synthesis of Target Compounds	66
General Procedure: Suzuki Couplings Towards Target Compounds.....	66
4,4'-(Thiophene-2,5-diyl)bis(<i>N,N</i> -bis(4-(2-(2-(2-methoxyethoxy)ethoxy)ethoxy)phenyl)aniline).....	67
4,4'-(Benzo[<i>c</i>][1,2,5]thiadiazole-4,7-diyl)bis(<i>N,N</i> -bis(4-(3,6,9,12,15,18,21,24,27-nonaoxaocacos-1-yloxy)phenyl)aniline)	68
4,4'-(Thiophene-2,5-diyl)bis(<i>N,N</i> -bis(4-(3,6,9,12,15,18,21,24,27-nonaoxaocacos-1-yloxy)phenyl)aniline)	69
4,4'-(Benzo[<i>c</i>][1,2,5]thiadiazole-4,7-diylbis(thiophene-5,2-diyl))bis(<i>N,N</i> -bis(4-(3,6,9,12,15,18,21,24,27-nonaoxaocacos-1-yloxy)phenyl)aniline)	70
4,4',4'',4'''-((Thiophene-2,5-diylbis(4,1-phenylene))bis(imino))tetrabenzoic acid	71
Sodium 4,4',4'',4'''-((thiophene-2,5-diylbis(4,1-phenylene))bis(imino))tetrabenzoate.....	72
D.3.2 Synthesis of Stoppers/Linkers for Rotaxane Synthesis.....	73
<i>N,N</i> -Bis(4-methoxy)phenyl)-4-(4,4,5,5-tetramethyl-1,3,2-dioxaborolan-2-yl)aniline	73
4-(5'-Bromo-[2,2'-bithiophen]-5-yl)- <i>N,N</i> -di-(<i>p</i> -tolyl)aniline.....	73

4-(5'-Iodo-[2,2'-bithiophen]-5-yl)- <i>N,N</i> -di-(<i>p</i> -tolyl)aniline	74
5,5'-Di(1,3,2-dioxaborolan-2-yl)-2,2'-bithiophene.....	75

E References	76
----------------------------------	-----------



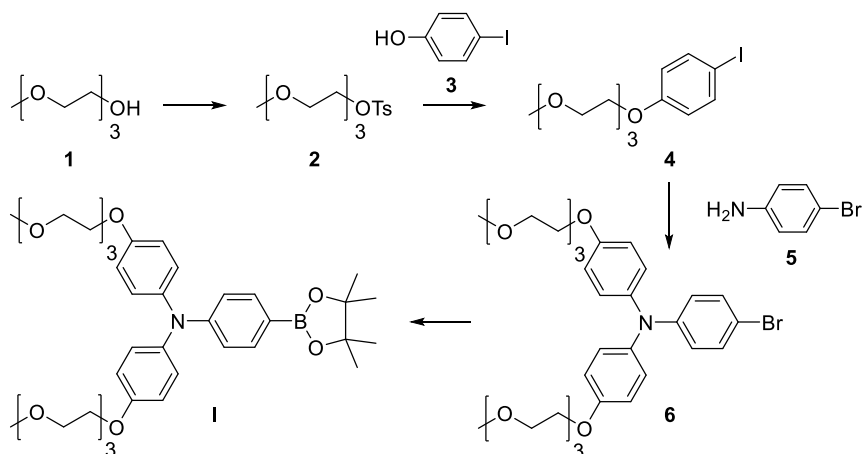
Die approbierte gedruckte Originalversion dieser Diplomarbeit ist an der TU Wien Bibliothek verfügbar.
The approved original version of this thesis is available in print at TU Wien Bibliothek.

A Formula Scheme

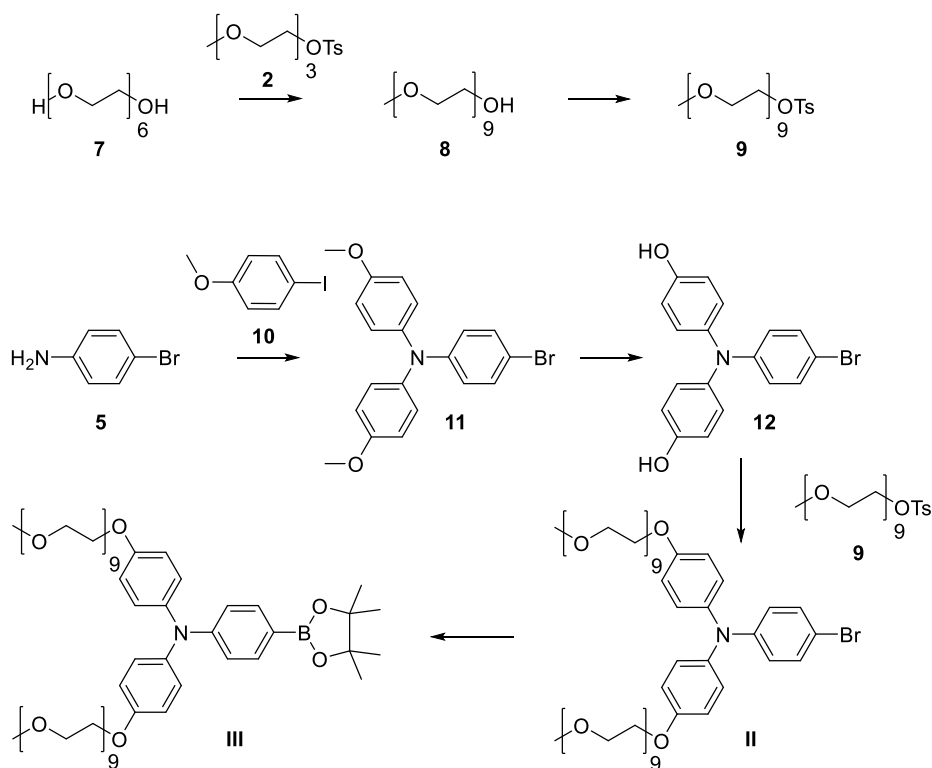
A.1 Synthesis of Cap Systems

A.1.1 PEG-substituted Triphenylamine Cap-Systems

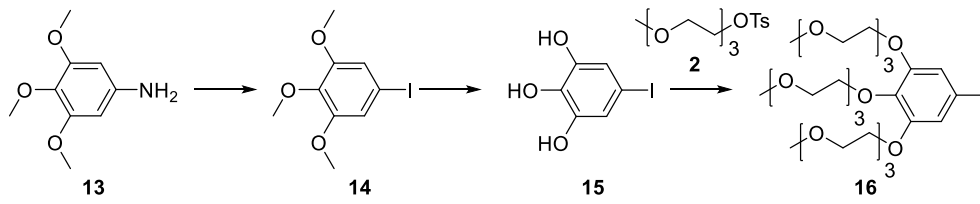
A.1.1.1 PEG (n = 3)-substituted Triphenylamine Cap-System



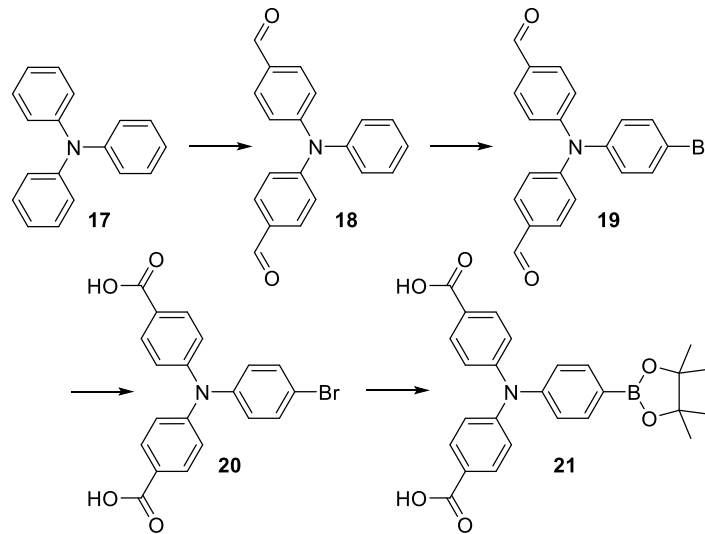
A.1.1.2 PEG (n = 9)-substituted Triphenylamine Cap-System



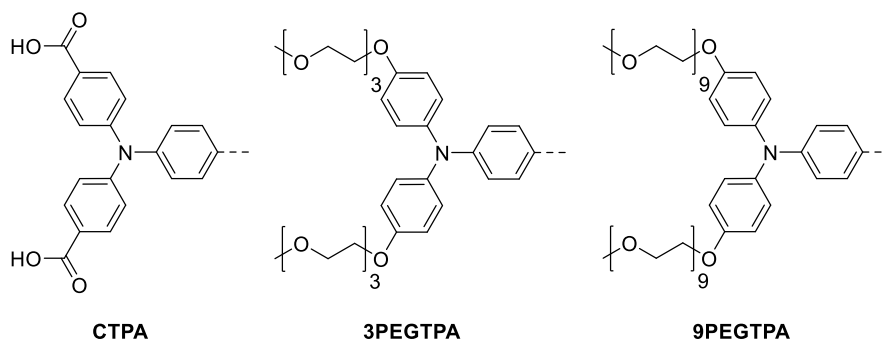
A.1.1.3 Multiple PEG Approach



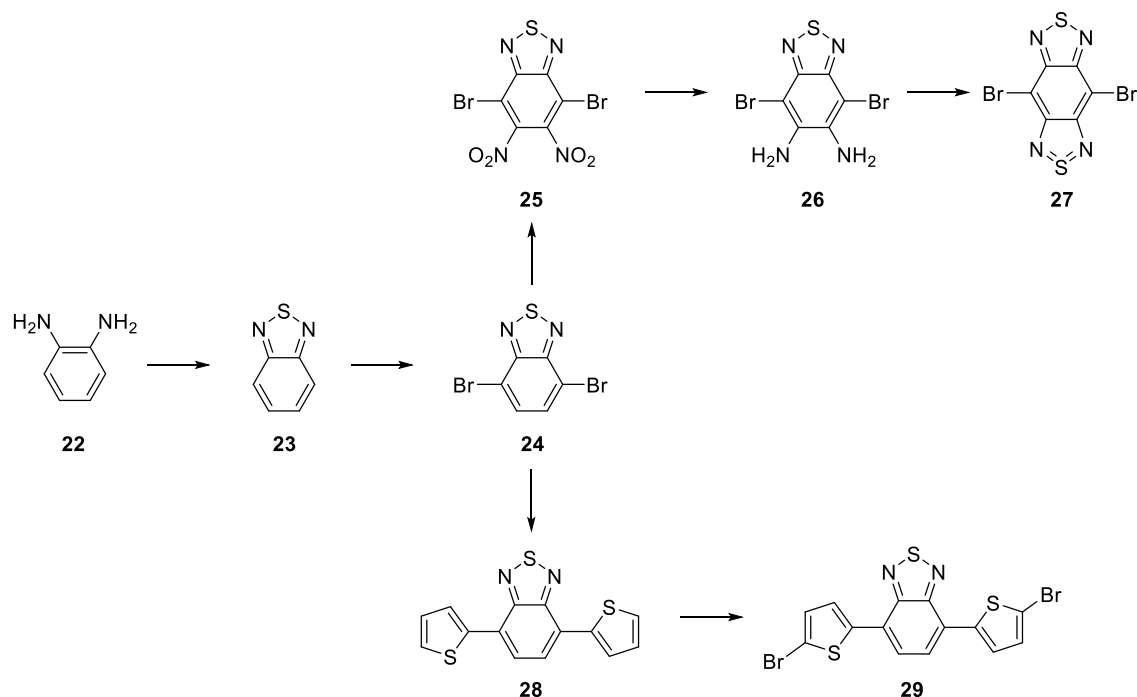
A.1.2 Carboxylic Acid-substituted Triphenylamine Cap-System



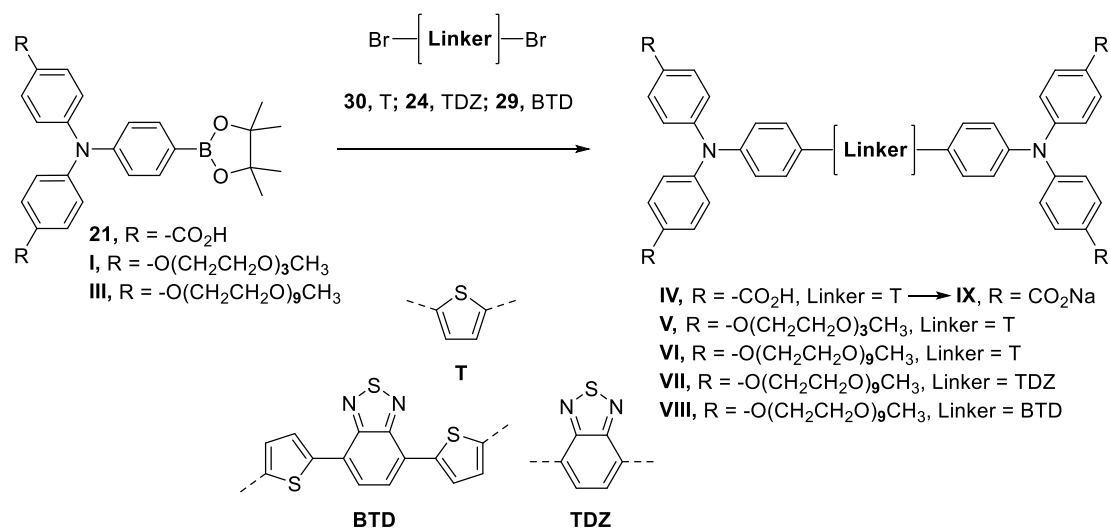
A.1.3 Cap Abbreviations



A.2 Linker Synthesis

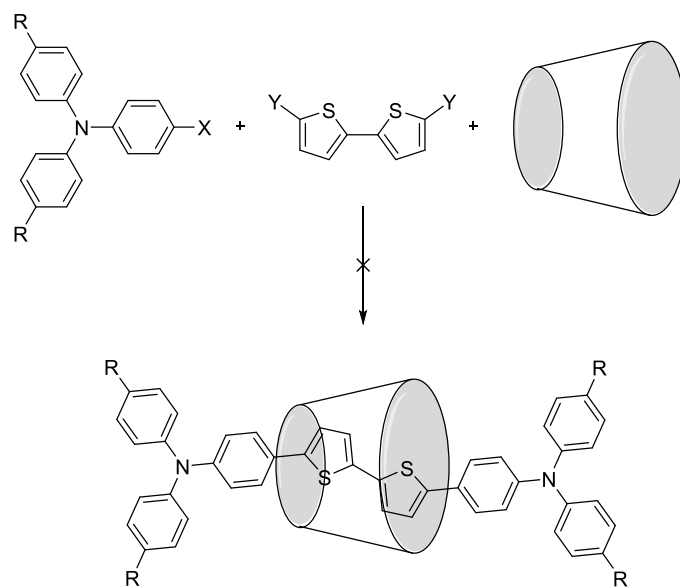


A.3 Synthesis of 2PIs



IV = BCAA-T, V = B3PEGA-T, VI = B9PEGA-T, VII = B9PEGA-TDZ, VIII = B9PEGA-BTD, IX = BCxA-T

A.4 Rotaxane Synthesis



B General Part

B.1 Two-Photon Absorption

The first theoretical analysis of the simultaneous absorption of two photons by the same molecule was realized by Göppert-Mayer^[1] in the 1930s and was demonstrated experimentally in 1961,^[2] soon after the invention of the laser. 2PA gathered much attention as sub-picosecond pulsed lasers were more readily available in the 1990s, particularly the Ti:sapphire laser. An explosion of interest in all types of multiphoton processes however occurred only after the invention of the two-photon fluorescence microscopy technique^[3] and its rapid adoption by manufacturers of confocal microscopes.^[4]

Contrary to linear absorption processes, that follow the Lambert-Beer law, 2PA is a non-linear optical event in which a molecule absorbs two photons instantaneously; the energy sum of these photons equals the energy of the 2PA transition energy. The transition probability of this process is inherently weak at normal light intensities.^[5-6] However, the use of an intense laser pulse allows the simultaneous absorption of two or more photons with the transition probability for the absorption of two identical photons being proportional to the square of the incident light intensity (Figure 1).^[7] The intensity of a focused laser beam decreases quadratically with distance from the lasers focal point, which means that the absorption probability is decreasing with the fourth power of distance from the focal point. This relation represents a crucial characteristic of the application of 2PA.^[6] Consequently, 2PA is a powerful tool to activate chemical or physical processes with high spatial resolution in three dimensions by applying tightly focused laser beams to induce excitation. Any following process, such as fluorescence or a chemical reaction, is also localized within this small volume.^[8]

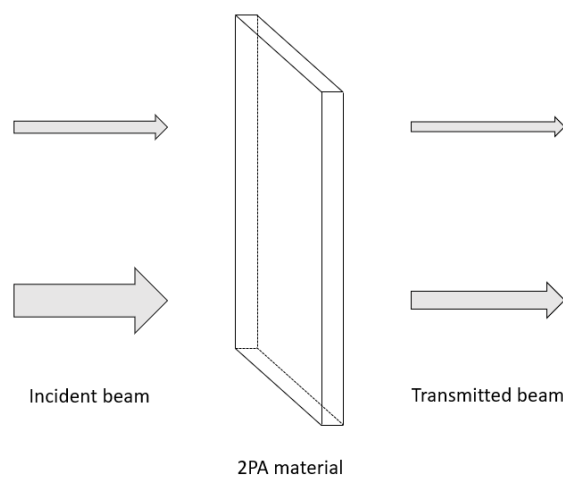


Figure 1: Attenuation of beams transmitting a 2PA material. Due to the non-linear optical event the attenuation of intense beams (below) occurs to a higher extent than the attenuation of weak beams (above).

A key characteristic of 2PA is that excited states get created with photons of only half the energy required for a 1PA transition, which provides improved penetration in absorbing or scattering media, such as tissue.^[7, 9] Figure 2 shows a fluorescent dye solution exposed to the application of an IR- and an UV-fs pulsed laser which were both narrowly focused.^[10] The caused fluorescence from 1PA can be

observed through the entire length of the vessel, while two-photon induced excitation is restricted to the center of a sharp focal point (voxel = volume element). The reason for the sharp excitation area is the before mentioned relation between distance from the focal point and 2PA probability, which results in no fluorescence above and beyond the focal point.^[5]

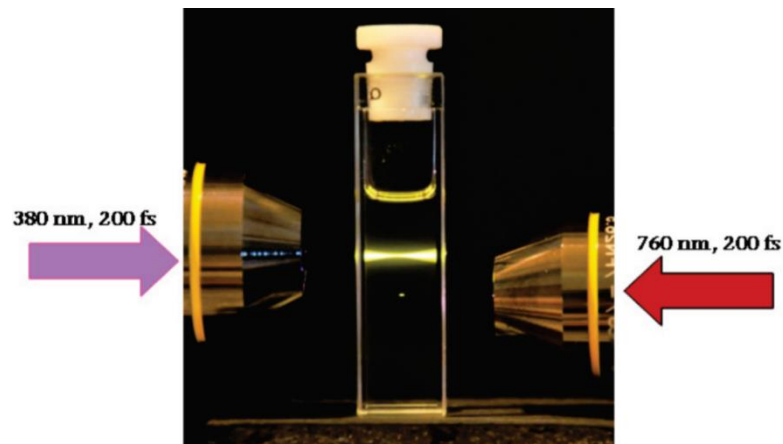


Figure 2: Excitation of a fluorescent dye *via* 1PA (above) and 2PA (below), using narrowly focused laser beams of the respective wavelength.^[10]

Compared to 1PA, 2PA has several benefits as the longer wavelengths show much smaller absorption and scattering losses and are less harmful to biological samples, due to lower energy input. Another advantage is that the sharper contrast in the excitation density prevents the occurrence of disruptive emission or photochemical reactions outside the focal volume.^[11-12] In order to characterize and compare 2PA materials for their efficiency to absorb two photons simultaneously the two-photon absorption cross section δ_{2PA} is a crucial parameter. The corresponding theoretical background (chapter B.1.1.1) and measures to increase δ_{2PA} (chapter B.1.2) are described below.

Consequently, the concept of 2PA offers applications in a wide range of research areas (Figure 3) including microfabrication,^[13] 3D-data-storage,^[14] microscopy,^[15] optical power limiting,^[16] up-converted lasing,^[17] photodynamic therapy,^[18] and the localized release of bio-active species.^[19]

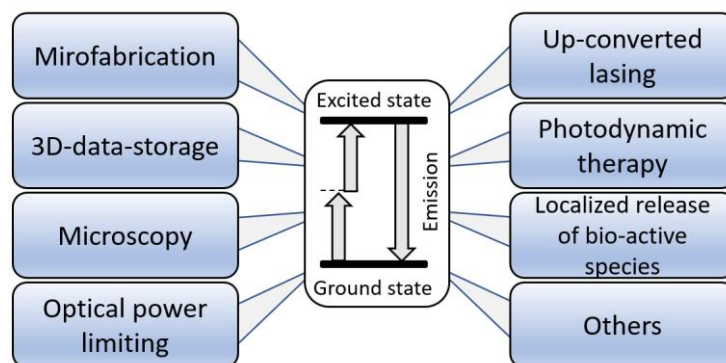


Figure 3: Research areas and applications based on 2PA.

B.1.1 Physical Principles

The process of 2PA involves the simultaneous absorption of two photons (energies E_1 and E_2) by a material, that occurs if one of the electronic states of the material is in resonance with $E_1 + E_2$. The result of this process is that the two absorbed photons are lost from the incident light beam (reducing their light intensity, Figure 1) and the material is brought to an excited state, followed by several possible excited state processes.

The initial interaction of a photon of energy E_1 leaves the system at a temporary virtual state of E_1 above the ground state. This virtual state is not a real state (eigenstate) of the molecule and it disappears after a very short time interval τ . If a second photon of energy E_2 interacts with the molecule during τ , it will be excited to state f . The duration of τ is about 10^{-15} - 10^{-16} s for photon energies in the VIS and NIR ranges. Hence it is not a simultaneous absorption of two photons, but rather a twofold absorption within τ .^[20] The values of E_1 and E_2 can be identical (degenerate case) or different (non-degenerate case) as illustrated in Figure 4a.

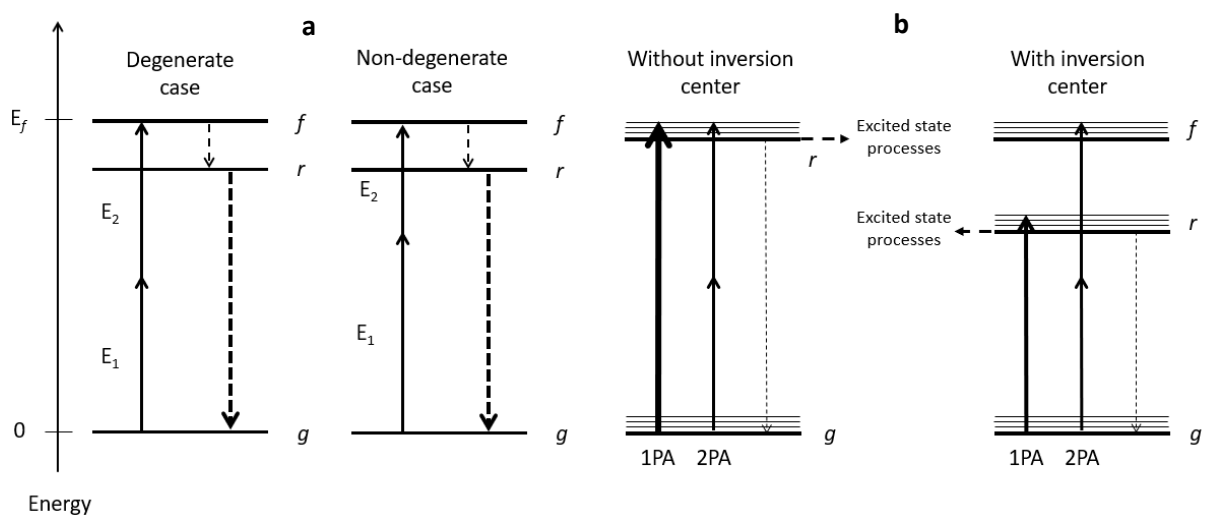


Figure 4: Schematic energy level diagram showing **a**: the excitation of a molecule from the ground state (g) to an excited state (f) by 2PA. The photons have either the same energy (degenerate case) or different energies (non-degenerate case), **b**: the 1PA and 2PA in case of centrosymmetric molecules (with inversion center) and molecules without an inversion center. The length and thickness of each arrow corresponds to the respective photon energies. Dashed arrows represent possible deexcitation pathways.^[6, 20]

Generally, a molecule can get excited to state r by 1PA, if the energy of this photon is equal to the respective transition energy ($g \rightarrow r$), assuming that this transition is quantum mechanically allowed. In the case of most molecules, which do not have an inversion center, 2PA leads to the same state r (Figure 4b). However, the selection rules of 1PA and 2PA are different for centrosymmetric molecules (Figure 4b). In that case a 1PA allowed state r cannot be reached directly *via* 2PA. Hence, the lowest electronic state in centrosymmetric systems accessible by 2PA f usually lies at higher energy than the 1PA allowed state r .^[6] After the absorption a molecule typically undergoes rapid internal conversion

until the lowest energy level of the excited state is reached (ps timescale). At that point the system can either drop back to the ground state *via* radiative or non-radiative relaxation (ns timescale) or it could lose the excess energy by several other processes that can take place from the excited state (e.g. energy transfer, electron transfer, reaction with other molecules, ...).^[20]

B.1.1.1 Two-Photon Absorption Cross Section δ_{2PA}

The 2PA cross section δ_{2PA} is a crucial parameter for the quantification of 2PA efficiency and will be described briefly below.^[21]

The attenuation of a light beam passing through an optical medium can be expressed by equation 1, under the conditions that there is no linear absorption at the wavelength of the incident light beam and only 2PA takes place.

$$\frac{dI(z)}{dz} = -\beta I^2(z) \quad (1)$$

$I(z)$ is the intensity of the incident light beam spreading along the z -axis and β is the 2PA coefficient of the transmitting medium. For simplicity, it was assumed that the light beam is of uniform transverse intensity and the initial intensity is not time dependent. The essence of equation 1 is that the 2PA probability of a molecule at a certain position is proportional to the square of the local light intensity, so the solution is:

$$I(z, \lambda) = \frac{I_0(\lambda)}{1 + \beta(\lambda)I_0(\lambda)z} \quad (2PA) \quad (2)$$

Here, $I_0(\lambda)$ is the incident light intensity, z is the propagation length in the medium and $\beta(\lambda)$ is the 2PA coefficient, which is a material parameter depending on the wavelength of the incident light. As $\beta(\lambda)$ [cm/GW] is a macroscopic parameter, that depends on the concentration of the two-photon absorbing molecules, it can be further expressed as:

$$\beta(\lambda) = \sigma_2(\lambda)N_0 = \sigma_2(\lambda)N_A d_0 * 10^{-3} \quad (3)$$

σ_2 is the molecular 2PA cross section [cm⁴/GW], N_0 is the molecular density [cm⁻³], N_A is the Avogadro's number and d_0 is the molar concentration of the absorbing molecules [M]. Despite σ_2 is a directly measurable quantity that characterizes the average two-photon absorbability per molecule, another parallel expression of the 2PA cross section is commonly used (equation 4).

$$\delta_{2PA} = \sigma_2(\lambda)h\nu \quad (4)$$

Here, $h\nu$ is the photon energy input by the incident light beam. Corresponding to equation 4 δ_{2PA} is in units of $\text{cm}^4/(\text{photon/s})$ or simply cm^4s . As most of the measured values of δ_{2PA} are in the range from 10^{-51} - 10^{-46} cm^4s researchers prefer to use a different informal unit [GM] (for Göppert-Mayer), defined by:

$$1 \text{ GM} = 10^{-50} \text{ cm}^4\text{s} \quad (5)$$

There are various methods to measure δ_{2PA} ,^[6] however the most common two techniques nowadays are z-scan and two-photon excited fluorescence (2PEF). 2PEF has the advantage of being highly sensitive, as a highly diluted solution (with an optical density of about 0.1) is used, requiring only a small amount of substance. However, it has the limitation that the analytes must be photoluminescent.^[4] In some cases, photoluminescence is an unwanted material feature, e.g. for 2PIs, where emission only liberates energy that is needed to induce polymerization. Hence, z-scan is the method of choice in such cases, as it is applicable for materials with very low fluorescence quantum yields. Compared to 2PEF a disadvantage of this technique is its relative low sensitivity, as a substantial amount of substance is required to obtain appropriate signal intensities.^[22]

B.1.2 Molecular Design

In the early days of 2PA chromophores developed for one-photon excitation have been employed in many 2PA applications, which was rather insufficient, due to their low δ_{2PA} .^[5] However, in the last decades a lot of work has been dedicated into the development of highly efficient 2PA materials,^[4, 20-21, 23-24] since for each application materials need to be identified that satisfy a certain set of requirements. That is typically the combination of a sizable probability of 2PA at a specific wavelength and high susceptibility for a process to take place after the absorption, such as fluorescence emission, a photochemical reaction, or the sensitization of another material.^[6]

Since organic molecules are in principle modular compounds, they offer a variety of tuning possibilities, which is fundamental for their application in various areas. Albota *et al.*^[7] discovered the relationship between intramolecular charge-transfer processes and two-photon absorptivity by the comparison of electronic structures with photophysical processes. Thus, a design concept was developed, which suggests that the functionalization of organic molecules with an electron-withdrawing (A) component, an electron-rich (D) component, or both, increases δ_{2PA} .^[4] Other important features are the degree of

conjugation, as it leads to states of extended charge separation,^[7] and coplanarity, since it enhances the efficiency of an intramolecular charge-transfer.^[25]

In summary, the requirements for maximizing δ_{2PA} are:^[4]

- long conjugated π -chains, with enforced coplanarity to ensure large conjugation length,
- centered or terminal A or D groups,
- centrosymmetric chromophores that exhibit a strong 1PA transition close to the 2PA laser wavelength and
- chromophores with narrow one- and two photon absorption bands.

Based on those findings certain design strategies were developed, as illustrated in Figure 5.^[25] Symmetrical chromophores (a), often referred to as “push-push” (D- π -D) or “pull-pull” (A- π -A) chromophores depending on whether the direction of intramolecular charge-transfer is from the ends to the center or the opposite, were firstly proposed as well as dipolar chromophores (b) (“push-pull”, A- π -D). However, quadrupolar chromophores (c) (A- π -D- π -A or D- π -A- π -D) were shown to be fourfold more efficient than their dipolar analogues.^[26] Since that discovery a rapidly growing collection of multi-branched 2PA organics (d), dendritic structures and hyperbranched polymers (e) were investigated.^[25]

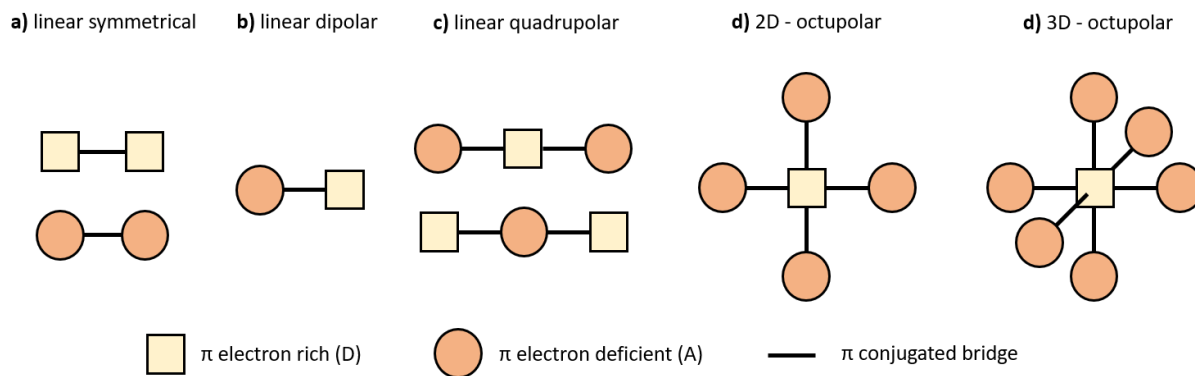


Figure 5: Structural motifs for molecules with improved 2PA performances.

B.2 Two-Photon Induced Photopolymerization

B.2.1 Radical Photopolymerization

Radical photopolymerization is the polymerization, or cross-linking of vinylic monomers or oligomers, upon exposure to light of a certain wavelength. In order to initiate a radical photopolymerization, photoinitiators (PI, usually photosensitive small molecules) are crucial elements of the monomer formulation, besides further additives and diluents. Thereby, the wavelength of the light source must lie within the absorption band of the PI and the dissociation energy acquired for bond cleavage must be lower than the excitation energy.^[27] The resulting excited state converts the absorbed energy to some degree into chemical energy and forms reactive radicals, which then initiate the polymerization.^[28] A one- ($h\nu_{UV}$) or two-photon ($h\nu_{NIR}$) initiated polymerization process consists of the following steps:

- Generation of a starter radical: $h\nu_{UV}$ or $2h\nu_{NIR} + Initiator \rightarrow R^\bullet$
- Chain initiation: $R^\bullet + M \rightarrow M^\bullet$
- Chain reaction (polymerization): $M^\bullet + M \rightarrow M-M^\bullet$

B.2.2 Photoinitiators

In general, PIs can be classified into type I (cleavable) or type II (hydrogen abstraction), corresponding to their mechanism of radical formation. As an example, the various pathways of activation and deactivation of the commercially available *Irgacure 369* 1PI are illustrated in Figure 6a.^[29] After absorbing light, the PI is excited from the ground state to the singlet state, followed by intersystem crossing to the triplet state. The absorbed energy can partly be lost due to internal conversion back to the ground state and some reactive triplet state intermediates can be quenched by oxygen, a monomer, or the recombination of intermediates. While a minor fraction of the excited initiator molecules abstract hydrogens from hydrogen donors, followed by a photo-induced electron transfer and fragmentation process (to produce efficient reactive intermediates), the majority of the reactive intermediates use their energy to cleave a carbon-hydrogen bond (α - or β -cleavage). Subsequently the formed radicals interact with reactive functionalities of monomers or oligomers, initiating the polymerization.^[28-29]

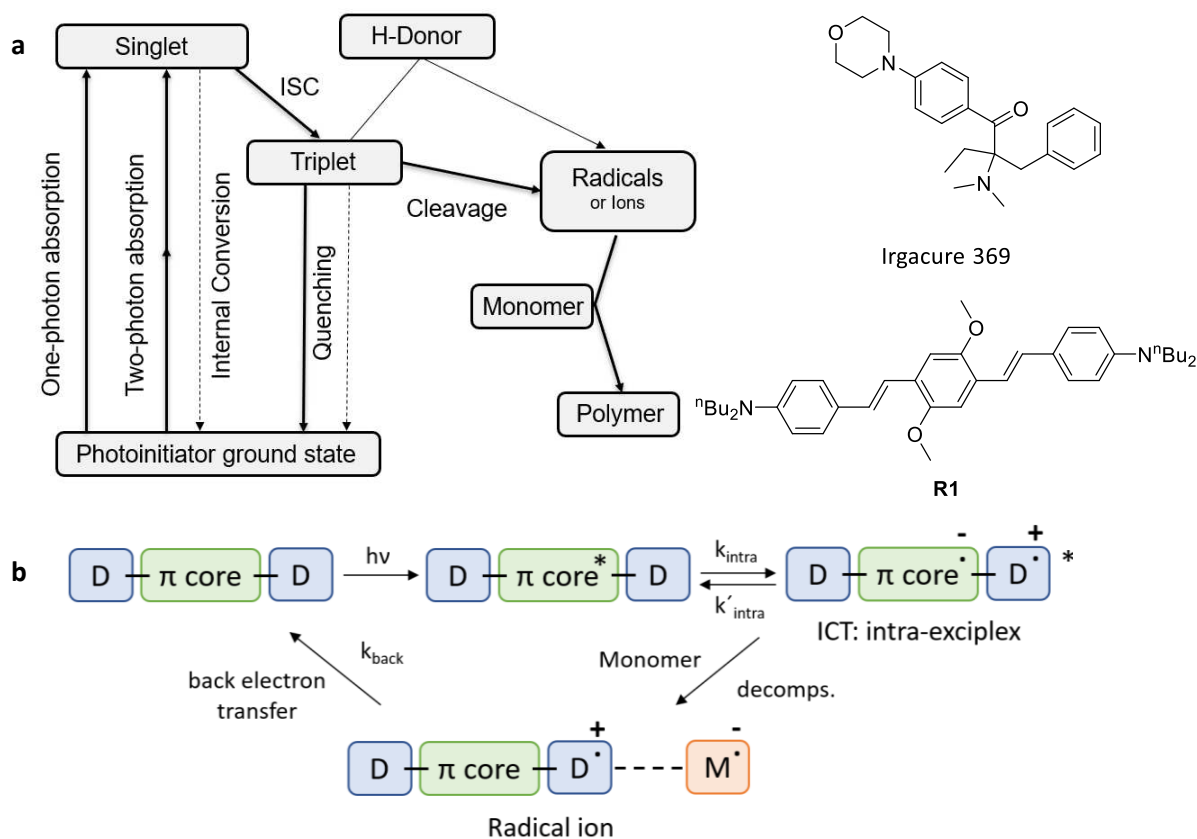


Figure 6: **a**: Pathways for activation and deactivation of PIs by the example of *Irgacure 369*. 1) absorption 2) inter-system crossing or internal conversion 3) radical formation or quenching 4) polymerization. **b**: A potential activation mechanism of D- π -D type 2PIs, such as **R1**.

The polymerization rate can be influenced by the intensity of the light source, the PI concentration, oxygen and additive presence, the quantum yield of the radical generation, and the initiation efficiency of the formed radicals. Higher rates can generally be achieved with more intense light sources, but not with higher PI concentrations. Though, the variation of PI concentrations give access to different molecular weight distributions, resulting in polymers with various mechanical properties.

2PP mechanisms (radical formation, initiation) are inherently difficult to study by spectroscopic methods since fs-pulsed lasers only generate a minor amount of radicals in a tiny voxel.^[30] Some well-proven 2PIs, like **R1** (Figure 6), contain no weak cleavable bonds or moieties known where hydrogen abstraction can take place, so the classical mechanisms (type I and II) seem unlikely to apply. However, Lu *et al.*^[31] proposed a mechanism for the activation of D- π -D type 2PIs that is outlined in Figure 6b. Here, an electron-rich 2PI forms an intra-excimer *via* intramolecular charge-transfer (ICT) upon excitation by 2PA. Subsequently an electron is transferred from the 2PI to the monomer, resulting in a pair of radical ions. The formed anionic monomer radicals can then initiate the polymerization. A good capability of the monomer to abstract electrons from the intra-excimer appears to be essential. This fact is in accordance with the particularly successful application of acrylates in 2PP, as the α,β -unsaturated carboxyl group serves as an electron acceptor and also stabilizes the formed radical anion mesomerically.

However, it is possible that such mechanisms suffer from a back electron transfer from the anionic monomer radical to the cationic 2PI radical, leading to a deactivation and hence a decrease in efficiency.^[30]

Ideally, PIs should have a high molar absorption coefficient and a well-adapted absorption spectral range. Furthermore, intermediates with excellent reactivity and photolysis by-products of low toxicity should be produced. For good processability, PIs should be compatible with monomers and oligomers, and should be homogeneously dispersed, or directly dissolved, in the monomer before the photo-reaction.^[28]

B.2.3 Two-Photon Microfabrication

Two-photon excitation is widely used to fabricate 3D microscopic structures with sub-micrometer resolution.^[4] Thereby the ability to induce photochemical or -physical processes within a very small confined volume (voxel) can be made use of in two-photon induced polymerization (2PP). 2PP enables computer-aided, single-step generation of 3D structures, while one-photon induced polymerization (1PP) is restricted to a layer-by-layer fabrication. The reason for this lies in the fact that two-photon-based approaches avoid problems of linear absorption, as resins are usually highly transparent at NIR wavelengths. Consequently, the excitation beam can penetrate deeply into the resin without loss of intensity, while leaving the layers above and beyond the focal plane unaffected (Figure 7, *left*). Contrary to that, 1PP approaches are limited to the resins surface, (Figure 7, *right*) since one-photon excitation provokes substantial photochemistry outside the focal volume (loss of lithographic contrast and definition).^[4]

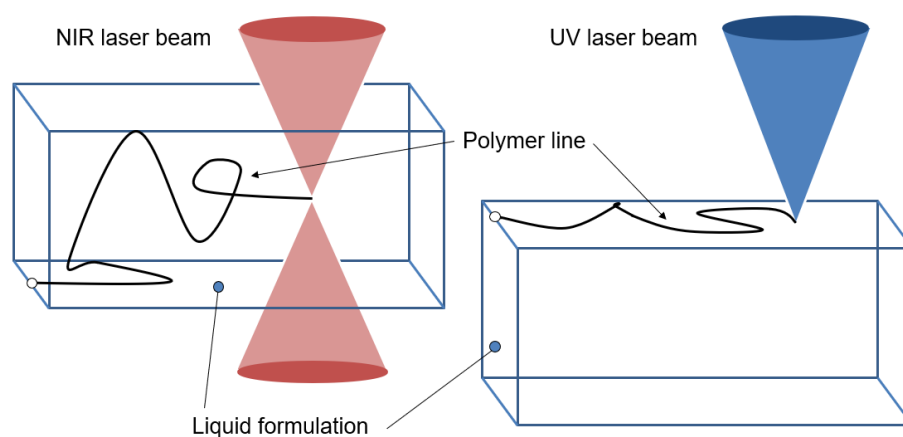


Figure 7: Comparison of a 2PP (*left*) and a 1PP (*right*). In a 2PP process NIR light can be focused in some depth of the 2PA-sensitive resin, while in a 1PP process the UV light can't penetrate the formulation due to absorption at the surface. Consequently, the 2PP technique achieves 3D structures, while 1PP is restricted to planar structures, within one processing step.

2PP has attracted a great deal of interest over the last decades^[32] due to its application in stereolithography and rapid prototyping of structures with resolutions in the sub-micrometer range. Several

potential applications of 2PP have been reported, including photonic crystals,^[33-34] microfluidic devices,^[35-36] microoptics,^[37-38] optical data storage,^[8] and biological applications^[39-42] including hydrogel-scaffold fabrication for cell-culturing and tissue engineering.

B.2.3.1 Two-Photon Initiators for Two-Photon Microfabrication

As mentioned above, initially 1PA chromophores were employed for 2PA applications. Common 1PIs usually have a very low δ_{2PA} of below 10 GM, reflecting in a poor 2PA sensitivity.^[8] Therefore, long exposure times and high laser powers were required for the 2PA-based structuring of a resin using 1PIs, resulting in frequent structural damage.^[4, 43] Consequently, highly potent 2PIs are needed for the application of two-photon microfabrication. In this regard, their requirements are listed below:^[44-45]

- High δ_{2PA}
- High radical quantum yield
- High initiating efficiency of the generated radicals

2PP offers the possibility to achieve realistic lateral resolutions of about 100 nm and even below,^[44, 46] since only the maximum intensity in the center of the focal volume is high enough to effectively initiate the polymerization, resulting in very small voxel dimensions.^[4] To achieve structuring resolution below the diffraction limit a precise control over the laser intensity and irradiation time is required. The laser intensity must stay within the boundaries of polymerization as illustrated in Figure 8. If the intensity is increased, the voxel sizes increase as well, as long as the upper threshold is reached, at which the energy input is too high and bubbles start to form.^[47]

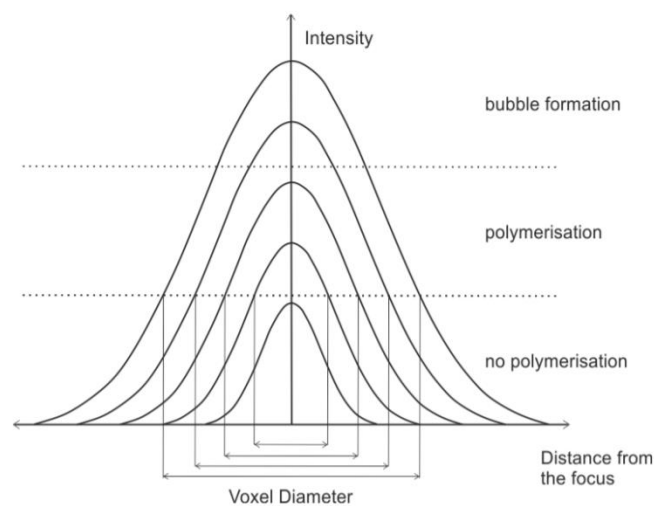


Figure 8: Illustration of the laser intensity influencing the voxel diameter.^[47]

By varying laser powers and writing speeds a photopolymerizable formulation can be benchmarked according to its lower and higher polymerization threshold, as well as its processing window.^[47]

B.2.4 State of the Art Two-Photon Initiators

To overcome the limitations of commercially available 1PIs and obtain 2PIs with increased efficiency several methods have been developed (e.g. combination of photosensitizers with commercial 1PIs or amines as co-initiators).^[48] The most obvious approach is the development of specialized 2PIs that feature a large δ_{2PA} (see chapter B.1.2) and have a high radical quantum yield with a high initiating efficiency.^[44-45] However, the establishment of reliable concepts explaining structure-property relationships of 2PIs still remains a challenge, as the efficiency of 2PP is affected by a multitude of parameters in complex relationship to each other. Consequently, the most efficient 2PIs have been the outcome of fortunate discoveries.^[4] Below symmetric TPA-substituted thiophenes are exemplified as state of the art 2PIs.

After first photophysical studies revealed the strong 2PA of triphenylamine-substituted thiophenes,^[49] and their suitability as 2PIs was proven, a series of triarylamine-substituted thiophenes with varying substituents was synthesized by Holzer *et al.* (Figure 9).^[50] Electron-withdrawing (-SO₂CH₃, -CN, -F), neutral (-H) and electron-donating (-TMS, -CH₃, -^tBu, -OCH₃) substituents were systematically introduced to fine-tune the photophysical properties of the 2PI scaffold.

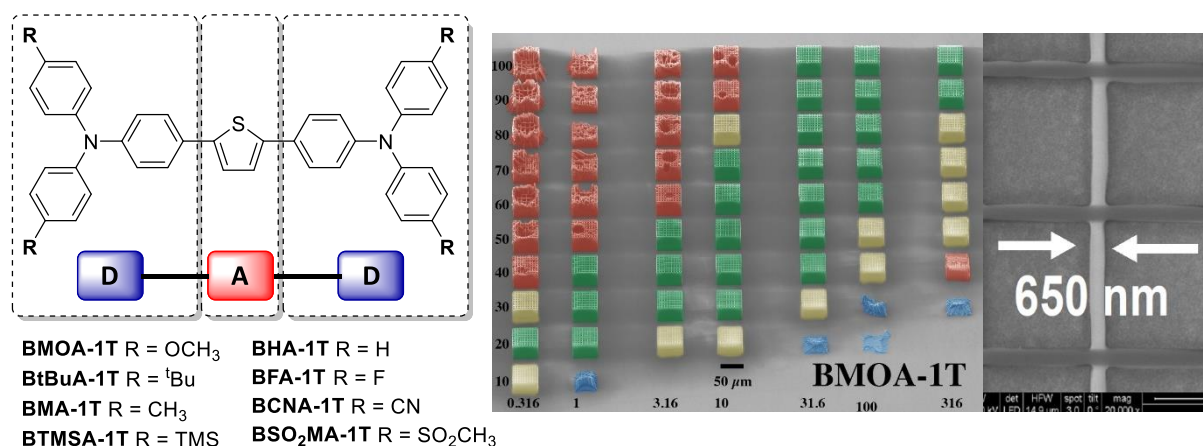


Figure 9: *left* Triphenylamine-substituted thiophene motifs. *middle*: Speed-power screening of BMOA-1T at different writing speeds (x-axis, [mm s⁻¹]) and laser powers (y-axis, [mW]) of an acrylate formulation (SEM pictures). The colour of each woodpile indicates the quality of the structure (green = excellent, yellow = good, red = small errors, blue = not identifiable). *right*: Line width of the speed-power screenings.^[50]

The results of the photophysical investigation showed that electron-withdrawing substituents shift the 2PA maximum to higher energies, which suggests a decrease in 2PA strength, however, stronger electron-donating substituents *i)* shift the optical bandgap to lower energies, *ii)* do not significantly alter the transition dipole moment, but *iii)* lead to an increased probability for excited state symmetry breaking and thus pronounced fluorescence solvatochromism. Despite their high fluorescence quantum yields, 2PP structuring tests with PI concentrations of only 5 $\mu\text{mol/g}$ revealed the high efficiency of these materials as 2PIs, as they all have large processing windows. In Figure 9 (*middle, right*) the

speed-power screening of BMOA-1T and the corresponding line width of below one micrometer are exemplified.^[50] However, the low solubility of this substance class in polar monomer formulations and especially in water is a major drawback of TPA-substituted thiophenes, hampering their potential use in biological applications.

B.2.5 Biological Applications

The investigation of mechanical properties of cells has attracted increasing interest in recent years, as new technologies are able to accurately probe cell's mechanical behavior. Particularly 3D scaffolding has elucidated several cell-structure interaction mechanisms by the possibility to analyze cell behavior within 3D artificial architectures. This has paved new ways for studying cell mechanics and the interplay with the surrounding environment.^[51] In this regard, two-photon microfabrication is a unique technique to realize complex 3D biomimetic scaffolds with excellent control over specific features like stiffness, topographic properties including roughness and porosity, and surface functionalization to tailor cell-structure biochemical interplays.^[52] Hence, the investigation of the influence of mechanical properties on basic cell processes, such as cell viability, proliferation, and migration, is not an obstacle anymore.^[42, 53] After sheer 3D microscuffolding the basic material does often not possess the characteristic information to induce specific cellular response hence surface coating with biomolecules is required.^[53]

As an example a poly(ethylene glycol) diacrylate (PEGDA) scaffold cultured with a neuronal cell line of mice (neuro2A) by Accardo *et al.*^[54] is shown in Figure 10.

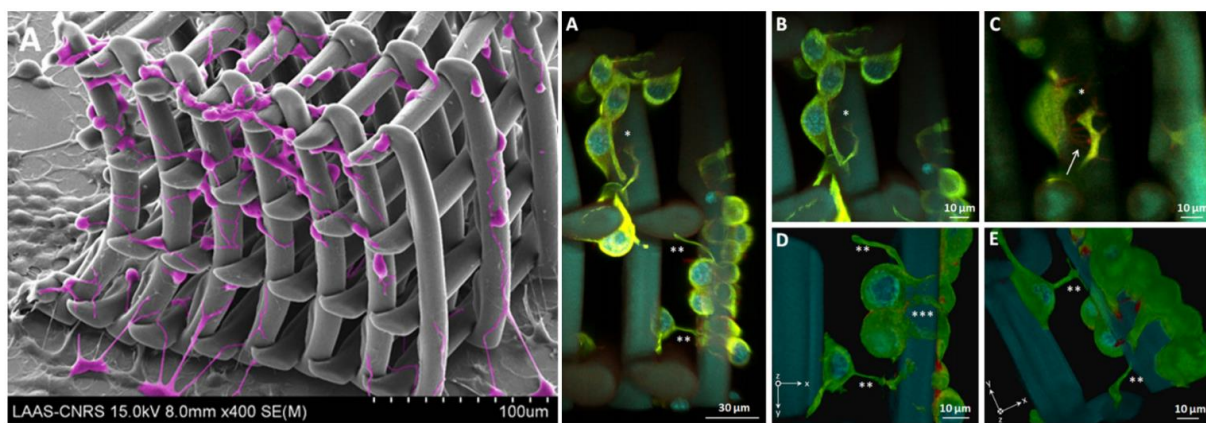


Figure 10: *Left:* SEM characterization. *Right:* Two-photon confocal imaging Z-stack of a lateral region of a 3D PEGDA hydrogel scaffold colonized by neuro2A cells.^[54]

The ability to precisely microfabricate hydrogels by 2PP has become critical for numerous biological applications including the construction of biosensors^[55] and the creation of soft scaffolds^[56] for tissue engineering.^[57] Besides its before mentioned features like high precision, excellent spatial control and high resolution in the sub-micrometer range, another aspect is the long wavelength of the excitation

source, offering the advantage of deeper tissue penetration with reduced risk for unintended photo-damage.

High initiation efficiency, good biocompatibility and sufficient hydrophilicity should constitute ideal 2PIs for biofabrication, however, the lack of efficient water-soluble 2PIs has been a critical obstruction of this technique.^[57] Furthermore, not only the 2PI and 2PI decomposition products but also the monomer and the emerging polymer scaffold are required to be biocompatible. While some polymers are not biocompatible or cause mutations, usually only the monomer is toxic (e.g. Bisphenol A), but after cross-linking cells are viable on these materials.^[53]

Microfluidics is a field of science that operates in the micrometer scale, whereby a microfluidic device consists of components such as valves, pumps and mixers for manipulating and transporting the fluid at this scale.^[58] Ovsianikov *et al.* utilized two-photon microfabrication to construct a microfluidic device as a placenta barrier model,^[59] which represents another interesting example of the potential biological application of 2PP. Given the many opportunities 2PIP offers for biological systems, water-soluble tunable initiators are desired for specific biological applications, thus enabling the writing of scaffolds either in the presence of biomolecules or directly around suspended biological moieties.

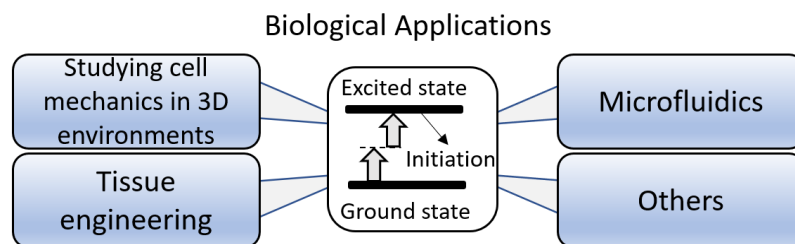


Figure 11: Biological applications of two-photon microfabrication.

B.3 Goal of this Thesis

On the basis of the 2PI shown in Figure 9, the aim of this work is to synthesize, characterize and evaluate water-soluble symmetrical α,ω -bis(triarylamine)-based compounds, linked by different π -conjugated heterocyclic units (linkers, Figure 12b), as potential initiators for two-photon microfabrication. The main objective of this thesis (i) is to introduce water-solubility to previously published triphenylamine-substituted thiophene 2PI scaffolds (Figure 9) by the introduction of highly polar groups of different electronic nature, such as PEG (electron-donating) or carboxylate (electron-withdrawing) functionalities (Figure 12a).

The enhancement of 2PI efficiency is a difficult matter, as it is affected by a multitude of parameters in complex relationship to each other.^[4] However, δ_{2PA} contributes as a major part in the overall efficiency of 2PIs and can be easily influenced (see chapter B.1.2, δ_{2PA} of BMOA-1T at 800 nm = 379 GM). One strategy that increases δ_{2PA} drastically is a high charge separation within the molecule. Hence, the higher the differences in electronic nature between A and D in quadrupolar D-A-D structures becomes, the further will δ_{2PA} most likely increase. Moreover, an increase in π -conjugation length and coplanarity will lead to higher δ_{2PA} as well, due to a better charge transfer. Therefore, the secondary aim (ii) of this thesis focuses on the incorporation of coplanar, π -conjugated and, compared to triphenylamine, electron-poor moieties like **T**, **BTD**, **TDZ** and **BBT** (Figure 12b) as linkers in the named cap-linker-cap systems. Benzothiadiazole units have been reported as excellent A units for a variety of applications,^[60-63] hence their incorporation as linkers in 2PIs features an interesting approach. Combined with the variation of electron-donating PEG and electron-withdrawing carboxylate substituents on the cap units a fine-tuning of the photophysical properties should be achieved (Figure 12), allowing the use of lasers in the IR range.

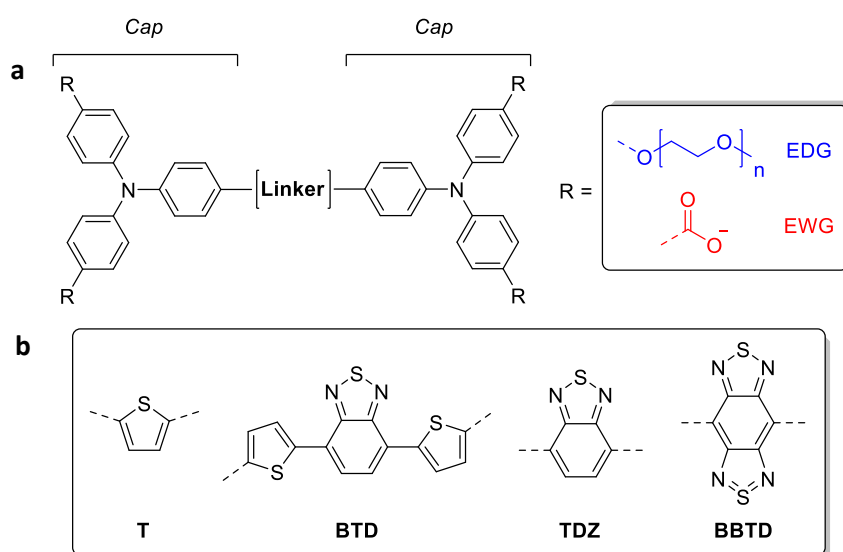


Figure 12: **a**: Cap-linker-cap motif with PEG or carboxylate substituents; **b**: Heterocyclic units as potential linkers (**T** = Thiophene, **BTD** = Bisthiophenebenzothiadiazole, **TDZ** = Benzothiadiazole, **BBTD** = Benzobisthiadiazole).

An alternatively pursued approach of introducing water-solubility to the 2PI scaffold (*iii*) is to synthesize respective rotaxanes whereby the 2PI scaffold is surrounded by a polar macrocycle. The structure of the target compounds consists of a stopper (substituted triphenylamine) and a linear component (thiophene) (Figure 13), which may be suitable as a dumbbell in rotaxane-based materials. Besides the possible water-solubility it was shown that the encapsulation of conjugated molecules by nonconjugated macrocycles to form rotaxanes represents a powerful method to achieve a high degree of control over several properties of molecular-based systems, as it can allow for simultaneous *i*) improvement of molecular rigidity, *ii*) prevention of aggregation, *iii*) enhanced chemical compatibility, as well as *iv*) protection of the functional unit.^[64]

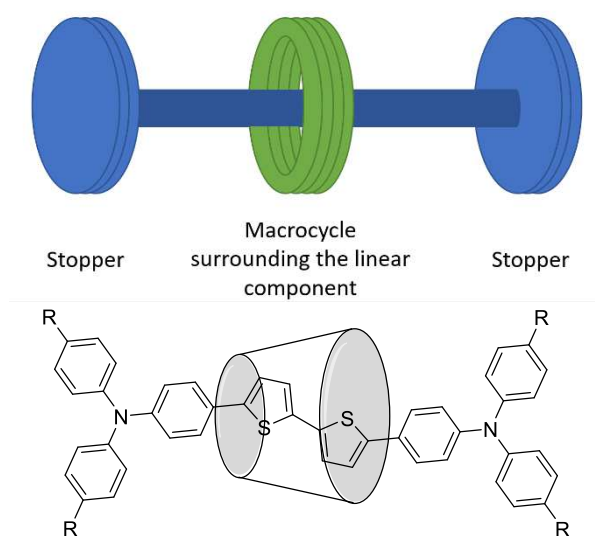


Figure 13: *Top*: General structure of a rotaxane. *Bottom*: Substituted rotaxane target compound.

C Specific Part

C.1 Introduction

D-A-D cap-linker-cap molecular assemblies (e.g. Figure 9) have been investigated intensively as potential OLED-materials in our research group over the past decade.^[65-67] Despite their high fluorescence quantum yields in solution (e.g. BHA-1T: 18 %, BMA-1T: 44 %, BMOA-1T: 56 %; Figure 9)^[65] several of these compounds were analyzed towards their applicability as 2PIs, with promising results.^[50]

As biological applications of two-photon polymerized structures gained a lot of attention in recent years^[42] and the lack of highly efficient water-soluble 2PIs restricts its possible potential,^[46, 57] the aim of this thesis is to design and synthesize water-soluble analogues of BMOA-1T scaffold (Figure 9). Consequently, the introduction of highly polar groups of varying electronic nature (electron-withdrawing $-\text{CO}_2^-$ and electron-donating -OPEG) is pursued also allowing an increased solubility in polar monomer formulations (e.g. for hydrogels), which is a crucial processing limitation of many PIs.

The quadrupolar D-A-D target compounds (Figure 12) can be synthesized from the respective precursors *via* Pd-catalyzed cross-coupling reactions. The Suzuki-Miyaura reaction was utilized in this study, since a reliable protocol, based on the application of pinacol boronic acid esters,^[65-67] was developed in our research group.

Besides the above described potentially water-soluble target compounds different molecular designs were pursued to ensure water-solubility of the targeted molecules in the course of this thesis. For instance, a cap substituted with multiple PEG groups was introduced to improve the water-solubility of the 2PI scaffold and bring interesting new properties with it, as its donor strength increases drastically. Further design approaches were investigated based on rotaxanes constituting of the 2PI scaffold as a dumbbell and a surrounding macrocycle (Figure 14). Cyclodextrins are conical in shape, hydrophobic on their interior and possess polar hydroxy groups on their exterior. Therefore, they are often used to solubilize hydrophobic compounds in water.^[68-69]

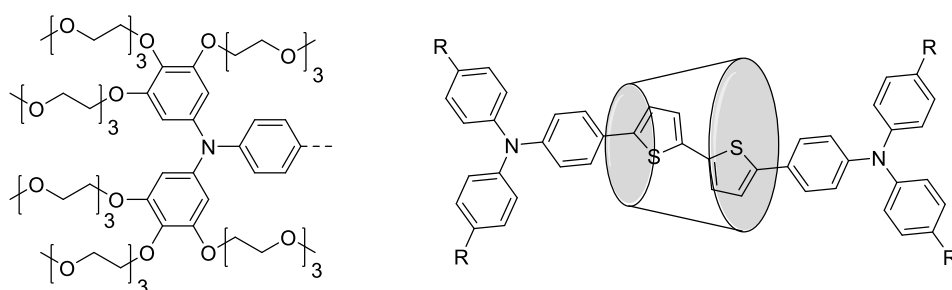


Figure 14: Alternative potentially water-soluble target compounds. *Left:* A triphenylamine-cap substituted with multiple PEG groups; *Right:* 2PI scaffold with a bithiophene linker as a dumbbell in a rotaxane.

C.2 Synthesis

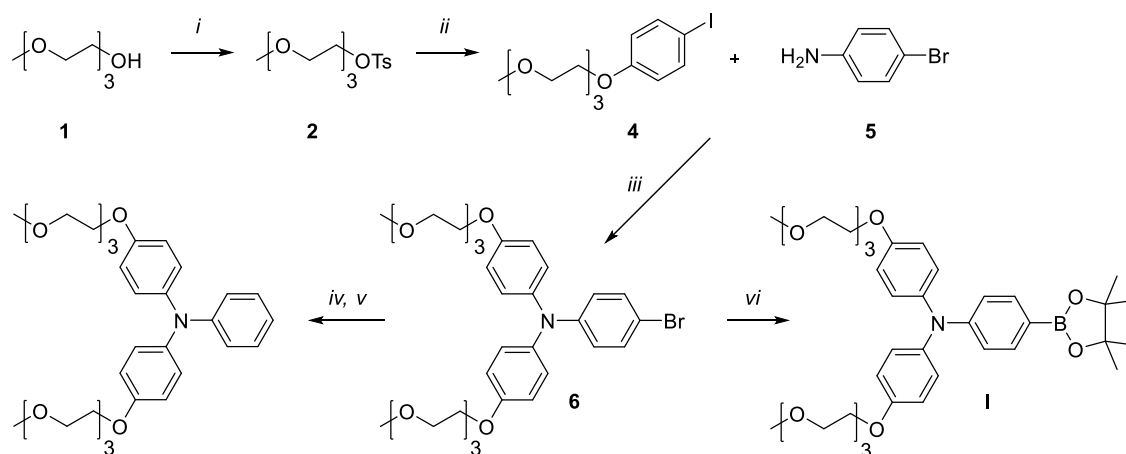
C.2.1 Synthesis of Cap Systems

C.2.1.1 Synthesis of 3PEGTPA

3PEGTPA substituted boronic ester **I** was synthesized as illustrated in Scheme 1 as a model compound, to analyze if the previously investigated synthetic pathway towards substituted triphenylamines^[11, 65] is also suitable for materials bearing PEG groups.

Tosylation of **1** (86 %) and subsequent pegylation (83 %) of **2**, according to Willinger,^[70] gave PEG substituted iodobenzene **4** in high yield. The synthesis of **6** was carried out *via* a ligand accelerated Ullmann condensation according to Goodbrand^[71] using 4-bromoaniline **5** achieving only a poor yield of 35 % after purification *via* column chromatography. In earlier studies it was shown, that differently substituted iodobenzenes work considerably better utilizing the same Ullmann conditions ($\approx 80\%$ ^[11, 65]). Hence, it can be concluded that the reaction may be hampered by catalyst coordination to the PEG group.

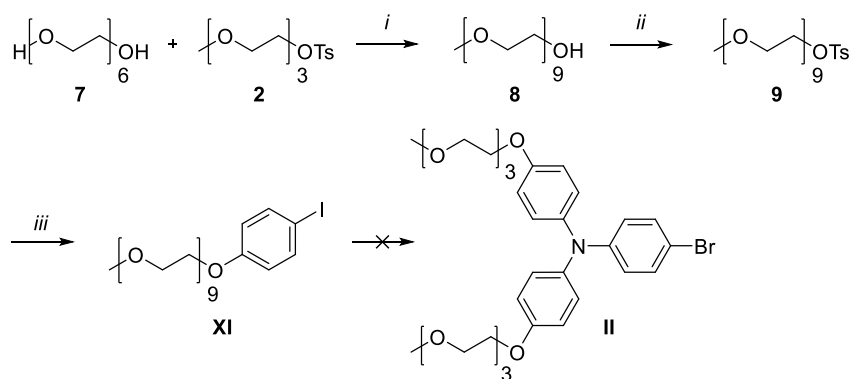
In a first approach, the synthesis of **I** was conducted according to previously published procedures. A lithium-halogen exchange using ⁿBuLi was used to convert the brominated precursor **6** to the boronic ester **I**. However, only dehalogenation of **6** could be observed after quenching the lithium species with Pinbop® (*iv*) or triisopropylborate (*v*) (Scheme 1). Therefore, a different approach was followed using Miyaura borylation conditions.^[72] **3PEGTPA** substituted boronic ester **I** could be obtained in 63 % after purification *via* column chromatography.



Scheme 1: Synthesis of **I**. *i*: TsCl, pyr, 0 °C to RT. *ii*: 4-iodophenol (**3**), K₂CO₃, MEK, reflux. *iii*: 4-bromoaniline (**5**), CuCl, KOH, 1,10-phenanthroline, toluene, reflux. *iv*: anh. THF, -78 °C, 1) ⁿBuLi; 2) Pinbop®. *v*: anh. THF, -78 °C, 1) ⁿBuLi; 2) triisopropyl borate. *vi*: Pd(dppf)Cl₂, KOAc, bis(pinacolato)diboron, DMF, 90 °C.

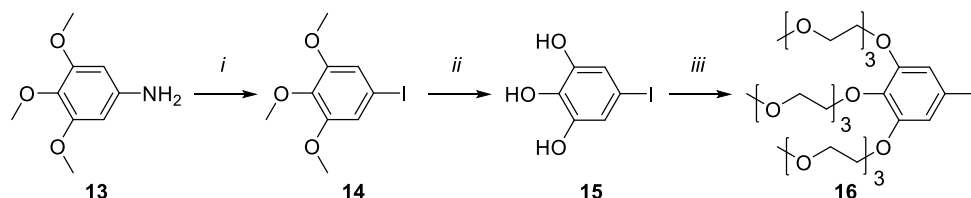
C.2.1.2 Synthesis of 9PEGTPA and Multiple PEG-substituted Caps

In a first attempt, the synthetic route targeting 9PEGTPA substituted boronic ester **III** was tried according to the above described route towards 3PEGTPA substituted boronic ester **I**. In this case, a chain extension of **2** with hexaethylene glycol **7** was initially performed, following a procedure developed by Hooper.^[73] Purification of **8** was achieved by bulb-tube distillation (57 %). As a main side product double side reacted product was identified. The tosylation of **8** was performed according to Heathcote^[74] and **9** could be obtained in 85 % yield. The nucleophilic substitution of **9** with 4-iodophenolate, adapted from Willinger,^[70] led to **XI** as a pure compound (41 %) by extracting the reaction mixture with *n*-hexanes and as a ~1:1 mixture with an unidentified side product followed by extraction with DCM. To obtain **II** two different Ullmann conditions were tried. The first approach followed the above described conditions according to Goodbrand,^[71] while the second approach was performed neat with copper powder at 170 °C. Unfortunately, both syntheses did not work (Scheme 2).



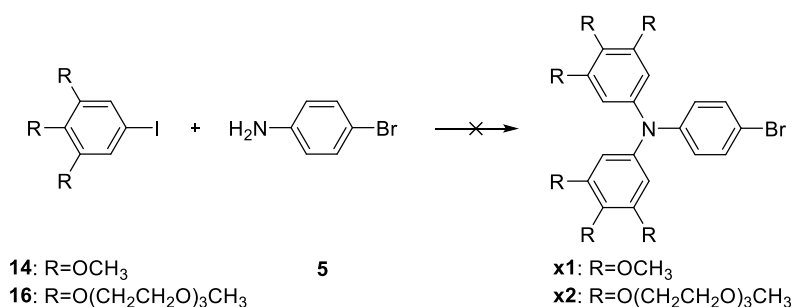
Scheme 2: PEG chain extension, tosylation and pegylation towards **XI**. *i*: NaH, THF, 0 °C to RT. *ii*: TsCl, KOH, H₂O, THF, 0 °C to RT. *iii*: 4-iodophenol, K₂CO₃, MEK, reflux.

The Ullmann conditions^[71] were further applied for the synthesis of TPAs bearing multiple PEG chains (**14**: R = OCH₃, **16**: R = O(CH₂CH₂)₃CH₃; Scheme 4). The corresponding substrates were synthesized according to the procedures of Han (*i*),^[75] Cardolaccia (*ii*)^[76] and Liang (*iii*)^[77] for the synthesis of **14**, **15** and **16** (Scheme 3).



Scheme 3: Synthetic route towards **16**. *i*: HCl, NaNO₂, KI, H₂O, CAN, 0 °C to RT. *ii*: BBr₃, DCM, -78 °C. *iii*: **2**, K₂CO₃, DMF, 100 °C.

14 was obtained after diazotization in excellent yield without the need of further purification (94 %). The subsequent straightforward demethylation using BBr_3 yielded **15** (54 %), which was then pegylated with **2**, obtaining **16** in moderate yield (41 %) after purification *via* column chromatography.

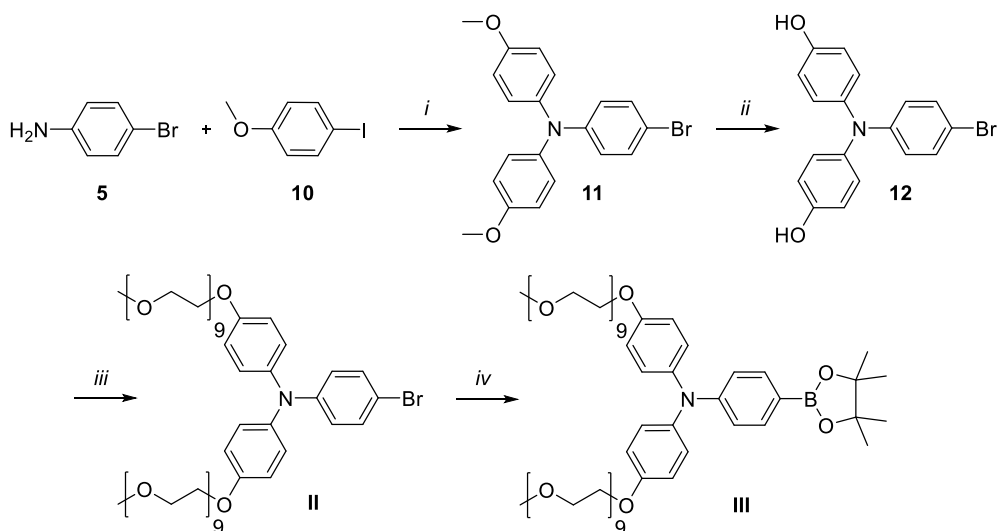


Scheme 4: Ullmann condensation or Buchwald-Hartwig amination of higher substituted starting materials (**14**, **16**).

Since the conditions used in the synthesis of **6** did not work towards compounds **x1** and **x2**, a Buchwald-Hartwig amination and different Ullmann conditions were tried. The attempt to synthesize **x2** also failed utilizing the Buchwald-Hartwig conditions investigated earlier in our research group (NaO^tBu , $(\text{NHC})\text{Pd}(\text{allyl})\text{Cl}$, toluene, reflux).^[65] The outcome of these syntheses may support the assumption that PEG groups coordinate to the catalyst and thereby hamper the reaction.

Since all reaction conditions described above did not yield any product **x2**, a different synthetic approach was chosen. The idea was to first synthesize **x1**, followed by a demethylation and a pegylation, leading to **x2**, whereby the coordination effects should be circumvented. A synthetic protocol was adopted from Lee,^[78] since this group was able to obtain **x1** in 26 % yield, differing only in a higher catalyst load (15 % instead of 4 %) from the Ullmann conditions depicted by Goodbrand,^[71] but only marginal amounts of one-sided product were isolated.

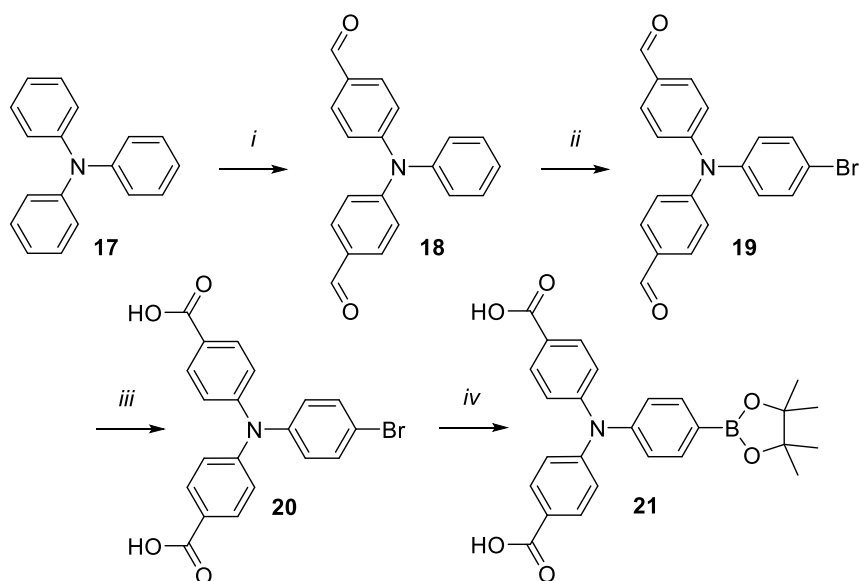
Another synthetic pathway towards **9PEGTPA** moiety (Scheme 5), similar to the described route towards **x2**, was chosen after Ullmann conditions with **XI** did not lead to the brominated precursor **II**. Thereby the Ullmann condensation was performed at an earlier stage avoiding the previously described problematic coordination effects of the catalyst, obtaining **11** (58 %). Demethylation of **11** was realized using BBr_3 , according to the protocol of Cardolaccia,^[76] and led to **12** (94 %). Important for the work-up of this synthesis is the disposal of the DCM layer after the reaction is quenched with water, as it contains mainly impurities. The first attempt to synthesize **II** was performed utilizing the conditions earlier used for pegylations.^[70] The desired product was formed, but it was not possible to separate it from a similar unidentified side product that appeared in the synthesis of **XI** (Scheme 2). To circumvent this problem different conditions according to Liu^[79] were used, which yielded **II** in 84 % without side products. The synthesis of **9PEGTPA** substituted boronic ester **III** was carried out similarly to the synthesis of **I** and provided **III** in excellent yield (85 %).



Scheme 5: Synthetic route towards **III**. *i*: CuCl, KOH, 1,10-phenanthroline, toluene, reflux. *ii*: 1 M BBr₃, anh. DCM, -78 °C. *iii*: **9**, K₂CO₃, ACN, reflux. *iv*: Pd(dppf)Cl₂, KOAc, bis(pinacolato)diboron, DMF, 90 °C.

C.2.1.3 Synthesis of CTPA

In the following the synthetic route towards the brominated precursor **20** is described. It was conducted according to a protocol developed by Ghosh.^[80] **21** was prepared as described by Wood.^[81] (Scheme 6)



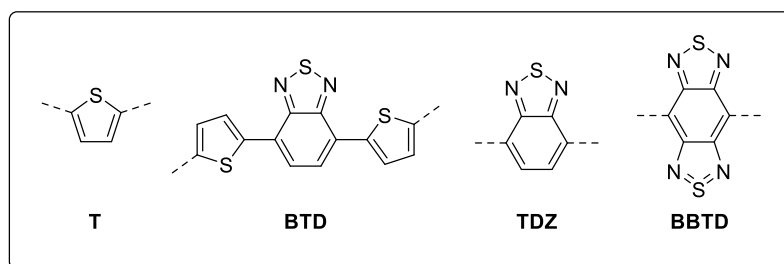
Scheme 6: Synthesis of **CTPA**. *i*: POCl₃, DMF, 100 °C. *ii*: NBS, CHCl₃, reflux. *iii*: KMnO₄, acetone:H₂O (4:1, v:v). *iv*: Pd(dppf)Cl₂, KOAc, bis(pinacolato)diboron, DMSO, 80 °C.

The conversion of triphenylamine to aldehyde **18** (49 %) was performed *via* a Vilsmeier-Haack formylation,^[82] followed by a bromination with NBS yielding **19** (quant.). Subsequently, KMnO₄ was used to oxidize aldehyde **19** to carboxylic acid **20** (78 %). The synthetic procedure towards boronic ester **21** deviated from the previously used Miyaura conditions only by the choice of solvent and a slightly lower

temperature, since the respective procedure is known in literature. **21** was obtained in 44 % yield after digestion in DCM.

C.2.2 Linker Synthesis

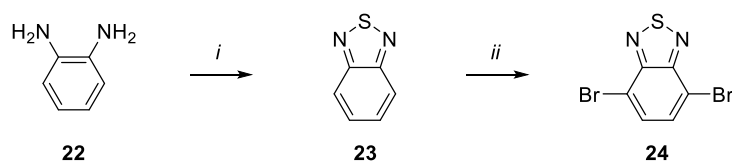
All dibromo substituted linkers were synthesized in the course of this thesis, except dibromo-**T**, which was commercially available (Scheme 7).



Scheme 7: Heterocyclic linkers.

C.2.2.1 Synthesis of TDZ

The synthesis towards linker **24** (Scheme 8) was performed according to Zhang (*i*)^[83] and Mancilha (*ii*).^[84]

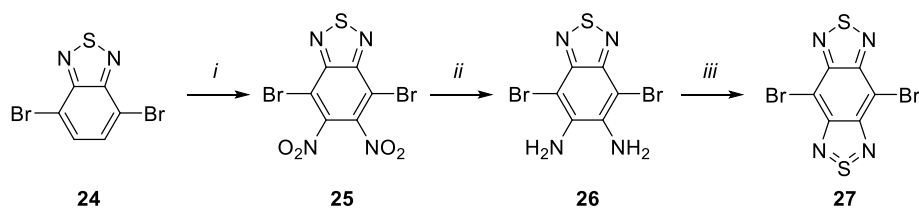


Scheme 8: Synthesis of **24**. *i*: SOCl₂, Et₃N, DCM, 0 °C to reflux. *ii*: Br₂, HBr, reflux.

Diamine **22** was subjected to a ring-closing reaction with SOCl₂ obtaining **23** (75 %). To synthesize **24** benzothiadiazole **23** was brominated in 4- and 7-position by an electrophilic aromatic substitution, giving **24** in 48 % yield after flash-chromatography. Dibromo substituted **TDZ** is not only a linker itself but also a precursor for every benzothiadiazole-based linker which was matter of interest in the course of this thesis.

C.2.2.2 Synthesis of BBTB

The protocols of Hassan^[85] (i), Tsubata^[86] (ii) and Murali^[87] (iii) were followed in the course of the synthesis of the linker **27** (Scheme 9).



Scheme 9: Synthesis of **27**. i: HNO₃, CF₃SO₃H, RT. ii: Fe, AcOH, 100 °C. iii: SOCl₂, Et₃N, DCM, 0 °C to reflux.

24 was converted into the electron-poor dinitro-precursor **25** (89 %) *via* twofold electrophilic aromatic substitution. Besides the above mentioned protocol also another procedure by Murali^[87] was used for the nitration. It deviated in the used equivalents of HNO₃ (2.6 eq. instead of 110 eq.) and the temperature was raised to 60 °C when Murali's procedure was followed. Both procedures worked but Hassan's protocol achieved higher yields, a higher conversion and no purification was necessary. However, a marginal amount of one-sided product stayed unconverted in both procedures.

Diamine **26** was synthesized *via* reduction of the nitro groups (54 %) with iron. The last step involved another ring-closing reaction with SOCl₂ yielding **27** (crude 72 %). The purification of dibromo **BBTB** was troublesome as it is almost insoluble in most organic solvents. Sublimation (140 °C, 1.7*10⁻⁶ Torr) was tried, following literature,^[88] but was not efficient enough. Extraction *via* a Soxhlet extractor with toluene did also not work. Flash-chromatography with DCM finally allowed purification. **27** was very difficult to characterize as conventional analytical approaches like NMR, GCMS, IR or the measurement of the melting point were not feasible. However, single crystals were grown out of a sat. solution in CHCl₃ covered with EtOH, since **27** revealed not to be stable in solution under air and measured confirming the molecular structure of **27** (Figure 15).

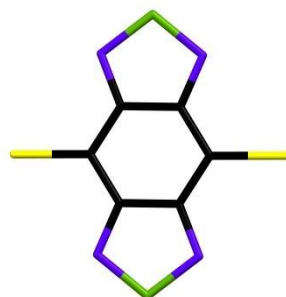
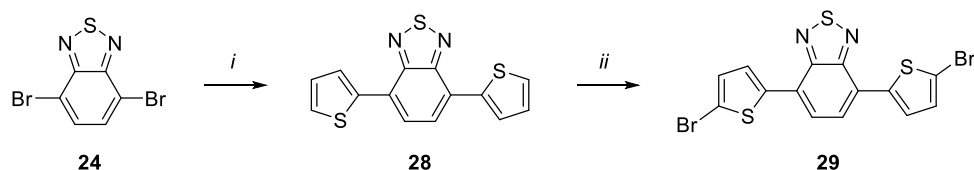


Figure 15: Molecular structure of **BBTB**.

C.2.2.3 Synthesis of BTD

The dibromo substituted **BTD** linker was synthesized as stated in the protocol of Kato (Scheme 10).^[89]

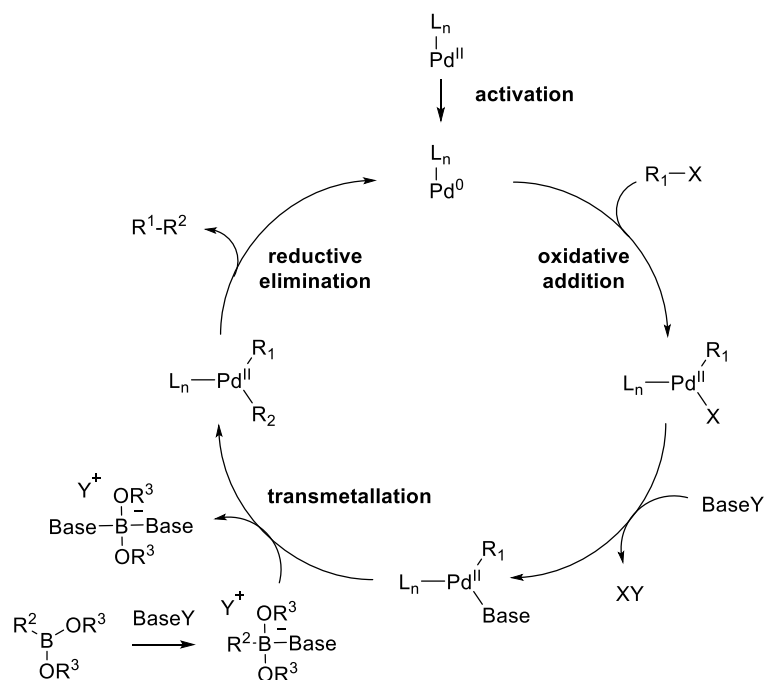


Scheme 10: Synthesis of **29**. *i*: thiophene-2-boronic acid pinacol ester, Na₂CO₃, Pd(PPh₃)₄, EtOH, H₂O, toluene, reflux. *ii*: NBS, CHCl₃, RT.

Dibromo-**TDZ** **24** was converted into **28** *via* a Suzuki-Miyaura cross-coupling. The purification was achieved by flash-chromatography, yielding 95 % of **28**. Subsequently, bromination with NBS gave **29** (95 %). Kato^[89] reported purification of **29** by recrystallization from chloroform. However, any attempts to recrystallize **29** did not improve the purity of the compound. Chromatography with PE:Et₂O achieved purification but proved to be troublesome due to insolubility of the product in the eluent.

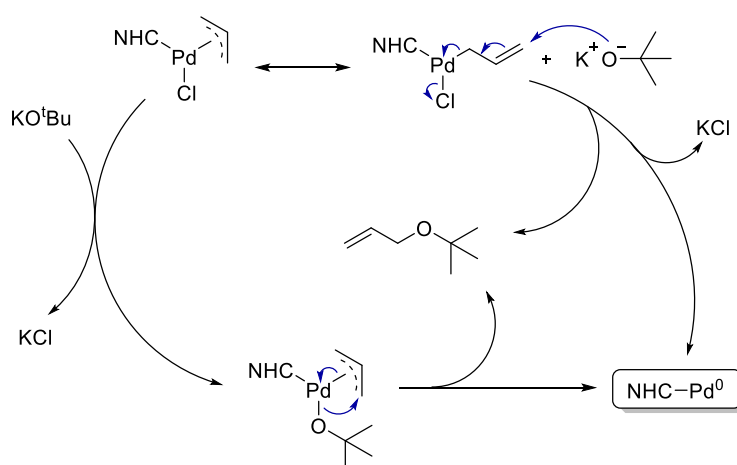
C.2.3 Target Compound Synthesis

The Suzuki-Miyaura reaction is an intensively investigated C-C coupling reaction and since it employs organoboron derivatives as organometallic reagents that are non-toxic, air- and moisture tolerant, and widely available, it is also one of the cross-couplings with the most important technological significance.^[90] In Scheme 11 a general mechanism of the reaction is illustrated. After the formation of the active Pd⁰ species an oxidative addition with the halide gives an organopalladium complex. The reaction with base activates the complex towards transmetalation with the boron ate-complex, which subsequently gives another organopalladium species. Upon reductive elimination the desired product is formed and the active Pd catalyst is restored.



Scheme 11: General mechanism of the Suzuki-Miyaura cross-coupling.

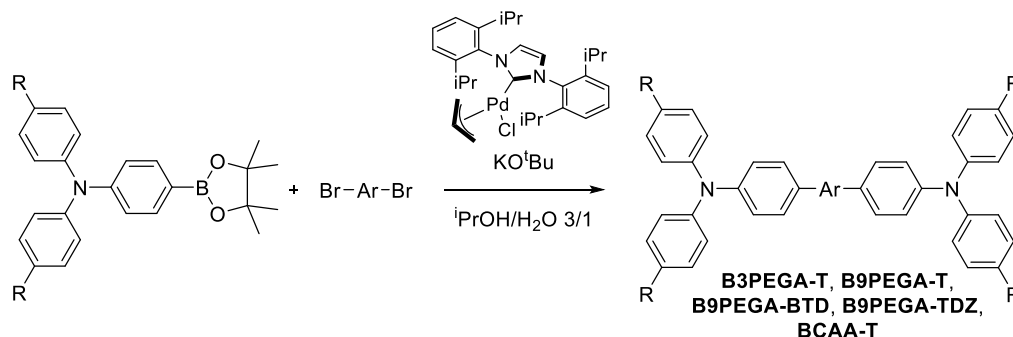
Due to the reasons mentioned above and the fact that a reliable protocol for Suzuki-Miyaura reactions was developed in our group^[65-67] this type of cross-coupling was applied for the synthesis of all target compounds. In the used protocol (NHC)Pd(allyl)Cl is applied as a catalyst. The corresponding activation pathway utilizing KO^tBu as the activation agent is illustrated in Scheme 12.^[91] Two pathways towards the active Pd⁰ species are shown. While one involves a conjugated addition on the allyl moiety the other includes an initial substitution of Cl by O^tBu. In the following step the activated Pd⁰ species is formed by the elimination of allyl-^tBu-ether.



Scheme 12: Two proposed activation pathways for (NHC)Pd(allyl)Cl.

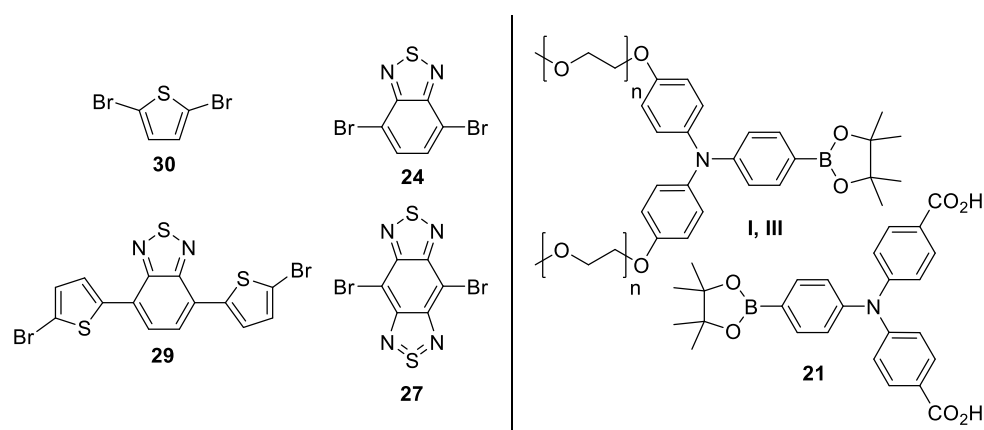
C.2.3.1 Synthesis of Target 2PIs

The methodology for Suzuki-Miyaura coupling of the respective pinacol boronic acid esters and dibromoaryl linkers applying (NHC)Pd(allyl)Cl as catalyst^[91] and KO^tBu as base in a 3:1-mixture of isopropanol and water proved to be highly efficient (Scheme 13).



Scheme 13: General reaction scheme of Suzuki-Miyaura coupling reactions of pinacol boronic acid esters and dibromoaryl linkers utilizing (NHC)Pd(allyl)Cl as catalyst.

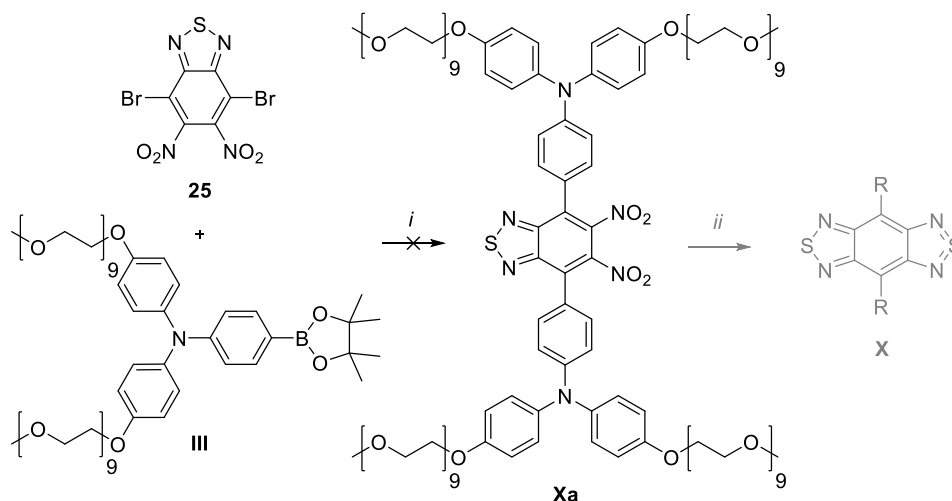
The building blocks used for the synthesis of target 2PIs are depicted in Scheme 14.



Scheme 14: Building blocks used for the synthesis of 2PIs. *Left*: Heteroaromatic Linkers (**24**, **27**, **29**, **30**); *Right*: Triphenylamine caps (**II** ($n = 3$), **III** ($n = 9$)).

Synthesis of Target Compounds with Electron-Donating Substituents

All reaction mixtures were refluxed in sealed vials until TLC showed full conversion. **B9PEGA-BBTD** was not obtained after the Suzuki-Miyaura coupling as the linker **27** proved to be unstable under basic conditions.^[60] Therefore, another route towards **X** according to Antaris^[60] was pursued. A Suzuki-Miyaura coupling of the nitrated **BBTD** precursor **25** with **9PEGTPA** substituted boronic ester was used, followed by a reduction with Fe and a ring-closing reaction using *N*-thionylaniline (Scheme 15). Unfortunately, the cross-coupling did not yield any **Xa**. Another alternative may be the utilization of the Stille coupling conditions, as no base is required.



Scheme 15: An alternative synthetic approach towards **X**. *i*: K_2CO_3 , $Pd(PPh_3)_4$, H_2O , toluene, reflux. *ii*: 1) Fe , $AcOH$, $100\text{ }^\circ C$; 2) *N*-thionylaniline, $TMSCl$, py , $80\text{ }^\circ C$.

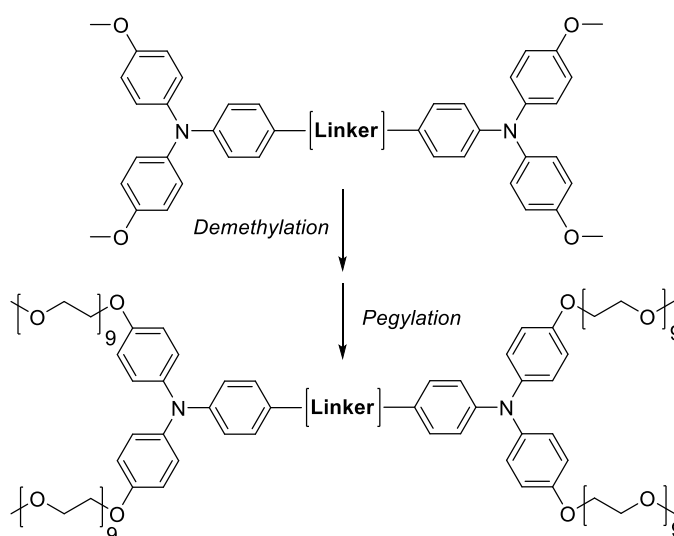
Besides several benefits that this Suzuki-Miyaura methodology features, such as low reaction times (2 h), easy reaction control and work-up, the purification was very difficult in most cases, as in total 36 ethylene glycol units hamper standard normal phase chromatography. After various chromatographic attempts including reversed phase and HILIC approaches finally a preparative HPLC method using a perfluorinated stationary phase and 80-90 % MeOH in H_2O as eluent allowed the purification of the target compounds. In Table 1 the substrates and yields of the target compound syntheses are summarized.

Table 1: Results of the target compound syntheses *via* Suzuki-Miyaura coupling.

	<i>Substrate</i>	<i>Product</i>	<i>Yield [%]</i>
B3PEGA-T	I + 30	V	40
B9PEGA-T	III + 30	VI	21
B9PEGA-TDZ	III + 24	VII	16
B9PEGA-BTD	III + 29	VIII	14
B9PEGA-BBTD	III + 27	X	-

B3PEGA-T was purified by normal phase MPLC, which was possible due to its shorter PEG chains. The residual target compounds were purified by preparative HPLC, which is reflected in the poor yield of the respective compounds. Before **B9PEGA-T**, **B9PEGA-TDZ** and **B9PEGA-BTD** were subjected to HPLC their work-up deviated from usual procedures as they are more soluble in water than in organic solvents used for extraction. Hence, catalyst- and base-residues were removed by the filtration through a pad of silica.

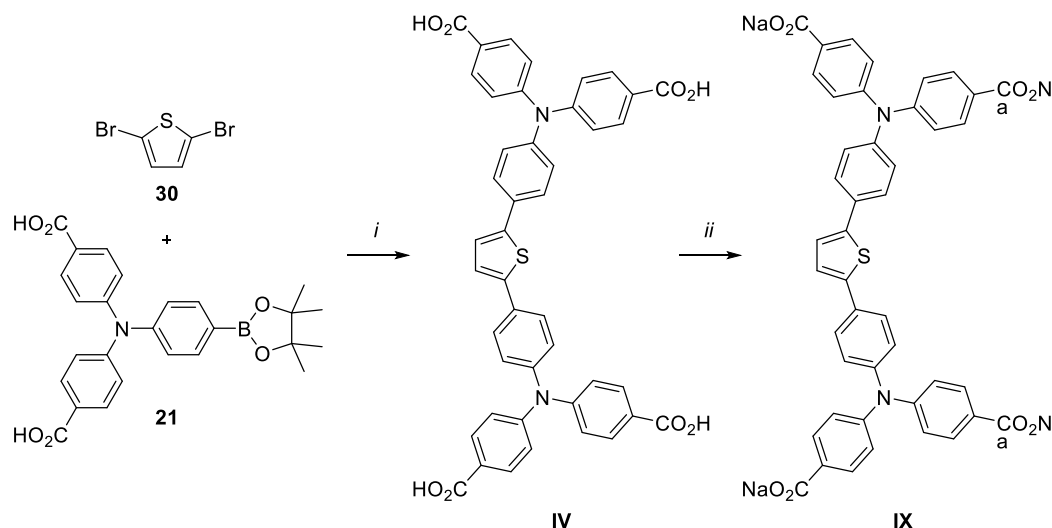
Due to very low yields it would be best to circumvent the need for prep. HPLC as the purification method. Therefore, a potential alternative synthetic pathway towards 2PI targets is presented in Scheme 16. It involves the synthesis of the methoxy substituted scaffold with any linker *via* the above described Suzuki-Miyaura conditions or other cross-couplings, followed by a demethylation with e.g. BBr_3 , giving the tetra alcohol and subsequent pegylation. The advantages of this route would include easier work-ups since the PEG groups get introduced at the last step, most probably higher yields and hence lower costs as large defined PEGs are relatively expensive. However, PEG functionalization after the coupling signifies several additional steps if the goal is to synthesize multiple compounds. Consequently, this alternative route is only advantageous when one specific target molecule shall be synthesized.



Scheme 16: Alternative potentially higher yielding approach towards target compounds. 1) Demethylation giving the tetra alcohol; 2) pegylation.

Synthesis of Target Compounds with Electron-Withdrawing Substituents

The synthesis of **BCAA-T** was performed utilizing the same conditions used for the previously described syntheses of target compounds (Scheme 13). However, the purification of **BCAA-T** deviated, since it was achieved by digestion in EE or recrystallization from $\text{MeOH}:\text{H}_2\text{O}$ (1:1), obtaining **IV** in 64 % yield. The conversion of **IV** to **BCxA-T** (quant.) was carried out with stoichiometric amounts of NaOH (Scheme 17). Although this reaction leaves no byproducts, inorganic salt impurities remain. A better way of synthesizing the tetra salt **IX** may be the utilization of an ion exchanger, following a protocol according to Ustyuzhanina.^[92] The Amberlite IR-20 (Na^+) ion exchanger was applied in this case but unfortunately, only NaOH led to **IX**. It was first tried to perform the reaction in MeOH but since no progress could be confirmed the solvent was changed to DMF , without success.



Scheme 17: Synthesis of IX. *i*: KO^tBu, (NHC)Pd(allyl)Cl, ⁱPrOH:H₂O (3:1), reflux. *ii*: NaOH, H₂O, RT.

C.2.4 Target 2PIs in β -Cyclodextrin-Rotaxanes

The lack of efficient 2PIs in aqueous medium may be tackled by using host-guest chemical interactions with β -cyclodextrin. Opting for water-solubility by the conversion of an efficient 2PI molecule into a rigid dumbbell in rotaxanes is a well-known approach. For instance Xing *et al.*^[68] was able to solubilize an anthraquinone-based 2PI in aqueous medium *via* host-guest interactions with 2-hydroxypropyl- β -cyclodextrin.

The 2PI scaffold discussed in B.2.4 consists of a stopper (substituted triphenylamine) and a linear component (thiophene) (Figure 16), which may be suitable as a dumbbell in rotaxane-based materials. Besides the possible water-solubility it was shown that the encapsulation of conjugated molecules by nonconjugated macrocycles to form rotaxanes represents a powerful method to achieve a high degree of control over several properties of molecular-based systems, as it can allow for simultaneous *i*) improvement of molecular rigidity, *ii*) prevention of aggregation, *iii*) enhanced chemical compatibility, as well as *iv*) protection of the functional unit.^[64]

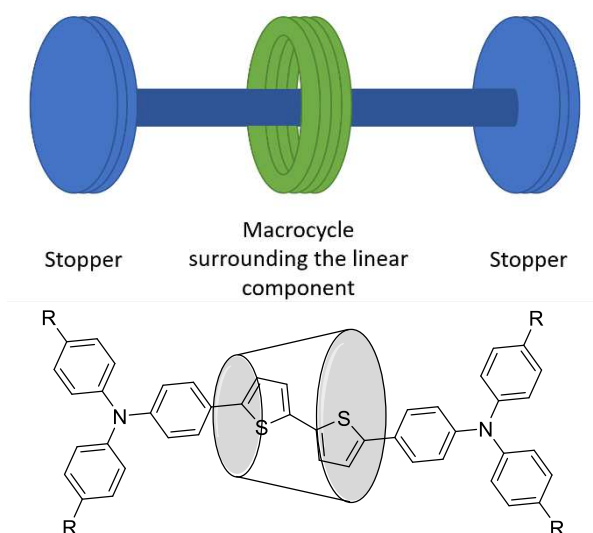


Figure 16: *Top*: General structure of a rotaxane. *Bottom*: Substituted rotaxane target compound.

Zalewski *et al.* synthesized a similar bithiophene-based rotaxane (Figure 17),^[64] which was incentive enough to use a similar approach towards the target 2PI scaffold shown in Figure 16.

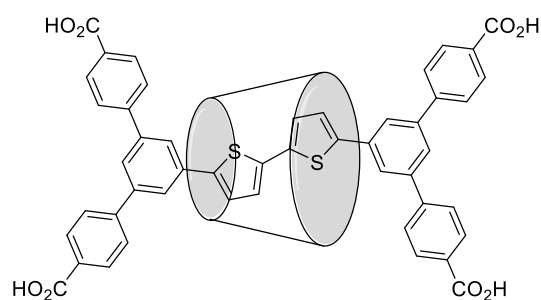


Figure 17: Rotaxane reference structure.

Intramolecular distance measurements of the molecular structures of TPA substituted thiophene, as well as β -cyclodextrin render these structures as suitable motifs for rotaxane materials (Figure 18).

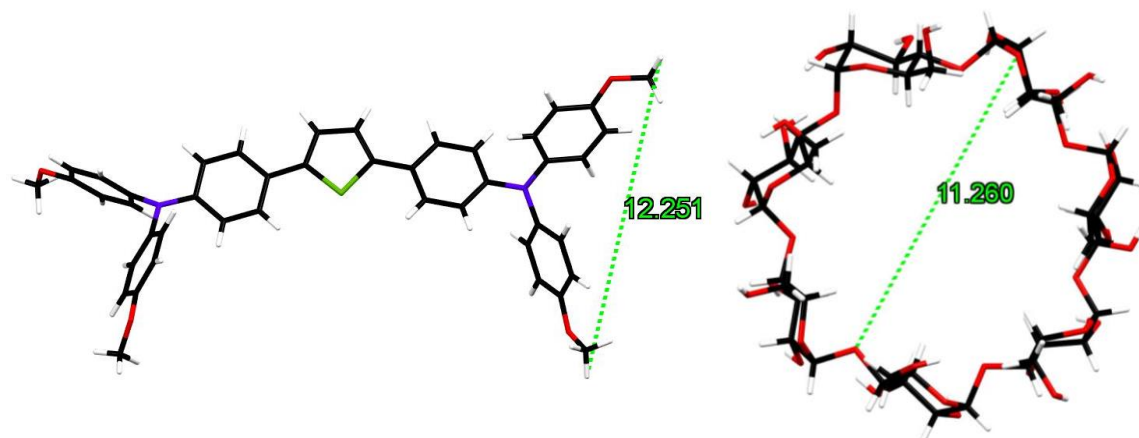
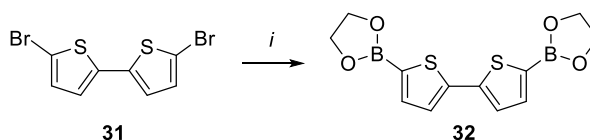


Figure 18: Molecular structures of BMOA-1T (*left*) and β -cyclodextrin (*right*). *Left*: Distance between the methoxy groups (12.251 Å). *Right*: Smallest diameter (11.260 Å).

The synthetic approach towards rotaxanes involves a water-based Suzuki-Miyaura coupling of the stoppers bearing carboxylic acid groups with the bithiophene linker, as Zalewski *et al.* reported.^[64] Since the protocol of Zalewski reports only a poor yield of 2 %, low yields were expected. Adjustment of both the reaction as well as the reaction conditions were pursued by means of varying halides on the stopper (Br, I), the use of single-branched templates and an inverse substitution pattern of the starting materials (boronic ester \leftrightarrow halide). Furthermore, the β -cyclodextrin concentration, the solvent and the temperature were varied.

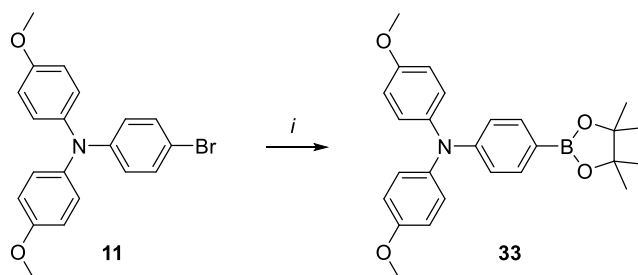
C.2.4.1 Synthesis of Rotaxane Precursors

In the following paragraph the syntheses of **32**, **33**, **35** and **36** are described. Bithiophene **32** and TPA **33** were synthesized since sterically demanding stoppers are required and Zalewski^[64] reported a successful synthesis of the reference structure (Figure 17) using **32** as boronic ester. **32** was synthesized according to Sakamoto^[93] *via* lithium-halogen exchange using bromide **31**, subsequent quenching with triisopropyl borate and hydrolysis of the resulting boronic ester with HCl. Esterification with ethylene glycol gave **32** in 50 % yield (Scheme 18).



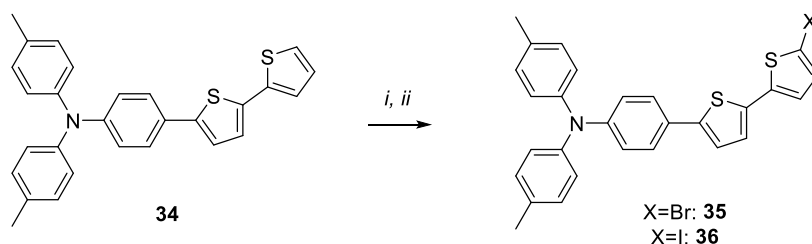
Scheme 18: Synthesis of **32**. *i*: 1) THF, -80 °C 1.1) ⁿBuLi, 1.2) B(OⁱPr)₃, HCl. 2) ethylene glycol, toluene, reflux.

The synthesis of **33** followed a protocol described by Anémian.^[94] **33** was synthesized *via* lithium-halogen exchange using bromide **11** and subsequent quenching with Pinbop®, obtaining **33** in 66 % yield (Scheme 19).



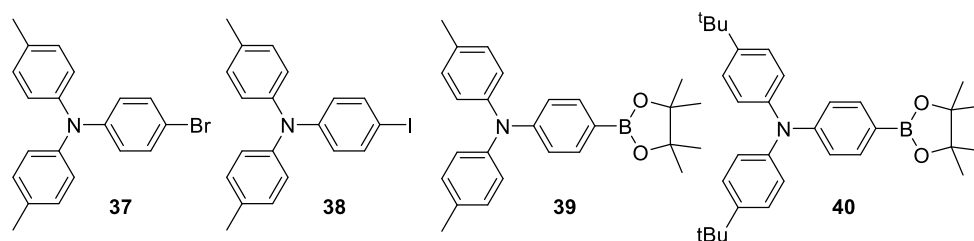
Scheme 19: Synthesis of **33**. *i*: THF, -80 °C 1) ⁿBuLi, 2) Pinbop®.

Single-branched templates **35** (95 %) and **36** (13 %) were synthesized according to Leliège^[95] by halogenation of **34** with the respective succinimide. The iodination worked with a poor yield (13 %) only after the addition of a catalytic amount of AcOH and heating to 50 °C (Scheme 20). Both halides were synthesized since the coupling parameters of the rotaxane synthesis needed adjustment. However, **36** was not used in the coupling, as the iodination gave only a marginal amount of product.



Scheme 20: Synthesis of single-branched templates **35** and **36**. *i* [X = Br]: NBS, CHCl₃, 0 °C to RT. *ii* [X = I]: NIS, AcOH, CHCl₃, 0 °C to 50 °C.

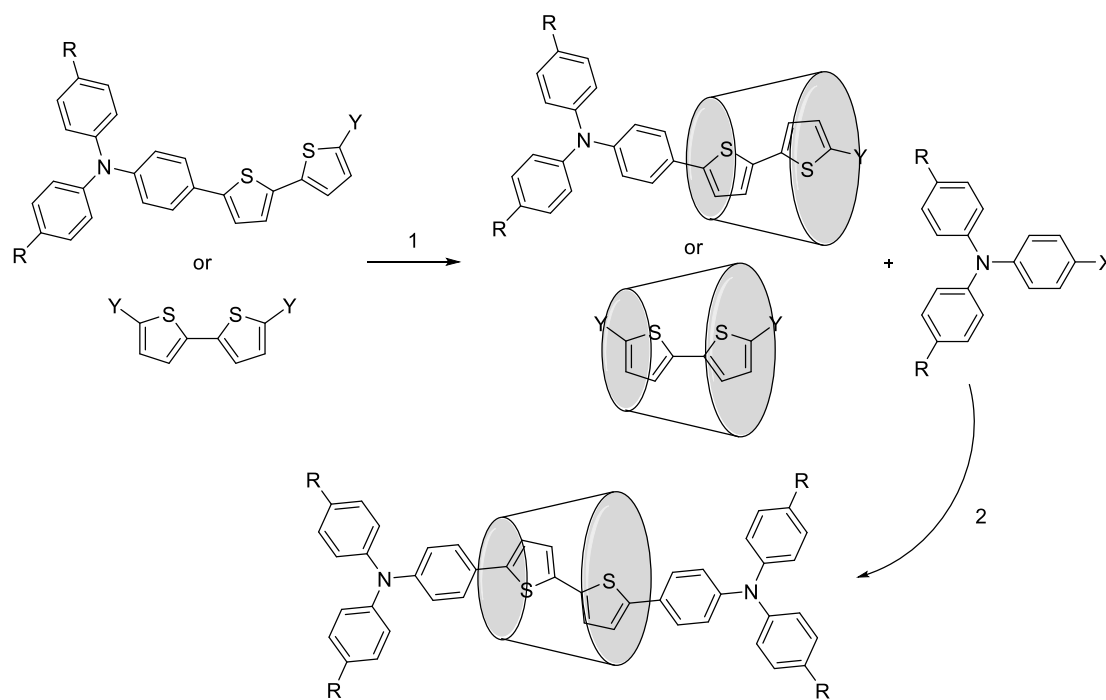
Due to previous synthetic efforts following TPA substrates bearing substituents with different steric demand are available and depicted in Scheme 21.



Scheme 21: Already available substrates for rotaxane synthesis.

C.2.4.2 Synthesis of β -Cyclodextrin Rotaxanes

The syntheses of rotaxanes were adapted from a Suzuki-Miyaura protocol described by Zalewski^[64] (Scheme 22). First, the respective linker or single-branched template was stirred with β -cyclodextrin in degassed solvent for a prolonged time (12h) to statistically prearrange the linker in the cavity of the cyclodextrin due to hydrophobic interactions.^[64, 69] Secondly, the stopper and the base were added.



Scheme 22: General rotaxane synthesis (X, Y = boronic ester or halide). 1) β -cyclodextrin, 2) Li_2CO_3 , $\text{Pd}(\text{OAc})_2$.

In Table 2 the reaction conditions for rotaxane syntheses are summarized. For the first syntheses (**R1-R4**) the Suzuki-Miyaura conditions reported by Zalewski^[64] were used. It was tried to adapt the reliable Suzuki-Miyaura coupling conditions which were developed in our group towards the rotaxane synthesis in **R5**. Hence, $(\text{NHC})\text{Pd}(\text{allyl})\text{Cl}$, KO^tBu and degassed $^i\text{PrOH}:\text{H}_2\text{O}$ (3:1) were used instead of $\text{Pd}(\text{OAc})_2$, KOAc and degassed H_2O . Unfortunately, only dumbbell was formed. Reactions **R6-R10** feature β -cyclodextrin saturation in the reaction mixture, to maximize the possibility of the linker moving into the hydrophobic cavity of cyclodextrin. For every reaction that involved β -cyclodextrin-saturation the pre-stirring occurred also at 80°C , to ensure the high concentration of cyclodextrin at this temperature. **R8** and **R9** were pre-stirred with base. It was discovered *via* TLC analysis of the pre-stirred solution of **R8**, that boronic ester **32** decomposes under basic conditions at 80°C .

Table 2: Conditions for the syntheses of rotaxanes.

Reaction	Boronic ester	Halide	β -Cyclodextrin load	T [°C]	Solvent	Reaction time
R1	32	38	4 eq.	80	H ₂ O	24 h
R2	32	37	4 eq.	80	H ₂ O	24 h
R3	39	31	4 eq.	reflux	H ₂ O	72 h
R4	39	35	4 eq.	reflux	H ₂ O	54 h
R5	39	31	4 eq.	reflux	¹ PrOH: H ₂ O	2.5 h
R6	32	37	saturated	80	H ₂ O	7 h
R7	32	11	saturated	80	H ₂ O	48 h
R8	32	-	saturated	80	H ₂ O	-
R9	40	31	saturated	80	H ₂ O	15 h
R10	33	31	saturated	80	DMF	48 h

The analysis towards rotaxane formation was performed *via* NMR-spectroscopy, LCMS or the growth of single crystals. In the NMR analysis the coexistence of aliphatic cyclodextrin signals and aromatic signals was pursued. Moreover, the splitting of the two thiophene signals into four distinct duplets, due to the influence of the conical cyclodextrin cavity,^[64] was looked out for.

The work-up strategies were varied for the performed syntheses since no reliable protocol regarding a similar synthetic problem was found in literature. A first work-up approach was to separate the remained starting materials and side products from the rotaxane and cyclodextrin mixture by liquid/liquid-extraction or digestion with an organic solvent (DCM or EE). If aromatic compounds remained in the mixture after the extraction it has been further investigated. A method separating α -cyclodextrin from the respective rotaxane *via* reversed phase column chromatography with Diaion HP-20 as stationary phase was reported^[96-98] and tried. Unfortunately, no separation was achieved as the grain size of the Diaion HP-20 did not allow the compounds to be retained. Another approach to remove excess cyclodextrin from the rotaxane was dissolving the mixture in DMF and precipitating the cyclodextrin with CHCl₃, which revealed that only a mixture of dumbbell and cyclodextrin could be obtained in this case. In another attempt the water-solubility of β -cyclodextrin^[99] was made use of, since it is most likely more soluble in water than the respective rotaxane. Hence, the mixture was neutralized, partially dissolved in H₂O (800 ml) and filtrated, but unfortunately, the residue consisted only of cyclodextrin. A further attempt to isolate any formed rotaxane was conducted by concentrating the organic extracts in *vacuo*. The obtained residue was subjected to normal phase column chromatography (SiO₂). By increasing the polarity to 10 % MeOH in DCM a fraction was obtained that may contain the desired

rotaxane according to NMR measurements, but it turned out to be only cyclodextrin and unidentified side product after single crystals were grown out of a MeOH/H₂O-solution (MeOH:H₂O, 3:1).

The rotaxane target compounds could not be isolated, but a series of reactions were screened, giving new insights into rotaxane synthesis.

C.3 Solubility of the Target Compounds

While exact solubility tests of the target compounds in water and polar monomer formulations still need to be performed a qualitative analysis of the solubility can be given. Target compounds featuring PEG groups are equally water-soluble, while **BCxA-T** seems to be more soluble in water. **BCxA-T** is only soluble in polar monomer formulations (ETA/TTA, PEGDA) if they feature a high water content, while PEG target compounds dissolve in a concentration of 1 µmol/g of resin without further addition of acetone, contrary to **BMOA-1T**. Since the PI needs to be homogeneously dispersed in the monomer formulation, the independence of organic solvents represents a considerable processing advantage of the PEG-based target compounds.

C.4 Photophysical Characterization of the Target Compounds

UV-VIS-Absorption and photoluminescence (PL) spectra of all synthesized target compounds were measured as 5 µM solutions in MeOH and will be discussed below. For experimental details see chapter D.2.3 and D.2.4. All absorption and fluorescence maxima are summarized in Table 3.

The absorption and fluorescence spectra of thiophene-based PEG substituted target compounds (**B3PEGA-T**, **B9PEGA-T**) were compared to the 2PI **BMOA-1T** (Figure 9)^[50] in Figure 19, showing that the introduction of PEG chains does not alter the photophysical properties as all spectra overlap almost perfectly. The absorption band at 296 nm can be attributed to a local TPA transition.

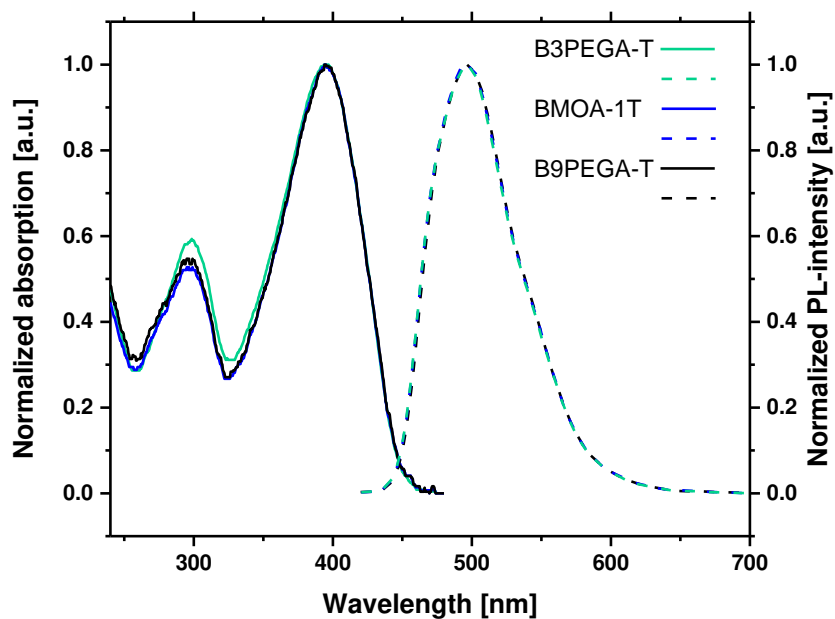


Figure 19: Absorption (*continuous*) and fluorescence (*dashed*, excitation wavelength: 400 nm) spectra of **B3PEGA-T**, **B9PEGA-T** and **BMOA-1T**.

BCAA-T and **BCxA-T** (Figure 20) follow the previously shown trend,^[50] which revealed a hypsochromic shift when changing from electron-donating to -withdrawing substituents on the TPA moiety, as they are blue shifted 15 nm and 10 nm, respectively, compared to e.g. **B9PEGA-T**. The two distinct absorption bands showed in Figure 19 overlap for **BCAA-T** and **BCxA-T** since electron-withdrawing substituents shift the local TPA transition band to higher wavelengths and simultaneously blueshift the energetically lowest absorption band.

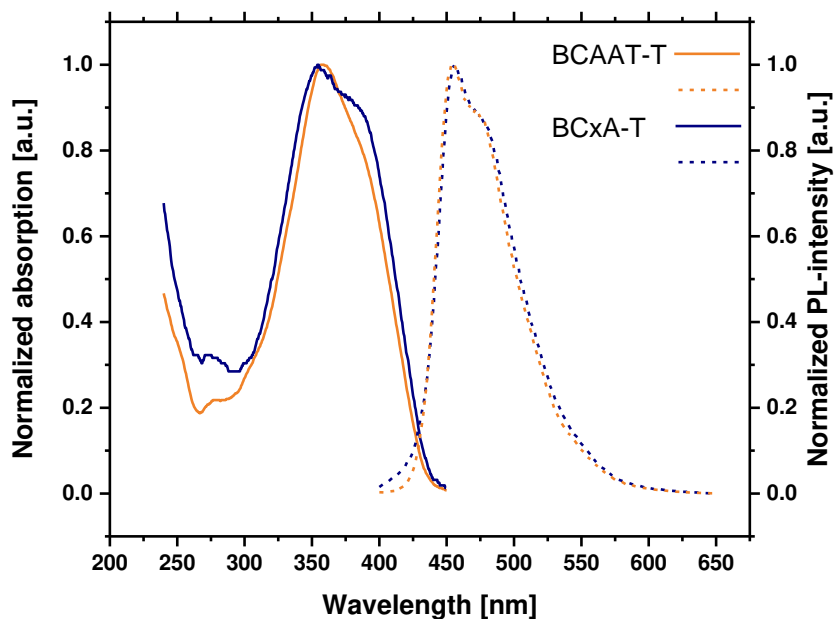


Figure 20: Absorption (*continuous*) and fluorescence (*dashed*, excitation wavelength: 370 nm) spectra of **BCAA-T** and **BCxA-T**.

B9PEGA-BTD and **B9PEGA-TDZ** show, compared to thiophene-based target compounds, significant differences in their absorption and fluorescence behavior, as the lowest energy absorption band is shifted to 537 nm for **B9PEGA-BTD** and to 477 nm for **B9PEGA-TDZ** (Figure 21). Interestingly, no fluorescence was observed at those wavelengths. **B9PEGA-BTD** is the only target compound that features three distinct absorption bands at 296 nm, 368 nm and 537 nm.

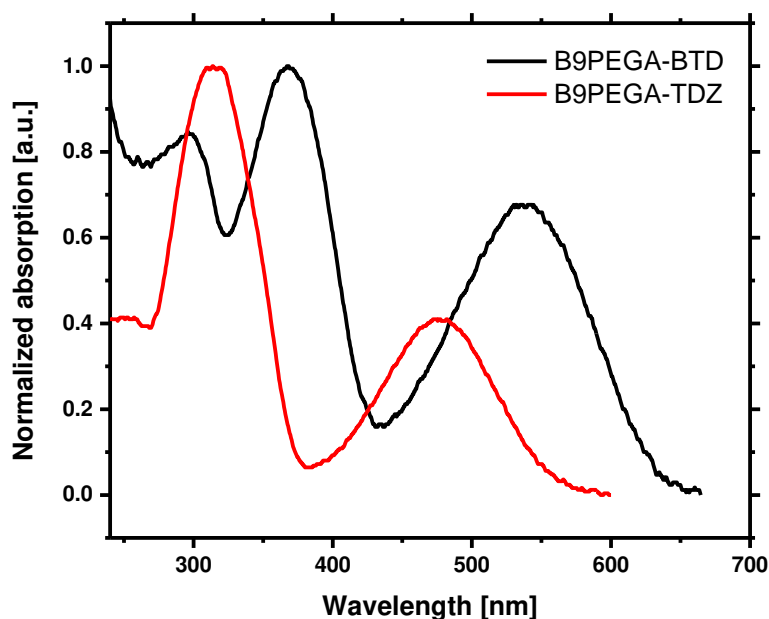


Figure 21: Absorption spectra of **B9PEGA-BTD** and **B9PEGA-TDZ**.

Table 3: All absorption and emission bands of target compounds.

	<i>Product</i>	λ_{Abs1} [nm]	λ_{Abs2} [nm]	λ_{Abs3} [nm]	λ_{Em1} [nm]	λ_{Em2} [nm]
BMOA-1T	ref.	395	296	-	497	-
B9PEGA-T	VI	395	296	-	497	-
B3PEGA-T	V	395	298	-	497	-
BCxA-T	IX	380	355	-	473	455
BCAA-T	IV	385	358	-	472	454
B9PEGA-BTD	VIII	537	368	296	-	-
B9PEGA-TDZ	VII	477	314	-	-	-

For comparison all absorption spectra were summarized in Figure 22.

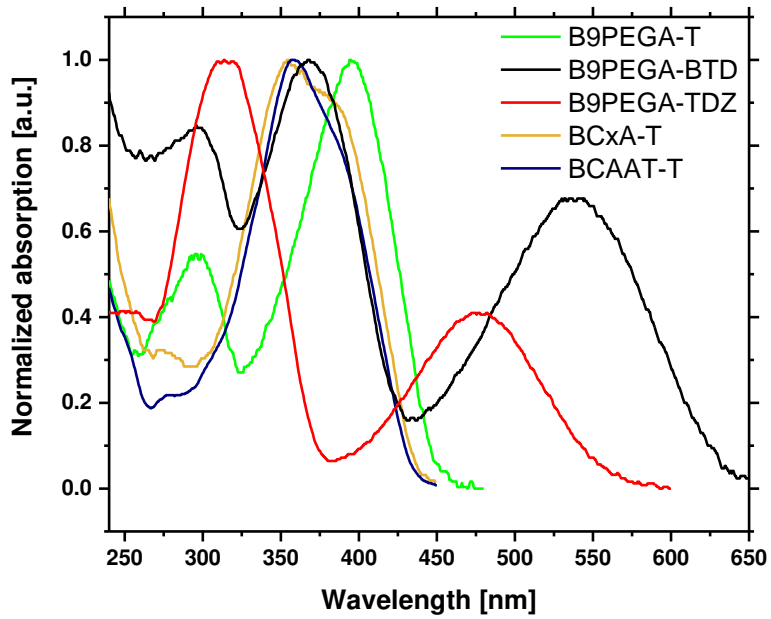


Figure 22: Absorption spectra of **B9PEGA-T**, **B9PEGA-BTD**, **B9PEGA-TDZ**, **BCAA-T** and **BCxA-T**.

B9PEGA-BTD and **B9PEGA-TDZ** feature exciting new absorption behavior, while **BCAA-T** and **BCxA-T** follow the previously discovered trend.^[50] **B9PEGA-T** shows the same absorption and emission maxima as the reference **BMOA-1T** which is promising in view of its potential efficiency as a 2PI.

C.5 Conclusion and Outlook

A series of symmetrically substituted α,ω -bis(triarylamine)-based water-soluble compounds have been synthesized. In order to increase the 2PA and thus the efficiency of these D-A-D type target molecules as potential PIs for two-photon-microfabrication, the structural motifs have been altered by either the introduction of electron-withdrawing carboxylate or electron-donating PEG groups on the TPA moiety. A new synthetic route towards pegylated as well as carboxylic acid bearing TPAs was developed, since the previously investigated lithium-halogen exchange strategy towards substituted TPA boronic esters was not expedient. Furthermore, the incorporation of varying linkers with different conjugation lengths and acceptor strengths allowed tuning the absorption maximum. Rotaxane target compounds could not be isolated, but a series of reactions were screened, giving new insights in rotaxane synthesis.

BCxA-T and target compounds featuring PEG groups with 9 units are water-soluble. While the PEG-based compounds are also soluble in polar monomer formulations (ETA/TTA, PEGDA; concentration of 1 $\mu\text{mol/g}$ of resin), **BCxA-T** seems to be only soluble if the water content is high. Furthermore, no acetone had to be added for the preparation of the PEG-based monomer formulations which features an important processing advantage.

All synthesized potential 2PIs were photophysically characterized. The results showed that the introduction of PEG substituents does not alter the one-photon absorption and emission properties of the reference 2PI **BMOA-1T**. Electron-withdrawing substituents (**BCAA-T**, **BCxA-T**) on the TPA moiety show an expected blue shift in absorption as well as in fluorescence. A strong shift towards higher wavelengths was observed for benzothiadiazole-based targets (**B9PEGA-BTD**: +142 nm, **B9PEGA-TDZ**: +82 nm) compared to thiophene-based targets **B3PEGA-T** and **B9PEGA-T**. Furthermore, **B9PEGA-BTD** and **B9PEGA-TDZ** show no fluorescence by excitation with the wavelength matching their energetically lowest absorption band.

Further investigations will be focused on the synthesis of the last target compound **B9PEGA-BBTD**, following the two possible routes described in chapter C.2.3 and the development of a reliable synthetic pathway towards higher substituted caps as well as 2PI rotaxanes. The determination of two-photon absorption cross sections $\delta_{2\text{PA}}$ will be essential for a comparison of the 2PA active materials in regard of their two-photon absorption maxima. Exact solubility tests in water and selected polar monomer formulations still need to be performed. Since the synthesized compounds should be applied in biological systems cell viability studies are of particular interest. Furthermore, appropriate 2PP structuring tests with excitation wavelengths within the absorption band of the respective 2PIs need to be performed.

D Experimental Part

D.1 General Remarks

All reagents from commercial suppliers were used without further purification. Anhydrous solvents like toluene, dioxane, DCM and THF were absolutized by a PURESOLV-system from it-innovative technology inc. Other anhydrous solvents were purchased from commercial suppliers. The lithiation reagent ⁿBuLi (2.5 M solution in hexanes) was purchased from Sigma-Aldrich® and used without additional quantitative analyses. All coupling reactions were performed using HPLC-grade isopropanol.

D.1.1 Chromatographic Methods

D.1.1.1 Thin Layer Chromatography

Thin layer chromatography (TLC) was performed using TLC-Silica gel 60 GF₂₅₄ (Merck).

D.1.1.2 Column Chromatography

Preparative MPLC

Preparative medium-pressure column chromatography was performed using a *Büchi* Sepacore™ Flash system, which was equipped with the following components:

- Pump-system: 2 *Büchi* pump modules C-605 *Büchi* pump manager C-615
- Detector: *Büchi* UV photometer C-635
- Fraction collector: *Büchi* fraction collector C-660

The appropriate PP-cartridges were packed with silica gel (Merck, 40-63 µm). Further details (eluent (distilled solvents), amount of stationary phase) are given in the respective experimental procedures.

Preparative HPLC

Preparative high-pressure column chromatography was performed using an autopurification system of *Waters* using an *ACQUITY* QDa detector in combination with a 2998 photodiode array detector. Analytical separation was conducted using *XSELECT* CSH Fluoro-Phenyl 5 µm 4.6 x 150 mm and *XSELECT* CSH C18 5 µm 4.6 x 150 mm columns. Preparative separation was performed using *XSELECT* CSH Prep Fluoro-Phenyl 5 µm 30 x 150 mm. As solvents HPLC grade methanol and HPLC grade H₂O were used containing 0.1 % formic acid.

D.2 Analytical Methods

D.2.1 GCMS Measurements

GCMS measurements were conducted *via* a GCMS interface from *Thermo Finnigan*:

- TRACETM 1300 Gas Chromatograph with a Restek® Rxi® -5Sil MS column (l = 30 m, Ø = 0.25 mm, 0.25 µm film, achiral).

- ISQTM LT Single Quadrupole Mass Spectrometer (electron ionization EI).

D.2.2 NMR-Spectroscopy

NMR spectra were recorded using a Bruker DPX-200 (200 MHz for ^1H ; 50 MHz for ^{13}C) or an Avance III HD (400 MHz for ^1H 100 MHz for ^{13}C) or an Avance III HD (600 MHz for ^1H ; 150 MHz for ^{13}C) Fourier transform spectrometer. ^1H - and ^{13}C -spectra are given as stated: chemical shift in parts per million (ppm) referenced to the according solvent (^1H : CDCl_3 δ = 7.26 ppm, DMSO-d_6 δ = 2.50 ppm, $(\text{CD}_3)_2\text{CO}$ δ = 2.05 ppm, CD_3OD δ = 3.31 ppm; ^{13}C : CDCl_3 δ = 77.0 ppm, DMSO-d_6 δ = 39.5, $(\text{CD}_3)_2\text{CO}$ δ = 29.9 ppm, CD_3OD δ = 49.1 ppm) with tetramethylsilane at δ = 0 ppm. Multiplicities of the signals are given as: ^1H : s = singlet, bs = broad singlet, d = doublet, dd = doublet of doublets, t = triplet, q = quartet, quin = quintet, sept = septet and m = multiplet.

D.2.3 Absorption Spectroscopy

Absorption spectroscopy was conducted using a NanoDrop™ One/OneC Microvolume UV-Vis Spectrophotometer from *Thermo Scientific™* in MeOH as a 5 μM solution.

D.2.4 Fluorescence Spectroscopy

Fluorescence spectra were recorded on a *PerkinElmer* LS 55 Fluorescence spectrometer in MeOH as a 5 μM solution.

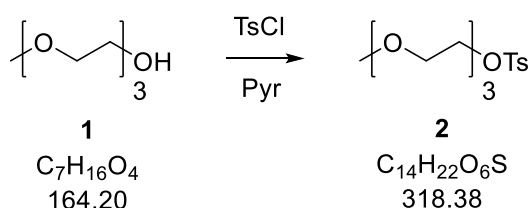
D.3 Synthesis and Characterization of the Compounds

Detailed experimental procedures for the synthesis of each compound as well as their characterization are presented in the following chapter.

D.3.1 Synthesis of Cap Systems

D.3.1.1 Synthesis of PEG (n=3)-substituted Triphenylamine Cap-System

2-(2-(2-Methoxyethoxy)ethoxy)ethyl 4-methylbenzenesulfonate



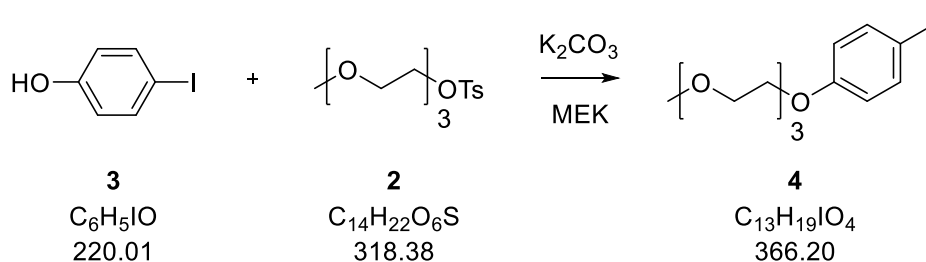
The synthesis of **2** was adapted from Willinger.^[70]

The alcohol **1** (13.14 g, 80 mmol, 1.0 eq.) was dissolved in pyridine (3 ml) and cooled to 0 °C under argon atmosphere. Then TsCl (16.78 g, 88 mmol, 1.1 eq.) dissolved in pyridine (15 ml) was added

dropwise within 1 h ($T < 10\text{ }^{\circ}\text{C}$). The color changed from yellow to pink and the reaction mixture became cloudy. The mixture was stirred at RT until TLC (PE:EE, 1:1) showed full conversion (3 h). Then ice was added, and the aqueous phase was extracted with EE repeatedly. The combined organic layers were washed with 2 M HCl (20 ml), sat. NaHCO_3 (20 ml) and H_2O (50 ml), dried over Na_2SO_4 , filtered and concentrated under reduced pressure. To remove pyridine residues the crude product was dried in HV yielding a colorless oil (21.80 g, 86 %).

$^1\text{H-NMR}$ (400 MHz, CDCl_3 , FID GEP019#10): $\delta = 7.80$ (d, $J = 8.4$ Hz, 2H), 7.34 (d, $J = 7.9$ Hz, 2H), 4.19 – 4.13 (m, 2H), 3.71 – 3.65 (m, 2H), 3.63 – 3.58 (m, 6H), 3.55 – 3.50 (m, 2H), 3.37 (s, 3H), 2.44 (s, 3H) ppm.

1-Iodo-4-(2-(2-(2-methoxyethoxy)ethoxy)ethoxy)benzene

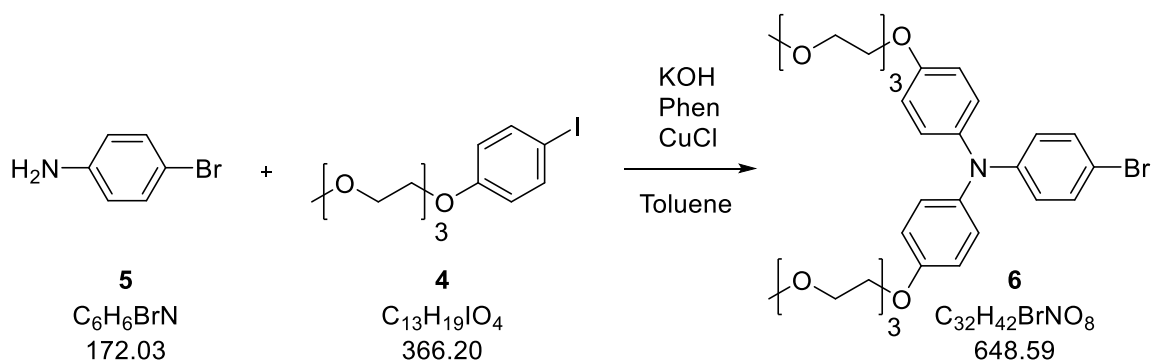


The reaction towards **4** was performed according to Willinger.^[70]

4-Iodophenol **3** (7.082 g, 32.2 mmol, 1.0 eq.) and K_2CO_3 (5.801 g, 42.0 mmol, 1.3 eq.) were suspended in MEK (30 ml) and heated to reflux under argon atmosphere. Then PEG dissolved in MEK (30 ml) was added dropwise within 40 min. During the addition another 60 ml of MEK were added, after precipitating solid disrupted the magnetic stir bar. The mixture was refluxed for 7 h. Then *n*-hexane (25 ml) was added and the mixture was refluxed for another 30 min. Ice water was added and the layers were separated. The organic layer was washed with water two times, dried over Na_2SO_4 and the solvent was removed in *vacuo*. The remaining starting material was removed by washing the in DCM dissolved crude product with aqueous 2 M NaOH. A brown liquid was obtained (9.826 g, 83 %).

$^1\text{H-NMR}$ (400 MHz, CDCl_3 , FID GEP020#40): $\delta = 7.54$ (d, $J = 9.0$ Hz, 2H), 6.69 (d, $J = 8.9$ Hz, 2H), 4.13 – 4.01 (m, 2H), 3.94 – 3.79 (m, 2H), 3.79 – 3.70 (m, 2H), 3.69 – 3.61 (m, 4H), 3.58 – 3.49 (m, 2H), 3.38 (s, 3H) ppm.

4-Bromo-*N,N*-bis(4-(2-(2-(2-methoxyethoxy)ethoxy)ethoxy)phenyl)aniline

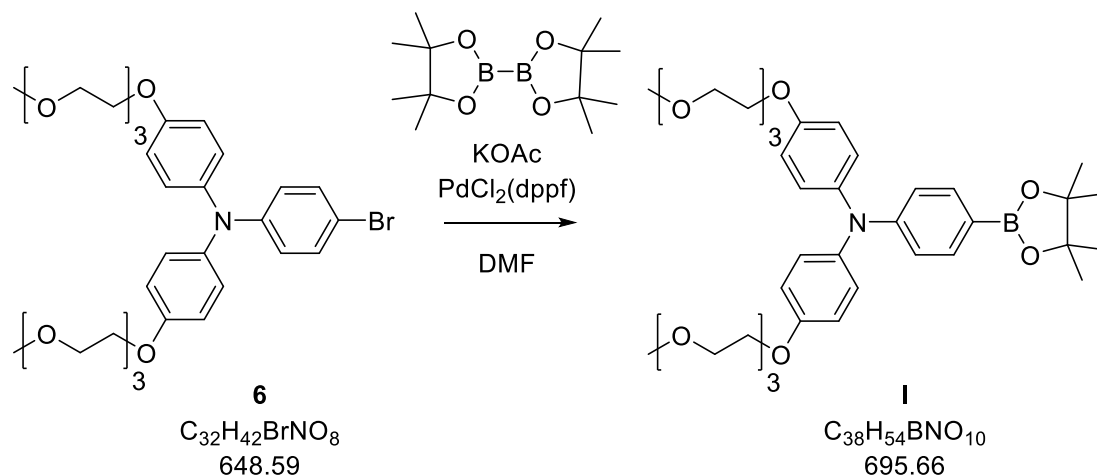


6 was synthesized according to Goodbrand.^[71]

4-Bromoaniline **5** (2.098 g, 12.2 mmol, 1.0 eq.), **4** (9.826 g, 26.8 mmol, 2.2 eq.), KOH (5.339 g, 95.2 mmol, 7.8 eq.), 1,10-phenanthroline monohydrate (97 mg, 0.49 mmol, 4 mol%) and CuCl (49 mg, 0.49 mmol, 4 mol%) were refluxed in anhydrous toluene (100 ml) under argon atmosphere using a Dean-Stark apparatus. After 27 h TLC (3 % MeOH in DCM) showed full conversion. H₂O (100 ml) was added and the mixture was stirred until most of the KOH dissolved. After the layers were separated the aqueous layer was extracted with toluene (3x). The combined organic layers were dried over Na₂SO₄ and concentrated under reduced pressure. The crude product was purified by column chromatography in two separate batches (180 g SiO₂, 120 g SiO₂, 1 % MeOH in DCM). A dark red oil was obtained (2.790 g, 35 %).

¹H-NMR (600 MHz, CDCl₃, FID GEP023#80): δ = 7.23 (d, J = 8.9 Hz, 2H), 6.99 (d, J = 8.9 Hz, 4H), 6.82 (d, J = 8.9 Hz, 4H), 6.78 (d, J = 8.9 Hz, 2H), 4.16 – 4.05 (m, 4H), 3.92 – 3.81 (m, 4H), 3.81 – 3.71 (m, 4H), 3.71 – 3.64 (m, 8H), 3.59 – 3.51 (m, 4H), 3.38 (s, 6H) ppm.

¹³C-NMR (150 MHz, CDCl₃, FID GEP023#81): δ = 155.3, 148.0, 140.82, 131.9, 126.6, 122.3, 115.6, 112.6, 72.1, 71.0, 70.8, 70.7, 69.9, 67.8, 59.2 ppm.

***N,N*-Bis(4-(2-(2-(2-methoxyethoxy)ethoxy)ethoxy)phenyl)-4-(4,4,5,5-tetramethyl-1,3,2-dioxaborolan-2-yl)aniline**

The borylation of **6** was performed according to Ishiyama.^[72]

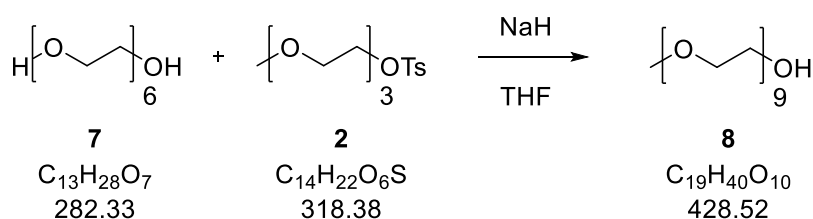
The brominated precursor **6** (193 mg, 0.30 mmol, 1.0 eq.), bis(pinacolato)diboron (84 mg, 0.33 mmol, 1.1 eq.), KOAc (88 mg, 0.90 mmol, 3.0 eq.) and Pd(dppf)Cl₂ (7 mg, 9 μmol, 3 mol%) were dissolved in dry DMF (3 ml) under argon atmosphere. The mixture was heated to 90 °C for 22 h. Subsequently the cooled mixture was poured on H₂O and extracted with DCM three times. Then the combined organic layers were dried over Na₂SO₄ and the solvents were removed in HV. **1** was isolated as a black oil (132 mg, 63 %) after column chromatography (9 g SiO₂, 2 % MeOH in DCM).

¹H-NMR (600 MHz, CDCl₃, FID GEP024#30): δ = 7.59 (d, J = 8.4 Hz, 2H), 7.03 (d, J = 8.9 Hz, 4H), 6.90 – 6.76 (m, 6H), 4.11 – 4.10 (m, 4H), 3.89 – 3.80 (m, 4H), 3.79 – 3.72 (m, 4H), 3.71 – 3.62 (m, 8H), 3.58 – 3.51 (m, 4H), 3.38 (s, 6H), 1.31 (s, 12H) ppm.

¹³C-NMR (150 MHz, CDCl₃, FID GEP024#31): δ = 155.3, 151.3, 140.5, 135.7, 127.0, 126.2, 118.7, 115.4, 83.4, 71.9, 70.8, 70.7, 70.6, 69.8, 67.6, 59.1, 24.8 ppm.

D.3.1.2 Synthesis of PEG (n=9)-substituted Triphenylamine Cap-System

3,6,9,12,15,18,21,24,27-Nonaoxaocacosan-1-ol

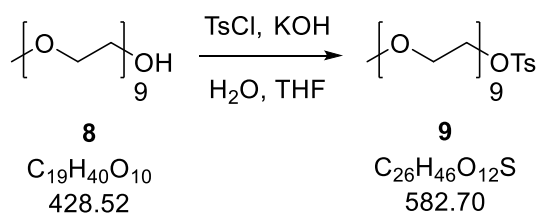


The synthesis of **8** was adapted from Hooper.^[73]

Hexaethylene glycol **7** (4.807 g, 17.0 mmol, 1.0 eq.) was dissolved in anh. THF (45 ml) and cooled to 0 °C. Then NaH (60 % in mineral oil; 0.882 g, 22.1 mmol, 1.3 eq.) was added in 5 portions and the red mixture was stirred at 0 °C for 1 h. Subsequently **2** (5.428 g, 17.0 mmol, 1.0 eq.) dissolved in anh. THF (15 ml) was added dropwise at 0 °C. After the addition the reaction mixture was stirred at RT overnight. The suspension was then filtered (Por 4) and the filtrate was concentrated in *vacuo*. The residue was partitioned between toluene and H₂O and the organic layer was extracted with H₂O (3x60 ml). The combined aqueous layers were then extracted with CHCl₃ (4x60 ml). The combined CHCl₃ layers were dried over Na₂SO₄ and the solvent was removed under reduced pressure. The crude product was subjected to bulb-tube distillation (3.0*10⁻¹ mbar, 200 °C) yielding a light-yellow oil (4.178 g, 57 %).

¹H-NMR (400 MHz, CDCl₃, FID GEP049#20): δ = 3.75 – 3.70 (m, 2H), 3.69 – 3.59 (m, 32H), 3.57 – 3.52 (m, 2H), 3.38 (s, 3H), 2.25 (bs, 1H) ppm.

3,6,9,12,15,18,21,24,27-Nonaoxaocacos-1-yl 4-methylbenzenesulfonate



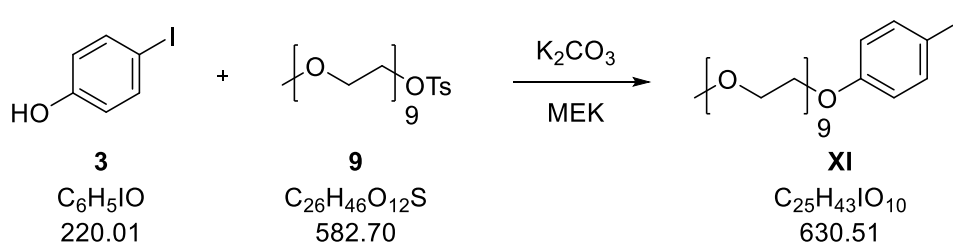
The synthesis of **9** was adopted from Heathcote.^[74]

KOH (0.524 g, 9.3 mmol, 2.8 eq.) was dissolved in H₂O (2 ml) and cooled to 0 °C. **8** (1.423 g, 3.3 mmol, 1.0 eq.) dissolved in THF (2 ml) was added and subsequently TsCl (1.147 g, 6.0 mmol, 1.8 eq.) dissolved in THF (2 ml) was added dropwise keeping the temperature below 5 °C. After the addition the mixture was slowly warmed to RT and stirred until TLC showed full conversion (4.5 h). Ice water (5 ml) was added and the mixture was extracted with DCM (2x10 ml). The combined organic layers were washed

with H₂O (2x3 ml) and brine (3 ml), dried over Na₂SO₄ and concentrated in *vacuo*. A colorless oil was obtained (1.615 g, 85 %).

¹H-NMR (400 MHz, CDCl₃, FID GEP046#10): δ = 7.80 (d, J = 8.4 Hz, 2H), 7.34 (d, J = 8.0 Hz, 2H), 4.34 – 3.94 (m, 2H), 3.78 – 3.46 (m, 34H), 3.38 (s, 3H), 2.45 (s, 3H) ppm.

1-Iodo-4-(3,6,9,12,15,18,21,24,27-nonaoxaoctacos-1-yl)benzene



The synthesis of **XI** was adapted from Willinger.^[70]

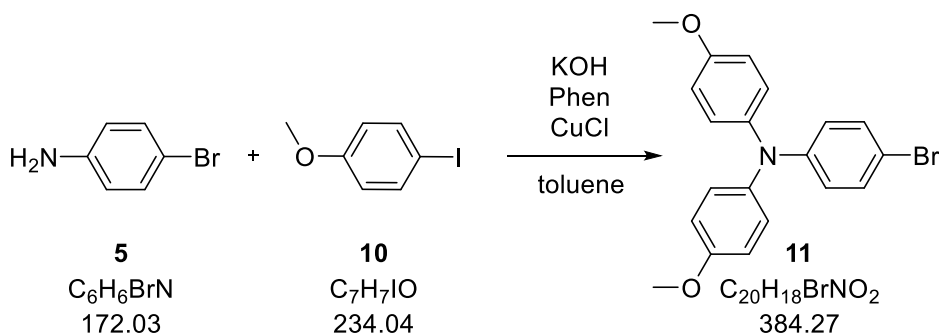
4-Iodophenol **3** (0.508 g, 2.30 mmol, 1.0 eq.) and K₂CO₃ (0.418 g, 2.99 mmol, 1.3 eq.) were refluxed in MEK (3 ml). **9** (1.615 g, 2.76 mmol, 1.2 eq.) dissolved in MEK (3 ml) was slowly added dropwise. MEK (3 ml) was added to improve the magnetic stirring efficiency. The mixture was refluxed until TLC (2 % MeOH in DCM) showed full conversion (4 h). Then *n*-hexane (3 ml) was added and refluxing was kept on for 30 min. Subsequently ice water (3 ml) was added to the cooled suspension and the layers were separated. The organic layer was washed with H₂O (2x2 ml), dried over Na₂SO₄ and concentrated in *vacuo*. To remove remaining starting material the crude product was dissolved in DCM and washed with 2 M NaOH. A light brown oil (0.595 g, 41 %) was obtained.

The aqueous layer was extracted with DCM (2x) and the combined DCM layers were dried over Na₂SO₄ and concentrated in *vacuo*. A mixture (~1:1 according to ¹H-NMR) of product and an unidentified side product were obtained (0.776 g).

¹H-NMR (400 MHz, CDCl₃, FID GEP047#30): δ = 7.54 (d, J = 9.0 Hz, 2H), 6.69 (d, J = 8.9 Hz, 2H), 4.20 – 3.99 (m, 2H), 3.90 – 3.78 (m, 2H), 3.76 – 3.59 (m, 30H), 3.58 – 3.50 (m, 2H), 3.38 (s, 3H) ppm.

HRMS (ESI) Calcd for: C₂₅H₄₄IO₁₀⁺ ([M+H]): 631.1974, found: 631.1982; Calcd for: C₂₅H₄₃IO₁₀Na⁺ ([M+Na]): 653.1793, found: 653.1802; Calcd for: C₂₅H₄₃IO₁₀K⁺ ([M+K]): 669.1532, found: 669.1542.

4-Bromo-*N,N*-bis(4-methoxyphenyl)aniline

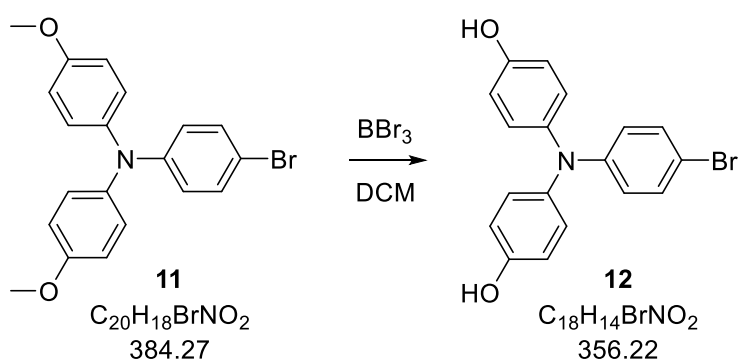


11 was synthesized analogous to Goodbrand.^[71]

4-Bromoaniline **5** (6.68 g, 38.8 mmol, 1.0 eq.), 4-iodoanisole (20.00 g, 85.5 mmol, 2.2 eq.), KOH (17.00 g, 303.0 mmol, 7.8 eq.), 1,10-phenanthroline monohydrate (308 mg, 1.6 mmol, 4 mol%) and CuCl (156 mg, 1.6 mmol, 4 mol%) were refluxed in anhydrous toluene (300 ml) under argon atmosphere using a Dean-Stark apparatus. After GCMS showed only traces of starting material (70 h) the mixture was cooled to RT and H₂O (200 ml) was added. The suspension was stirred until most of the KOH was dissolved. Subsequently the layers were separated, and the aqueous layers was extracted with toluene (3x). The combined organic layers were dried over Na₂SO₄ and the solvent was removed in *vacuo*. **11** was obtained as a white solid (8.71 g, 58 %) after bulb-tube distillation ($3.0 \cdot 10^{-1}$ mbar, 200 °C) and subsequent recrystallization from MeOH.

¹H-NMR (400 MHz, CDCl₃, FID GEP083#70): δ = 7.23 (d, *J* = 8.9 Hz, 2H), 7.02 (d, *J* = 8.9 Hz, 4H), 6.82 (d, *J* = 9.0 Hz, 4H), 6.79 (d, *J* = 8.9 Hz, 2H), 3.79 (s, 6H) ppm.

4,4'-[(4-Bromophenyl)imino]bisphenol



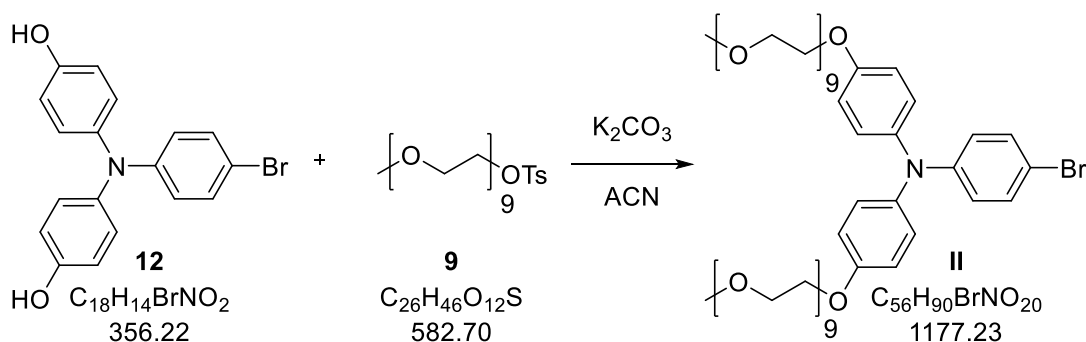
The synthesis towards **12** was performed according to Cardolaccia.^[76]

In a dry flask **11** (1.921 g, 5.0 mmol, 1.0 eq.) was dissolved in anh. degassed DCM (15 ml) under argon atmosphere. At -78 °C BBr₃ (1 M in DCM; 10.0 ml, 10.0 mmol, 2.0 eq.) was added dropwise *via* a dropping funnel. The green reaction mixture was slowly warmed to RT overnight. After TLC (10 % acetone

in DCM) showed full conversion the mixture was degassed with argon for 30 min. Subsequently H₂O (50 ml) was added, the layers were separated, and the aqueous layer was extracted with EE (3x). The combined EE layers were dried over Na₂SO₄ and after the solvent was removed under reduced pressure to obtain **12** (1.665 g, 94 %) as a black solid.

¹H-NMR (400 MHz, (CD₃)₂CO, FID GEP091#10): δ = 8.29 (s, 2H), 7.25 (d, J = 9.0 Hz, 2H), 6.98 (d, J = 8.8 Hz, 4H), 6.82 (d, J = 8.8 Hz, 4H), 6.70 (d, J = 8.9 Hz, 2H) ppm.

4-Bromo-*N,N*-bis(4-(3,6,9,12,15,18,21,24,27-nonaoxaococos-1-yloxy)phenyl)aniline



The synthesis of **II** was adapted from Liu.^[79]

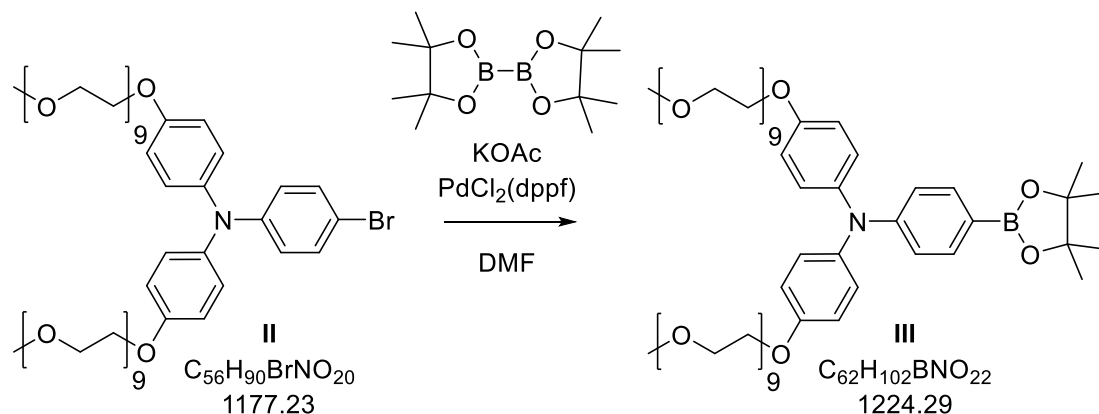
12 (1.425 g, 4.0 mmol, 1.0 eq.), **9** (5.365 g, 9.2 mmol, 2.3 eq.) and K₂CO₃ (2.230 g, 16.0 mmol, 4.0 eq.) were refluxed in anhydrous ACN (50 ml) overnight. After TLC showed full conversion the solvent was removed in *vacuo* and the residue was partitioned between EE and H₂O. The organic layer was washed with H₂O (2x) and brine (1x), dried over Na₂SO₄ and concentrated under reduced pressure. A brown oil (3.945 g, 84 %) was obtained.

¹H-NMR (600 MHz, CDCl₃, FID GEP063#70): δ = 7.23 (d, J = 9.0 Hz, 2H), 6.99 (d, J = 9.0 Hz, 4H), 6.82 (d, J = 9.0 Hz, 4H), 6.78 (d, J = 8.9 Hz, 2H), 4.15 – 3.99 (m, 4H), 3.93 – 3.79 (m, 4H), 3.78 – 3.69 (m, 4H), 3.68 – 3.62 (m, 56H), 3.57 – 3.50 (m, 4H), 3.37 (s, 6H) ppm.

¹³C-NMR (150 MHz, CDCl₃, FID GEP063#71): δ = 155.4, 148.0, 140.9, 131.9, 126.6, 122.3, 115.7, 112.6, 72.1, 71.0, 70.8 – 70.7 (m), 70.7, 69.9, 67.8, 59.2 ppm.

HRMS (ESI) Calcd for C₅₆H₉₀BrNO₂₀K⁺ ([M+K]): 1214.4871, found: 1214.4852.

***N,N*-Bis(4-(3,6,9,12,15,18,21,24,27-nonaoxaocacos-1-yloxy)phenyl)-4-(4,4,5,5-tetramethyl-1,3,2-dioxaborolan-2-yl)aniline**



The borylation of **II** was performed according to Ishiyama.^[72]

The brominated precursor **II** (2.353 g, 2.0 mmol, 1.0 eq.), bis(pinacolato)diboron (0.561 g, 2.2 mmol, 1.1 eq.), KOAc (0.592 g, 6.0 mmol, 3.0 eq.) and Pd(dppf)Cl₂ (44 mg, 60 μmol, 3 mol%) were dissolved in dry DMF (30 ml) under argon atmosphere. The mixture was heated to 90 °C for 23 h. Subsequently the cooled mixture was poured on H₂O and extracted with DCM three times. Then the combined organic layers were dried over Na₂SO₄ and the solvents were removed in HV. **III** was isolated as a black oil (2.083 g, 85 %) after flash chromatography (10 % MeOH in DCM).

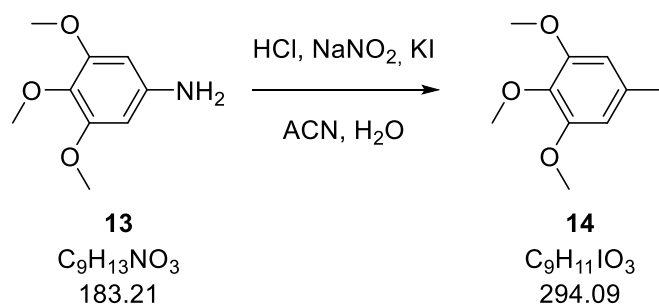
¹H-NMR (600 MHz, CDCl₃, FID GEP077#50): δ = 7.58 (d, *J* = 8.6 Hz, 2H), 7.02 (d, *J* = 8.9 Hz, 4H), 6.92 – 6.75 (m, 6H), 4.10 – 4.09 (m, 4H), 3.89 – 3.80 (m, 4H), 3.73 – 3.71 (m, 4H), 3.69 – 3.58 (m, 56H), 3.57 – 3.49 (m, 4H), 3.37 (s, 6H), 1.31 (s, 12H) ppm.

¹³C-NMR (150 MHz, CDCl₃, FID GEP077#51): δ = 155.3, 151.3, 140.5, 135.7, 126.9, 126.2, 118.7, 115.4, 83.3, 71.9, 70.8, 70.6 – 70.5 (m), 69.7, 67.6, 59.0, 24.8 ppm.

HRMS (ESI) Calcd for C₆₂H₁₀₂BNO₂₂K⁺ ([M+K]): 1262.6618, found: 1262.6618; Calcd for C₆₂H₁₀₂BNO₂₂Na⁺ ([M+Na]): 1246.6879, found: 1246.6905.

D.3.1.3 Multiple PEG-Approach

5-Iodo-1,2,3-trimethoxybenzene

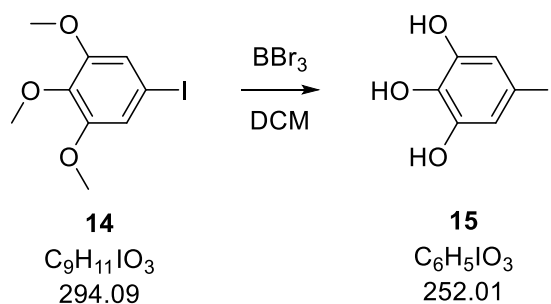


14 was synthesized analogous to Han.^[75]

Amine **13** (10.99 g, 60 mmol, 1.0 eq.) was dissolved in ACN (170 ml) and cooled to 0 °C. A mixture of conc. HCl/ACN (3/2; 60 ml) was added dropwise and the mixture was stirred for 20 min at 0 °C. Subsequently NaNO₂ (4.97 g, 72 mmol, 1.2 eq.) dissolved in H₂O (40 ml) was added dropwise and the mixture was stirred at 0 °C for 1 h. Then KI (29.88 g, 180 mmol, 3.0 eq.) dissolved in H₂O (60 ml) was added dropwise and the mixture was slowly warmed to RT, where it was stirred overnight. The reaction mixture was quenched by pouring it on a Na₂S₂O₃-solution and stirring it for 15 min. Subsequently the suspension was filtered, and the residue was washed with water vigorously. A light pink solid (16.55 g, 94 %) was obtained.

¹H-NMR (200 MHz, CDCl₃, FID GEP069#10): δ = 6.88 (s, 2H), 3.83 (s, 6H), 3.81 (s, 3H) ppm.

5-iodobenzene-1,2,3-triol



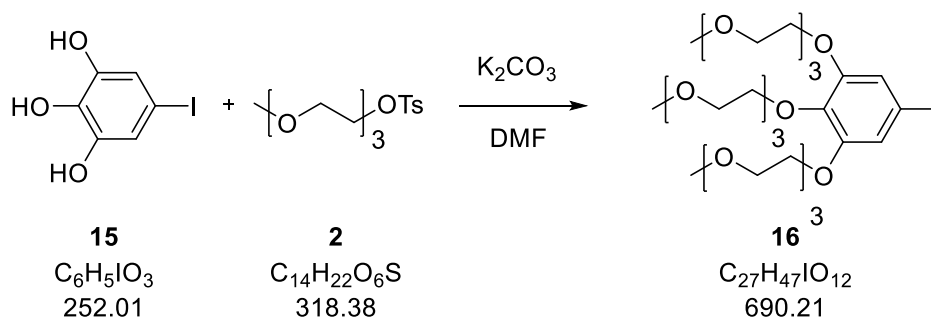
The synthesis of **15** followed the protocol of Cardolaccia.^[76]

In a dry flask under argon atmosphere **14** (2.060 g, 7.0 mmol, 1.0 eq.) was dissolved in anh. DCM (15 ml). The light-red solution was cooled to -78 °C before BBr₃ (1 M solution in DCM; 21.0 ml, 21.0 mmol, 3.0 eq.) was added dropwise. The reaction mixture was allowed to warm to RT slowly and it was stirred overnight. The mixture was quenched with ice water (15 ml) carefully and stirred for 30 min. The aqueous layer was then extracted with EE (3x) and the combined organic layers were

washed with Na₂SO₃-solution, dried over Na₂SO₄ and concentrated under reduced pressure. The product (0.934 g, 53 %) was obtained as a grey powder after purification by digestion in CHCl₃.

¹H-NMR (400 MHz, CD₃OD, FID GEP035#20): δ = 6.64 (s, 2H), 4.86 (s, 3H) ppm.

5-Iodo-1,2,3-tris(2-(2-(2-methoxyethoxy)ethoxy)ethoxy)benzene



16 was synthesized according to Liang.^[77]

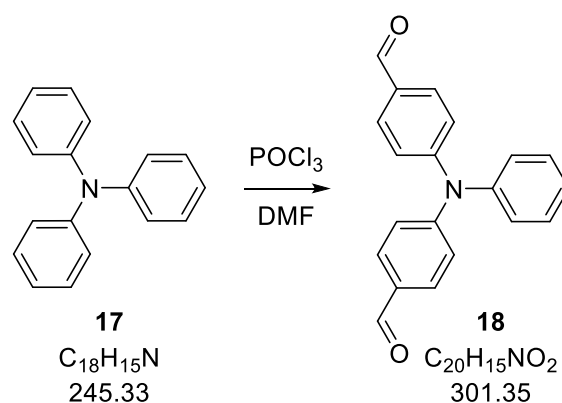
Triol **15** (0.889 g, 3.5 mmol, 1.0 eq.) was dissolved in anh. DMF (18 ml) under argon atmosphere and K₂CO₃ (5.780 g, 42.0 mmol, 12.0 eq.) was added. The mixture was heated to 100 °C and stirred for 20 min before **2** (4.470 g, 14.0 mmol, 4.0 eq.) was added slowly. The temperature was kept at 100 °C for 24 h. Then the solvent was removed in HV and the residue was taken up in EE (100 ml). The organic layer was washed with H₂O (3x20 ml), dried over Na₂SO₄ and concentrated in *vacuo*. After repeated purification *via* MPLC (90 g SiO₂, 90 g SiO₂, 3 % MeOH in DCM) a yellow oil (1.010 g, 42 %) was obtained.

¹H-NMR (400 MHz, CDCl₃, FID GEP036#50): δ = 6.90 (s, 2H), 4.16 – 4.06 (m, 6H), 3.89 – 3.79 (m, 3H), 3.79 – 3.74 (m, 3H), 3.73 – 3.68 (m, 6H), 3.67 – 3.61 (m, 12H), 3.59 – 3.50 (m, 6H), 3.37 (s, 6H), 3.37 (s, 3H) ppm.

¹³C-NMR (100 MHz, CDCl₃, FID GEP036#51): δ = 153.4, 138.8, 117.5, 85.7, 72.3, 72.0, 70.9, 70.8 – 70.7 (m), 70.6, 70.6 – 70.5 (m), 69.7, 69.1, 59.1, 59.0 ppm.

D.3.1.4 Carboxylic Acid-substituted Triphenylamine Cap-System

4,4'-(Phenylimino)bisbenzaldehyde

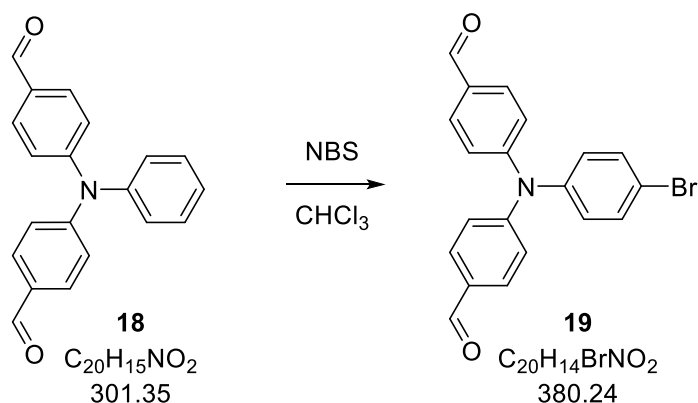


The synthesis towards **18** was performed as described by Ghosh.^[80]

17 (19.63 g, 80 mmol, 1 eq.) was dissolved in anh. DMF (166 ml) and cooled to 0 °C under argon atmosphere. Then POCl₃ (184.08 g, 1200 mmol, 15 eq.) was added dropwise *via* a dropping funnel, while keeping the temperature below 5 °C. After complete addition the reaction mixture was slowly heated to 100 °C and stirred overnight. After GCMS showed full conversion the mixture was hydrolyzed with H₂O and neutralized with 2 M NaOH carefully. The mixture was extracted with DCM several times. The combined organic layers were dried over Na₂SO₄, concentrated in *vacuo* and dried in HV. The crude product was purified by column chromatography (360 g SiO₂, toluene/CHCl₃/Et₂O; 20/1/1) yielding a yellow solid (11.88 g, 49 %).

¹H-NMR (200 MHz, CDCl₃, FID LUJ006#110): δ = 9.89 (s, 2H), 7.78 (d, J = 8.8 Hz, 2H), 7.49 – 7.32 (m, 2H), 7.32 – 7.04 (m, 7H) ppm.

4,4'-[(4-Bromophenyl)imino]bisbenzaldehyde

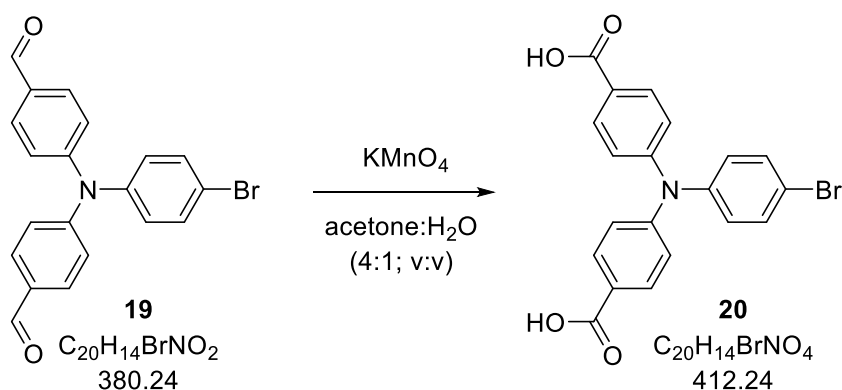


The synthesis of **19** followed the protocol of Ghosh.^[80]

18 (3.020 g, 10.0 mmol, 1.0 eq.) was dissolved in CHCl₃ (150 ml) under argon atmosphere. NBS (1.960 g, 11.0 mmol, 1.1 eq.) was added and the mixture was refluxed overnight. After GCMS showed full conversion the mixture was washed with 2 M NaOH. The aqueous layer was extracted with CHCl₃ (2x) and the combined organic layers were dried over Na₂SO₄ and concentrated in *vacuo*. A yellow solid was obtained (3.899 g, quant.).

¹H-NMR (400 MHz, CDCl₃, FID GEP037#10): δ = 9.91 (s, 2H), 7.79 (d, J = 8.8 Hz, 4H), 7.50 (d, J = 8.8 Hz, 2H), 7.18 (d, J = 8.5 Hz, 4H), 7.05 (d, J = 8.8 Hz, 2H) ppm.

4,4'-[(4-Bromophenyl)imino]bisbenzoic acid

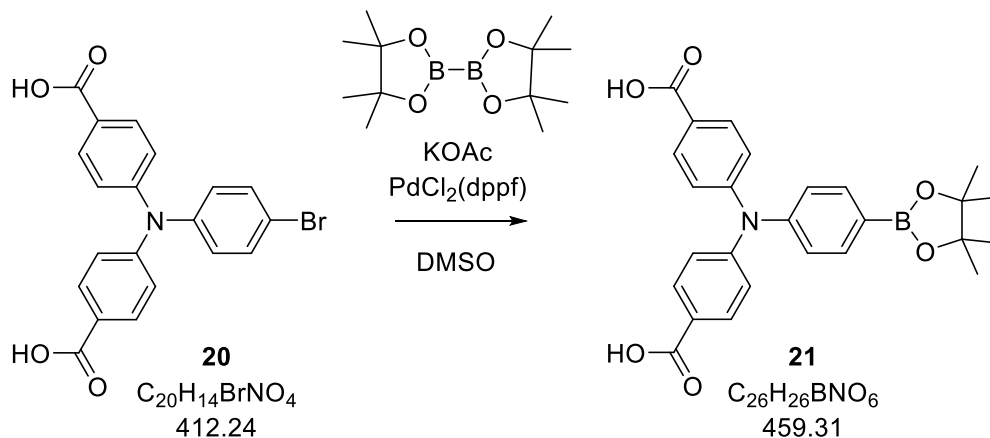


The synthesis of **20** was performed as described in the protocol of Ghosh.^[80]

19 (1.901 g, 5.0 mmol, 1.0 eq.) was heated to 60 °C in a mixture of acetone/H₂O (4/1). Then KMnO₄ (3.953 g, 25.0 mmol, 5.0 eq.) was added in 4 portions and the reaction mixture was stirred at 60 °C overnight. After TLC showed full conversion acetone was removed under reduced pressure and H₂O (50 ml) was added. The mixture was filtered (por 4) and acidified with HCl. The precipitating off-white solid was filtered off, washed with H₂O and dried in HV (1.617 g, 78 %).

$^1\text{H-NMR}$ (400 MHz, DMSO, FID GEP039#10): δ = 12.75 (bs, 2H), 7.87 (d, J = 8.8 Hz, 4H), 7.58 (d, J = 8.8 Hz, 2H), 7.17 – 7.00 (m, 6H) ppm.

4,4'-[(4-(4,4,5,5-Tetramethyl-1,3,2-dioxaborolan-2-yl)phenyl)imino]bisbenzoic acid



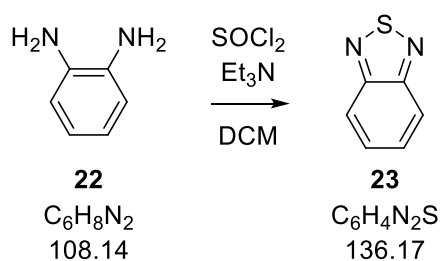
21 was synthesized following the protocol of Wood.^[81]

20 (1.237 g, 3.00 mmol, 1.0 eq.), bis(pinacolato)diboron (0.801 g, 3.15 mmol, 1.05 eq.), KOAc (0.883 g, 9.00 mmol, 3.0 eq.) and Pd(dppf)Cl₂ (123 mg, 0.17 mmol, 5 mol%) were dissolved in anhydrous DMSO (35 ml) under argon atmosphere. The mixture was heated to 80 °C for 22 h. Then DCM (200 ml) was added to the cooled mixture and the organic layer was washed with H₂O (4x50 ml). After the organic layer was dried over Na₂SO₄ and concentrated in *vacuo*, the crude product was purified by digestion in DCM (30 ml) (0.606 g, 44 %).

$^1\text{H-NMR}$ (400 MHz, DMSO, FID GEP044#10): δ = 12.74 (bs, 2H), 7.87 (d, J = 8.8 Hz, 4H), 7.67 (d, J = 8.5 Hz, 2H), 7.21 – 6.96 (m, 6H), 1.29 (s, 12H) ppm.

D.3.1.5 Linker Synthesis

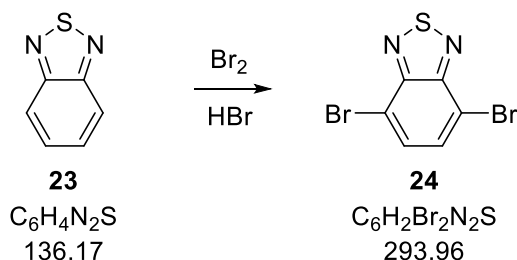
Benzo[c][1,2,5]thiadiazole



The reaction towards **23** was performed according to Zhang.^[83]

Diamine **22** (10.01 g, 92.6 mmol, 1.00 eq.) was dissolved in CH_2Cl_2 (300 ml) and Et_3N (51.5 ml, 369.5 mmol, 4.00 eq.) was added. Under an argon atmosphere and ice bath cooling $SOCl_2$ (11.60 g, 97.5 mmol, 1.05 eq.) was added within 1 h. The solution changed its color after every drop of $SOCl_2$ to red and loses the color shortly after. White solid formed after 30 min. Subsequently the reaction mixture was heated to reflux for 4 h. The next day GCMS still showed starting material, so $SOCl_2$ (5.90 g, 49.6 mmol, 0.53 eq.) was added under ice bath cooling. Afterwards the mixture was heated to reflux for 5 h. The next day GCMS showed complete conversion. The solvent was removed in *vacuo* and the residue was taken up in H_2O (700 ml). The pH-value was adjusted with conc. HCl to 2 and the aqueous phase was extracted 3 times with 100 ml CH_2Cl_2 . The organic layers were combined, dried over Na_2SO_4 and the solvent was removed in *vacuo*. 10.54 g brownish crude product was obtained. The solid was dissolved in CH_2Cl_2 and stirred with activated carbon for 15 min. The suspension was filtered over Celite and the solvent of the now clear yellow solution was removed in *vacuo*. An orange solid was obtained (9.44 g, 75 %).

1H -NMR (400 MHz, $CDCl_3$, FID GEP001#30): δ = 8.01 (dd, J_1 = 6.8 Hz, J_2 = 3.2 Hz, 2H), 7.59 (dd, J_1 = 6.7 Hz, J_2 = 3.2 Hz, 2H) ppm.

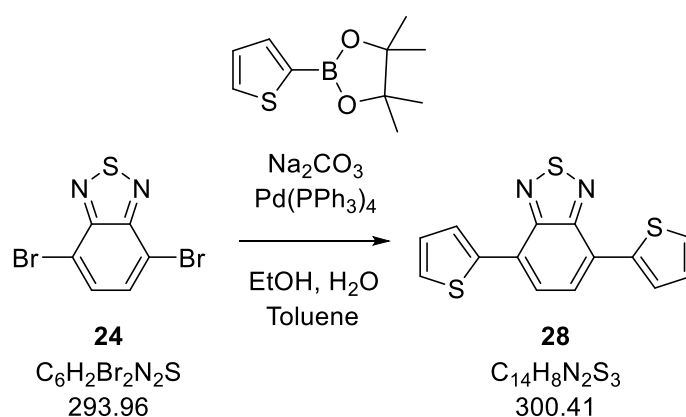
4,7-Dibromobenzo[*c*][1,2,5]thiadiazole

The synthesis towards **24** followed a procedure described by Mancilha.^[84]

Thiadiazole **23** (9.40 g, 69 mmol, 1.0 eq.) was suspended in aqueous HBr (150 ml, 48 %) and Br_2 (33.09 g, 207 mmol, 3 eq.) dissolved in aqueous HBr (100 ml, 48 %) was added dropwise carefully. Another 50 ml of aqueous HBr (48 %) were added, after a lot of solid precipitated at the beginning of the Br_2 addition. The reaction mixture was then heated to reflux until GCMS showed no more starting material or intermediate to be present. The reaction was quenched with an aqueous $Na_2S_2O_3$ solution, filtered and washed with water and cold Et_2O . The dried crude product was further purified by flash-chromatography (pure PE). Off-white needles were obtained after recrystallization from $CHCl_3$ (9.74 g, 48 %).

1H -NMR (600 MHz, $CDCl_3$, FID GEP003#140): δ = 7.71 (s, 2H) ppm.

^{13}C -NMR (150 MHz, $CDCl_3$, FID GEP003#141): δ = 152.9, 132.3, 113.9 ppm.

4,7-Di(thiophen-2-yl)benzo[*c*][1,2,5]thiadiazole

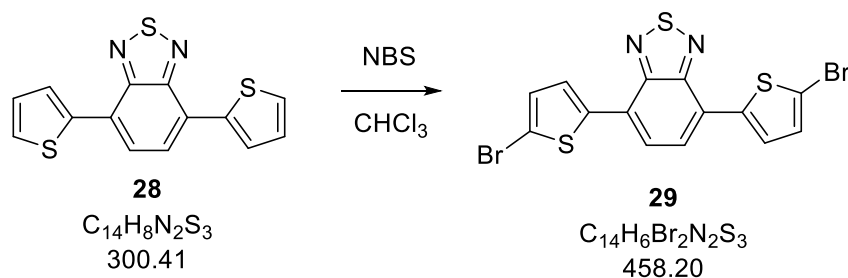
The following synthesis was performed analogous to Kato.^[89]

Thiadiazole **24** (2.060 g, 7.0 mmol, 1.0 eq.) and $Pd(PPh_3)_4$ (0.526 g, 0.5 mmol, 6.5 mol%) were dissolved in toluene (70 ml) and heated to 55 °C. Then thiophene-2-boronic acid pinacol ester (4.702 g, 22.4 mmol, 3.2 eq.) dissolved in EtOH and 2 M Na_2CO_3 (35.0 ml, 70.0 mmol, 10.0 eq.) were added and the temperature was raised to reflux. After TLC showed full conversion (24 h), all solvents were

removed under reduced pressure and the residue was distributed between DCM and H₂O. The organic layer was washed with water (2x), dried over Na₂SO₄ and concentrated in *vacuo*. Further purification was done *via* flash chromatography (PE/DCM; 1/4). **28** was obtained as a fluorescent orange solid (1.992 g, 95 %).

¹H-NMR (200 MHz, CDCl₃, FID GEP060#20): δ = 8.12 (d, J = 3.7 Hz, 2H), 7.88 (d, J = 0.6 Hz, 2H), 7.46 (d, J = 5.1 Hz, 2H), 7.22 (ddd, J₁ = 5.1 Hz, J₂ = 3.7 Hz, J₃ = 0.6 Hz, 2H) ppm.

4,7-Bis(5-bromothiophen-2-yl)benzo[c][1,2,5]thiadiazole

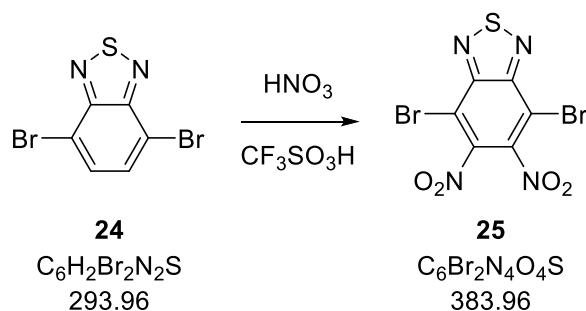


The synthesis of **29** followed a procedure described by Kato.^[89]

Thiadiazole **28** (1.992 g, 6.6 mmol, 1.0 eq.) and NBS (2.479 g, 13.9 mmol, 2.1 eq.) were dissolved in CHCl₃ (120 ml) and stirred at RT for 48 h. During the reaction a red solid precipitated, which was then filtered off, washed with H₂O, MeOH and CHCl₃ and dried in *vacuo* (2.866 g, 95 % crude). A small sample was successfully purified by column chromatography (2 % Et₂O in PE).

¹H-NMR (600 MHz, CDCl₃, FID GEP065#90): δ = 7.81 (d, J = 4.0 Hz, 2H), 7.80 (s, 2H), 7.16 (d, J = 4.0 Hz, 2H) ppm.

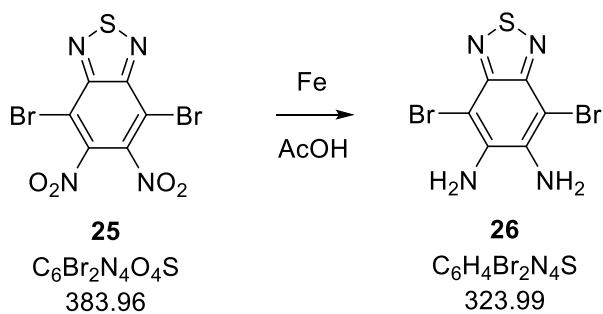
¹³C-NMR (150 MHz, CDCl₃, FID GEP065#91): δ = 152.2, 140.5, 130.8, 127.3, 125.4, 125.1, 114.8 ppm.

4,7-Dibromo-5,6-dinitrobenzo[*c*][1,2,5]thiadiazole

The synthesis of **25** was adopted from the protocol described by Hassan.^[85]

Fuming triflic acid (15 ml, excess) was cooled to 0 °C and **24** (0.955 g, 3.25 mmol) was added in several portions. Subsequently fuming HNO₃ (15 ml, excess) was added slowly dropwise. The suspension was allowed to warm to RT and stirred overnight. After TLC confirmed full conversion the mixture was poured on ice and the precipitate was filtered off. It was washed with water and dried in *vacuo*. The desired product was obtained as a slightly yellow powder (1.111 g, 89 %).

¹³C-NMR (150 MHz, CDCl₃, FID GEP098#11): δ = 151.4, 144.9, 110.3 ppm.

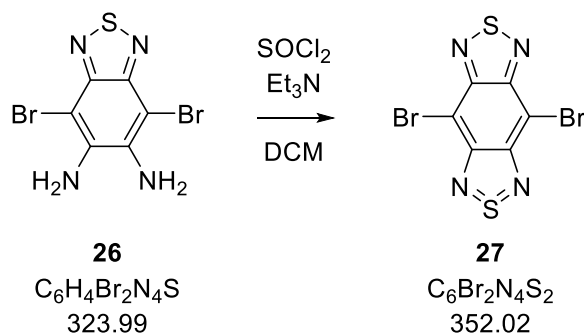
4,7-Dibromobenzo[*c*][1,2,5]thiadiazole-5,6-diamine

The following procedure was adapted from Tsubata.^[86]

Thiadiazole **25** (1.508 g, 3.9 mmol, 1 eq.) was heated to 100 °C in AcOH (20 ml). Then iron (2.630 g, 47.1 mmol, 12 eq.) was added in 4 portions over 10 min. After 1.5 h EtOH (5 ml) was added and the mixture was further heated for 1 h (GCMS showed full conversion). The cooled suspension was filtered and washed with H₂O. Flash chromatography (PE/EE; 1/1) and a subsequent soxhlet-extraction (EE) of the used SiO₂ yielded **26** as a yellow solid (0.715 g, 54 %).

¹³C-NMR (150 MHz, CDCl₃, FID GEP026#21): δ = 147.8, 140.0, 88.5 ppm.

4,8-Dibromobenzo(1,2-*c*;4,5-*c'*)bis(1,2,5)thiadiazole



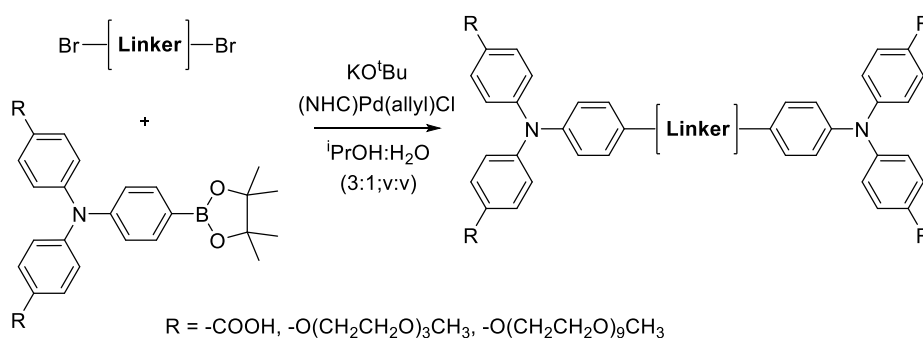
27 was synthesized as described in the protocol by Murali.^[87]

26 (0.387 g, 1.2 mmol, 1 eq.) and Et_3N (0.7 ml, 5.0 mmol, 4 eq.) were suspended in anh. DCM (10 ml) under argon atmosphere. Then $SOCl_2$ (0.328 g, 2.8 mmol, 2 eq.) was added slowly dropwise. Subsequently the mixture was refluxed until GCMS and TLC showed full conversion (5.5 h). The suspension was poured on ice and acidified with HCl. The precipitate was filtered off and dried under reduced pressure obtaining a dark-red solid (0.305 g, crude 72 %). Further purification was achieved by flash-chromatography (pure DCM).

27 was characterized by x-ray crystallography of single crystals grown out of a sat. $CHCl_3$ -solution covered with an EtOH-layer.

D.3.1.6 Synthesis of Target Compounds

General Procedure: Suzuki Couplings Towards Target Compounds

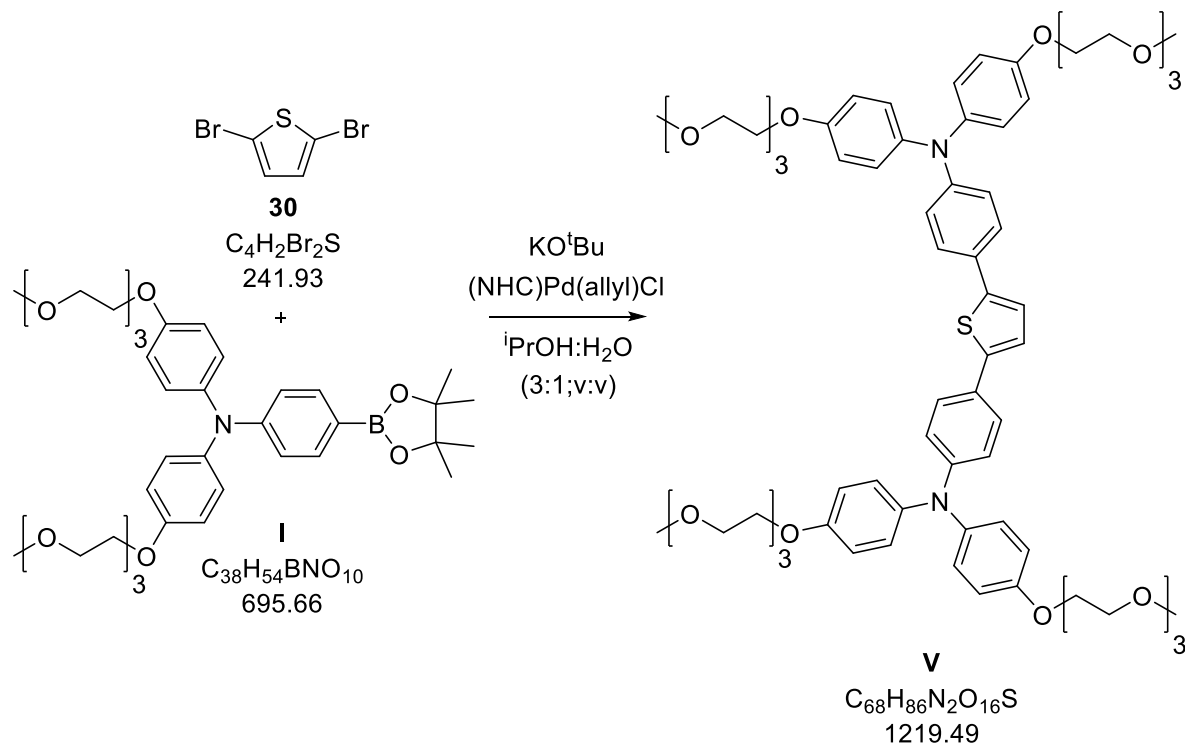


(NHC)Pd(allyl)Cl catalyzed Suzuki-coupling reactions were performed according to Marion.^[100]

To a suspension of the linker (1.0 eq.), the boronic ester (2.3 – 2.5 eq.) and KO^tBu (3.0 eq., $R = -COOH$: 7.0 eq.) in a mixture of degassed $iPrOH:H_2O$ (3:1) under argon atmosphere (NHC)Pd(allyl)Cl (2 mol%)

was added. The reaction mixture was refluxed until TLC showed full conversion (2 h). The work-up and purification was performed as stated in the detailed descriptions.

4,4'-(Thiophene-2,5-diyl)bis(*N,N*-bis(4-(2-(2-(2-methoxyethoxy)ethoxy)ethoxy)phenyl)aniline)



The synthesis of **V** was performed as described in the general procedure.

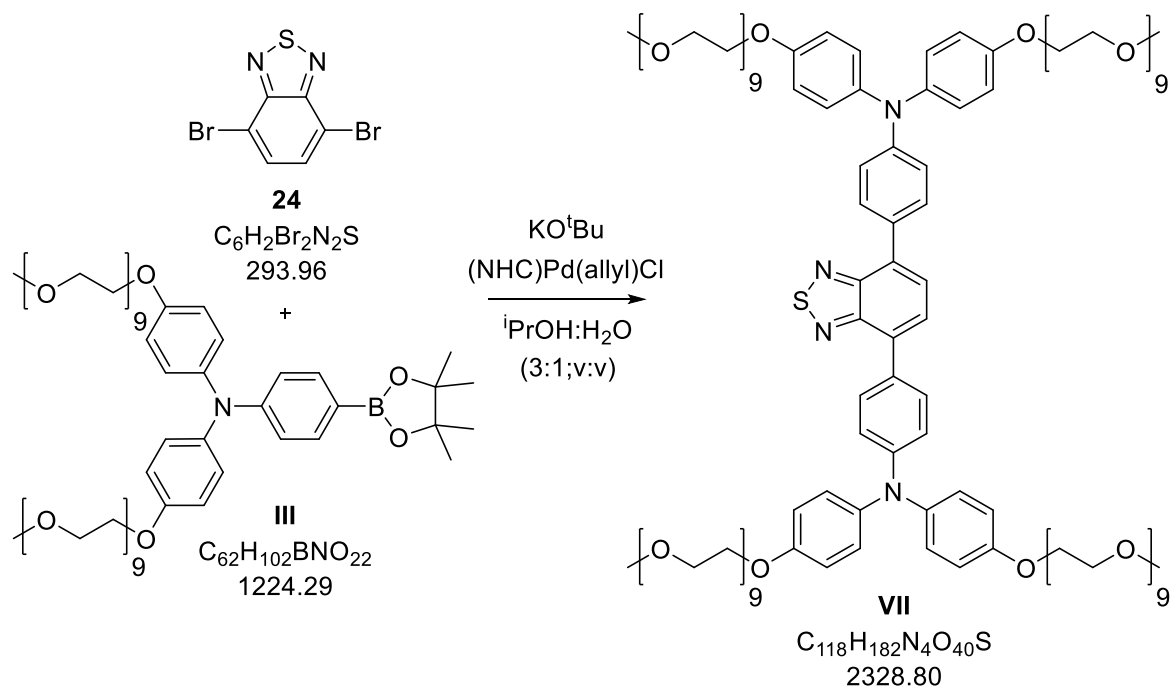
I (100 mg, 144 μ mol, 2.05 eq.), **30** (17 mg, 70 μ mol, 1.00 eq.), KO^tBu (21 mg, 187 μ mol, 2.70 eq.) and $(NHC)Pd(allyl)Cl$ (2 mg, 3 μ mol, 5 mol%) were refluxed in a mixture of degassed $iPrOH:H_2O$ (3:1, 2 ml) for 2 h. The reaction mixture was partitioned between DCM and H_2O and the aqueous layer was extracted with DCM (3x). The combined organic layers were dried over Na_2SO_4 and concentrated in *vacuo*. A yellow-green oil (34 mg, 40 %) was provided after column chromatography (9 g SiO_2 , 3 % MeOH in DCM).

1H -NMR (600 MHz, CD_3OD , FID GEP028#100): δ = 7.37 (d, J = 8.8 Hz, 4H), 7.11 (s, 2H), 6.98 (d, J = 9.0 Hz, 8H), 6.86 (d, J = 9.0 Hz, 8H), 6.82 (d, J = 8.8 Hz, 4H), 4.13 – 4.00 (m, 8H), 3.87 – 3.75 (m, 8H), 3.72 – 3.65 (m, 8H), 3.64 – 3.56 (m, 16H), 3.54 – 3.47 (m, 8H), 3.32 (s, 12H) ppm.

^{13}C -NMR (150 MHz, CD_3OD , FID GEP028#101): δ = 156.8, 149.5, 143.6, 142.2, 128.1, 127.7, 127.0, 123.8, 121.8, 116.7, 73.0, 71.8, 71.6, 71.40, 70.9, 68.9, 59.1 ppm.

HRMS (ESI) Calcd for $C_{68}H_{87}N_2O_{16}S^+$ ([M+H]): 1219.5771, found: 1219.5786; Calcd for $C_{68}H_{86}N_2O_{16}SNa^+$ ([M+Na]): 1241.5590, found: 1241.5616; Calcd for $C_{68}H_{86}N_2O_{16}SK^+$ ([M+K]): 1257.5330, found: 1257.5354.

4,4'-(Benzo[c][1,2,5]thiadiazole-4,7-diyl)bis(*N,N*-bis(4-(3,6,9,12,15,18,21,24,27-nonaoxaoctacos-1-yloxy)phenyl)aniline)



The synthesis of **VII** was performed as described in the general procedure.

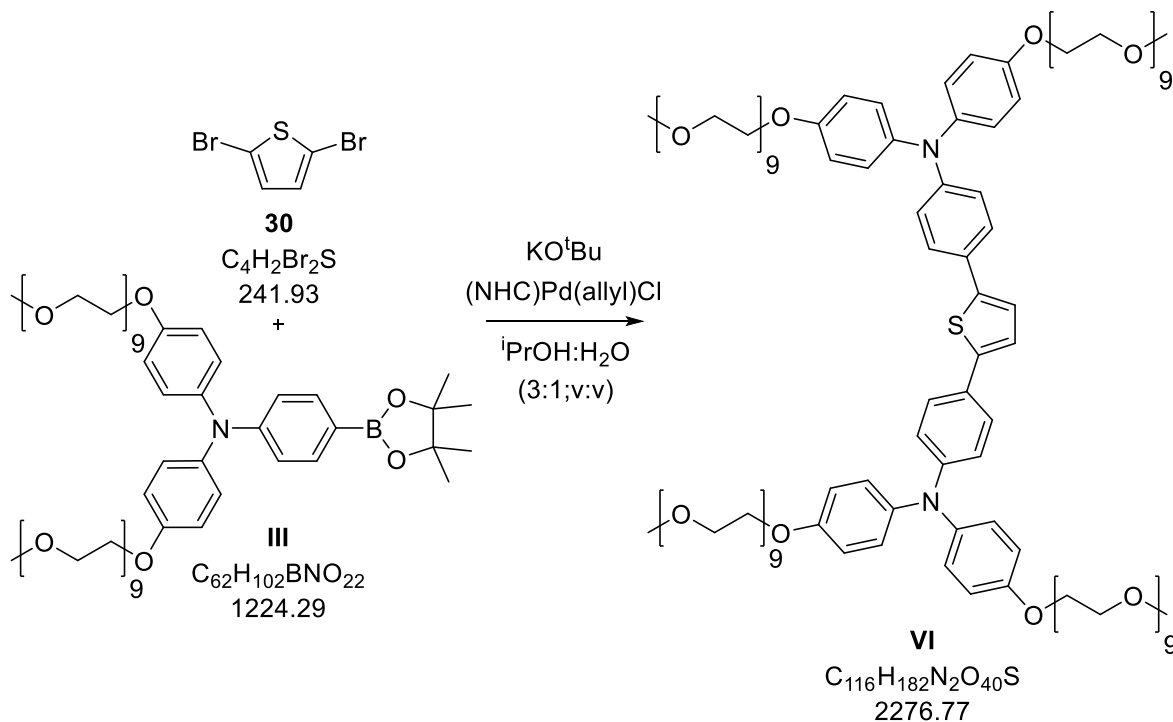
III (563 mg, 0.46 mmol, 2.3 eq.), **24** (59 mg, 0.2 mmol, 1.00 eq.), KO^tBu (67 mg, 0.6 mmol, 3.0 eq.) and (NHC)Pd(allyl)Cl (2 mg, 4 μmol, 2 mol%) were refluxed in a mixture of degassed ⁱPrOH:H₂O (3:1, 8 ml) for 2 h. The solvents were removed in *vacuo* and the residue was subjected to flash chromatography (10 % MeOH in DCM) before prep. HPLC (82 % MeOH in H₂O) yielded a red oil (73 mg, 16 %).

¹H-NMR (600 MHz, (CD₃)₂CO, FID GEP085#20): δ = 7.94 (d, J = 8.8 Hz, 4H), 7.85 (s, 2H), 7.16 – 7.10 (m, 8H), 7.02 – 6.96 (m, 12H), 4.21 – 4.09 (m, 8H), 3.90 – 3.76 (m, 8H), 3.72 – 3.65 (m, 8H), 3.65 – 3.50 (m, 112H), 3.48 – 3.42 (m, 8H), 3.27 (s, 12H) ppm.

¹³C-NMR (150 MHz, (CD₃)₂CO, FID GEP085#21): δ = 156.8, 155.0, 149.9, 141.4, 132.6, 130.7, 129.8, 128.0, 127.9, 120.1, 116.5, 72.7, 71.5, 71.3, 71.3 – 71.2 (m), 71.1, 70.40, 68.7, 58.8 ppm.

HRMS (ESI) Calcd for C₁₁₈H₁₈₅N₄O₄₀S³⁺ ([M+3H]): 776.7423, found: 776.7437.

4,4'-(Thiophene-2,5-diyl)bis(*N,N*-bis(4-(3,6,9,12,15,18,21,24,27-nonaoxaocacos-1-yloxy)phenyl)aniline)



The synthesis of **VI** was performed as described in the general procedure.

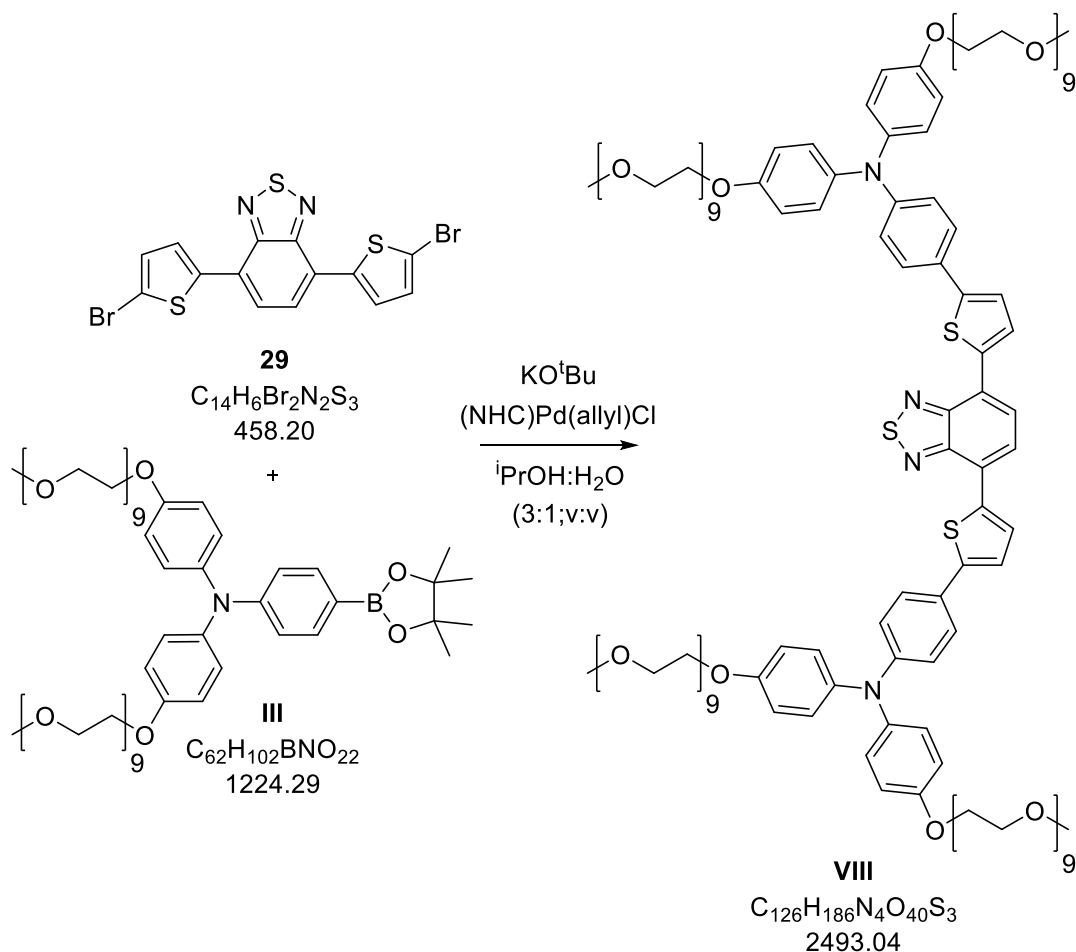
III (704 mg, 575 μ mol, 2.3 eq.), **30** (60 mg, 250 μ mol, 1.00 eq.), KO^tBu (85 mg, 750 μ mol, 3.0 eq.) and $(NHC)Pd(allyl)Cl$ (3 mg, 5 μ mol, 2 mol%) were refluxed in a mixture of degassed $iPrOH:H_2O$ (3:1, 10 ml) for 2 h. The solvents were removed in *vacuo* and the residue was subjected to flash chromatography (10 % MeOH in DCM) before prep. HPLC (82 % MeOH in H_2O) yielded a yellow-green oil (119 mg, 21 %).

1H -NMR (600 MHz, $(CD_3)_2CO$, FID GEP082#40): δ = 7.49 (d, J = 8.8 Hz, 4H), 7.26 (s, 2H), 7.07 (d, J = 8.9 Hz, 8H), 6.95 (d, J = 9.0 Hz, 8H), 6.88 (d, J = 8.8 Hz, 4H), 4.19 – 4.00 (m, 8H), 3.88 – 3.75 (m, 8H), 3.67 – 3.65 (m, 8H), 3.64 – 3.52 (m, 112H), 3.49 – 3.42 (m, 8H), 3.28 (s, 12H) ppm.

^{13}C -NMR (150 MHz, $(CD_3)_2CO$, FID GEP082#41): δ = 156.7, 149.3, 143.2, 141.5, 127.8, 127.3, 126.9, 123.8, 121.1, 116.5, 72.8, 71.5, 71.4, 71.4 – 71.3 (m), 71.2, 70.5, 68.8, 58.9 ppm.

HRMS (ESI) Calcd for $C_{116}H_{185}N_2O_{40}S^{3+}$ ($[M+3H]$): 759.4069, found: 759.4080.

4,4'-(Benzo[c][1,2,5]thiadiazole-4,7-diylbis(thiophene-5,2-diyl))bis(*N,N*-bis(4-(3,6,9,12,15,18,21,24,27-nonaoxaocacos-1-yloxy)phenyl)aniline)



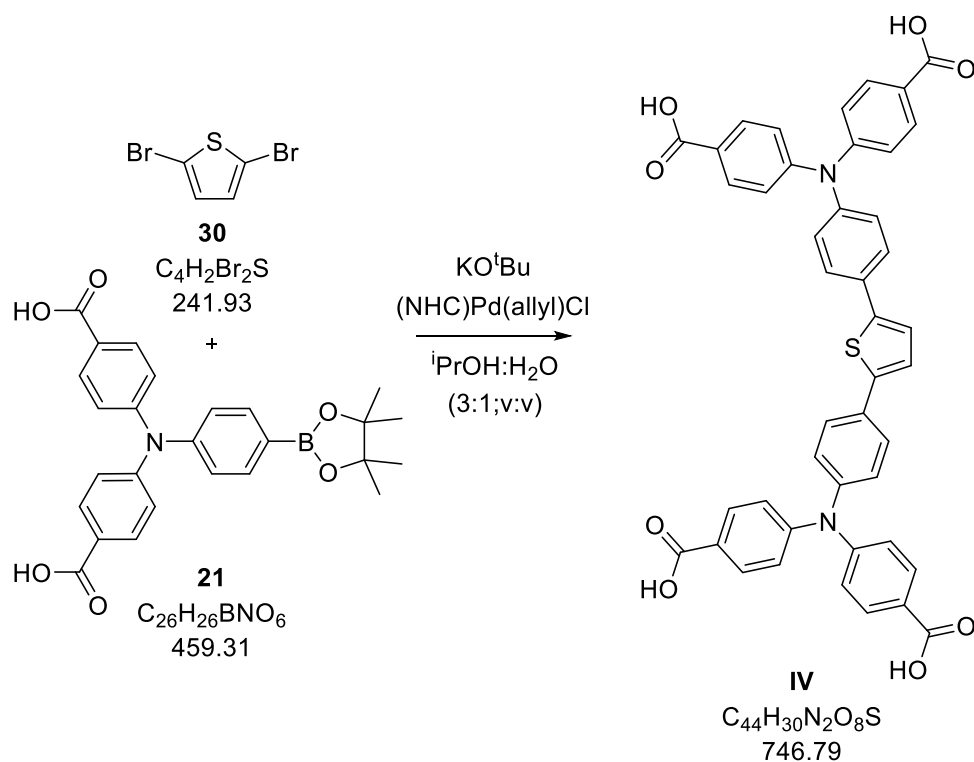
The synthesis of **VIII** was performed as described in the general procedure.

III (830 mg, 0.68 mmol, 2.3 eq.), **29** (136 mg, 0.30 mmol, 1.00 eq.), KO^tBu (101 mg, 0.90 mmol, 3.0 eq.) and $(NHC)Pd(allyl)Cl$ (3 mg, 6 μ mol, 2 mol%) were refluxed in a mixture of degassed $iPrOH:H_2O$ (3:1, 12 ml) for 2 h. The starting material was not fully converted so TPA **III** (184 mg, 0.15 mmol, 0.5 eq.) was added. After reflux overnight the conversion was still incomplete. The solvents were removed in *vacuo* and the residue was subjected to flash chromatography (10 % MeOH in DCM) before prep. HPLC (90 % MeOH in H_2O) yielded a purple oil (104 mg, 14 %).

1H -NMR (600 MHz, $(CD_3)_2CO$, FID GEP096#50): δ = 8.22 (d, J = 3.9 Hz, 2H), 8.06 (s, 2H), 7.62 (d, J = 8.7 Hz, 4H), 7.46 (d, J = 3.9 Hz, 2H), 7.13 (d, J = 8.9 Hz, 8H), 7.00 (d, J = 8.9 Hz, 8H), 6.93 (d, J = 8.8 Hz, 4H), 4.27 – 4.08 (m, 8H), 3.99 – 3.79 (m, 8H), 3.77 – 3.67 (m, 8H), 3.67 – 3.54 (m, 112H), 3.51 – 3.44 (m, 8H), 3.30 (s, 12H) ppm.

^{13}C -NMR (150 MHz, $(CD_3)_2CO$, FID GEP096#21): δ = 155.9, 152.3, 148.9, 145.8, 140.4, 137.0, 128.9, 127.0, 126.3, 125.8, 125.3, 125.1, 122.8, 119.7, 115.6, 71.8, 70.6, 70.5 – 70.2 (m), 70.1, 69.5, 67.8, 57.9 ppm.

HRMS (ESI) Calcd for $C_{126}H_{188}N_4O_{40}S_3^{3+}$ ($[M+3H]$): 831.4008, found: 831.4016.

4,4',4'',4'''-((Thiophene-2,5-diylbis(4,1-phenylene))bis(imino))tetrabenzoic acid

The synthesis of **IV** was performed as described in the general procedure.

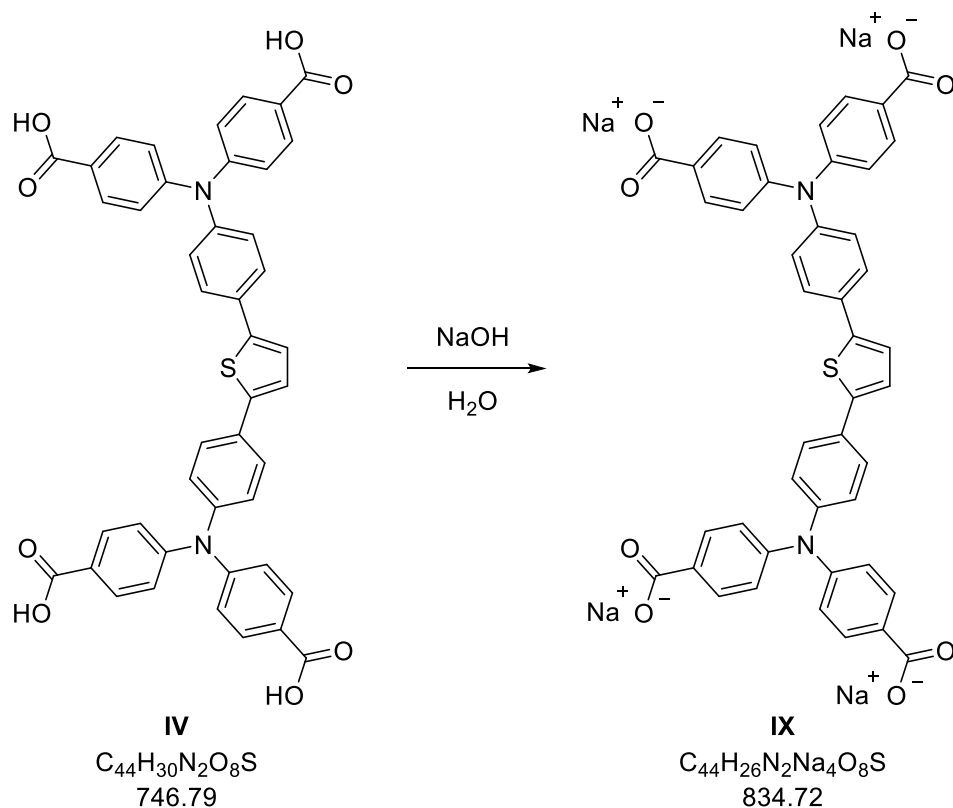
TPA **21** (274 mg, 600 μmol, 2.5 eq.), thiophene **30** (58 mg, 240 μmol, 1.00 eq.), KO^tBu (189 mg, 1.68 mmol, 7.0 eq.) and (NHC)Pd(allyl)Cl (3 mg, 5 μmol, 2 mol%) were refluxed in a mixture of degassed iPrOH:H₂O (3:1, 10 ml) for 2 h. H₂O (15 ml) was added to the cooled mixture and it was acidified with HCl. The mixture was extracted with EE (3x) and the combined organic layers were dried over Na₂SO₄ and concentrated in *vacuo*. A yellow solid (114 mg, 64 %) was obtained after digestion in EE and recrystallization in MeOH/H₂O (1/1).

¹H-NMR (600 MHz, DMSO, FID GEP048#50): δ = 12.73 (s, 4H), 7.88 (d, J = 8.8 Hz, 8H), 7.72 (d, J = 8.6 Hz, 4H), 7.54 (s, 2H), 7.18 (d, J = 8.6 Hz, 4H), 7.12 (d, J = 8.8 Hz, 8H) ppm.

¹³C-NMR (150 MHz, DMSO, FID GEP048#51): δ = 166.8, 150.1, 145.1, 141.8, 131.1, 130.3, 126.8, 126.5, 125.0, 125.0, 122.5 ppm.

HRMS (ESI) Calcd for C₄₄H₃₀N₂O₈S⁺ ([M+H]): 747.1796, found: 747.1794.

Sodium 4,4',4'',4'''-((thiophene-2,5-diylbis(4,1-phenylene))bis(imino))tetrabenzoate



IV (44.8 mg, 60 μmol , 1.0 eq.) was suspended in H_2O (10 ml) and 0.1 M NaOH (2.4 ml, 240 μmol , 4.0 eq.) was added. The solution was filtered and concentrated under reduced pressure. A brown/yellow solid (50 mg, quant.) was obtained.

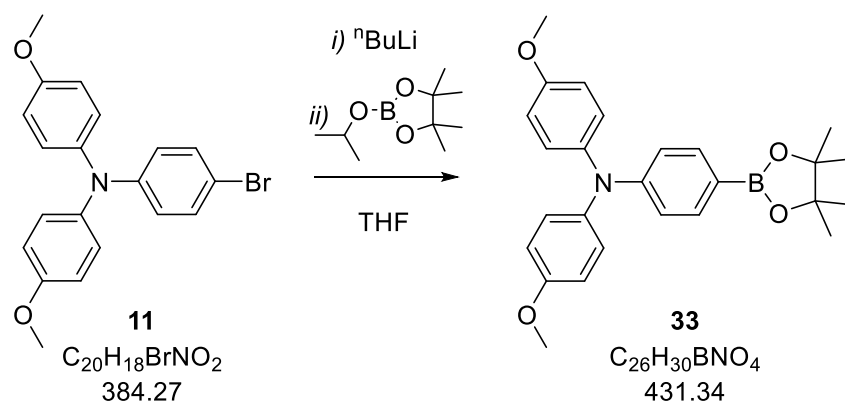
$^1\text{H-NMR}$ (600 MHz, CD_3OD , FID GEP067#30): δ = 7.88 (d, J = 8.7 Hz, 8H), 7.61 (d, J = 8.7 Hz, 4H), 7.32 (s, 2H), 7.11 (d, J = 8.7 Hz, 4H), 7.05 (d, J = 8.7 Hz, 8H) ppm.

$^{13}\text{C-NMR}$ (150 MHz, CD_3OD , FID GEP067#31): δ = 175.0, 150.5, 147.9, 143.9, 133.6, 131.7, 131.1, 127.5, 126.3, 124.9, 123.9 ppm.

HRMS (ESI) Calcd for $\text{C}_{44}\text{H}_{30}\text{N}_2\text{O}_8\text{S}^+$ ($[\text{M}-4\text{Na}+5\text{H}]$): 747.1796, found: 747.1797.

D.3.2 Synthesis of Stoppers/Linkers for Rotaxane Synthesis

N,N-Bis(4-methoxy)phenyl)-4-(4,4,5,5-tetramethyl-1,3,2-dioxaborolan-2-yl)aniline

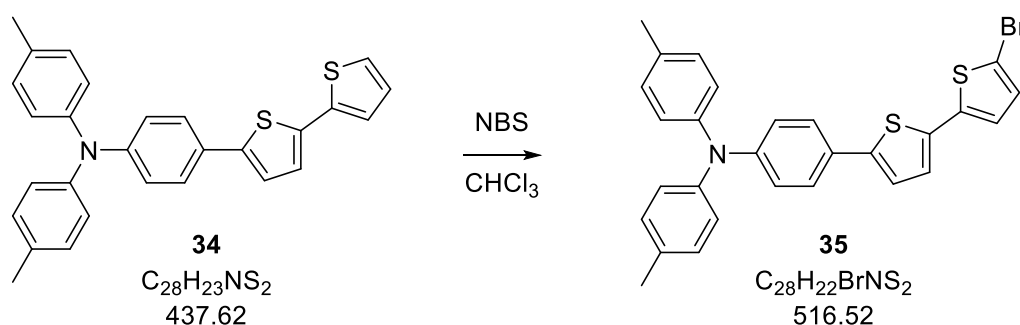


The synthesis of **33** followed a protocol described by Anémian.^[94]

11 (1.921 g, 5.0 mmol, 1.0 eq) was dissolved in anh. THF (25 ml) under argon atmosphere and cooled below $-78\text{ }^{\circ}\text{C}$. To the stirred solution $^n\text{BuLi}$ (2.40 ml, 6.0 mmol, 1.2 eq.; 2.5 M in hexanes) was added dropwise and the reaction mixture was stirred below $-65\text{ }^{\circ}\text{C}$ for 2.5 h before Pinbop® (1.116 g, 6.0 mmol, 1.2 eq.) was added. After warming the solution to RT slowly it was stirred overnight. THF was removed in *vacuo* before the residue was partitioned between DCM and water. The aqueous phase was extracted with DCM (3x). The combined organic layers were dried over Na_2SO_4 followed by evaporation of the solvent in *vacuo*. A white powder (1.435 g, 66 %) was obtained after recrystallization from ACN.

$^1\text{H-NMR}$ (600 MHz, CDCl_3 , FID GEP095#10): δ = 7.60 (d, J = 8.6 Hz, 2H), 7.06 (d, J = 8.9 Hz, 4H), 6.86 (d, J = 8.6 Hz, 2H), 6.86 (d, J = 8.6 Hz, 4H), 3.80 (s, 6H), 1.32 (s, 12H) ppm.

4-(5'-Bromo-[2,2'-bithiophen]-5-yl)-*N,N*-di-(*p*-tolyl)aniline



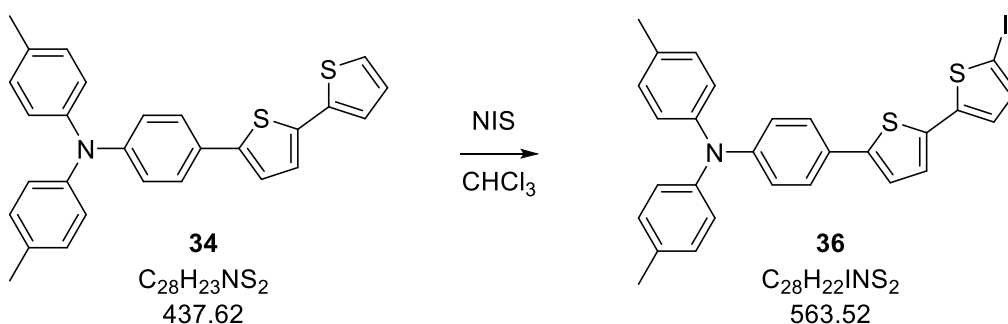
The synthesis of **35** was adapted from the protocol of Leliège.^[95]

34 (150 mg, 0.34 mmol, 1.0 eq.) was dissolved in CHCl_3 (1 ml) under argon atmosphere and cooled to $0\text{ }^{\circ}\text{C}$. NBS (61 mg, 0.34 mmol, 1.0 eq.) was added in two portions and the color changed from yellow to green. After complete addition the reaction mixture was allowed to warm to RT and it was stirred

until GCMS showed full conversion. Subsequently the mixture was quenched with 2 M NaOH (5 ml) and the aqueous layer was extracted with Et₂O (3x). The combined organic layers were dried over Na₂SO₄ and concentrated under reduced pressure. After purification *via* flash chromatography (PE:EE, 10:1) the desired product was obtained as a brown/yellow solid (169 mg, 95 %).

¹H-NMR (400 MHz, CDCl₃, FID GEP005#40): δ = 7.39 (d, J = 8.1 Hz, 2H), 7.12 – 6.93 (m, 13H), 6.90 (d, J = 3.7 Hz, 1H), 2.32 (s, 6H) ppm.

4-(5'-Iodo-[2,2'-bithiophen]-5-yl)-N,N-di-(p-tolyl)aniline

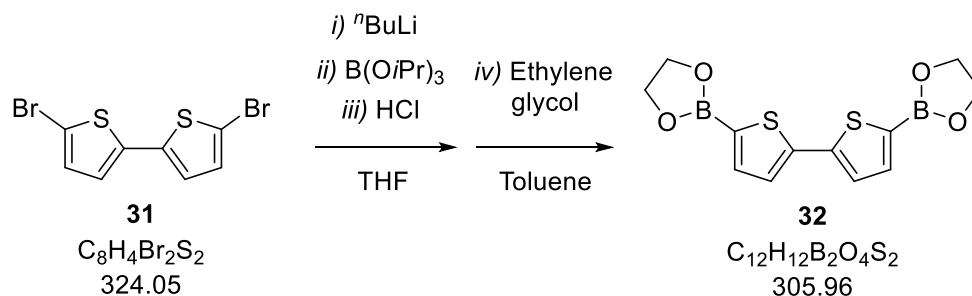


36 was synthesized according to Leliège.^[95]

34 (301 mg, 0.69 mmol, 1.0 eq.) was dissolved in CHCl₃ (2 ml) under argon atmosphere and cooled to 0 °C. NIS (154 mg, 0.69 mmol, 1.0 eq.) was added in two portions. After complete addition the reaction mixture was allowed to warm to RT. AcOH (1 drop) was added and the mixture was heated to 50 °C overnight. Subsequently the mixture was quenched with 2 M NaOH (5 ml) and the aqueous layer was extracted with Et₂O (3x). The combined organic layers were dried over Na₂SO₄ and concentrated under reduced pressure. After purification *via* column chromatography (18 g SiO₂, PE:DCM, 9:1) the desired product was obtained as an orange solid (51 mg, 13 %).

¹H-NMR (400 MHz, CDCl₃, FID BRO006#20): δ = 7.41 – 7.28 (m, 2H), 7.08 – 6.98 (m, 8H), 6.98 – 6.90 (m, 6H), 2.26 (s, 6H) ppm.

5,5'-Di(1,3,2-dioxaborolan-2-yl)-2,2'-bithiophene



32 was prepared as described in the protocol from Sakamoto.^[93]

5,5'-Dibromobithiophene **31** (3.24 g, 10 mmol, 1.0 eq.) was dissolved in anh. THF (60 ml) under argon atmosphere before it was cooled to $-80\text{ }^\circ\text{C}$. Then $nBuLi$ (2.5 M in hexanes; 9.2 ml, 23 mmol, 2.3 eq.) was added dropwise within 30 min. After 2.5 h stirring at $-80\text{ }^\circ\text{C}$ GCMS showed full lithiation. Subsequently a solution of triisopropylborate (9.40 g, 50 mmol, 5.0 eq.) in anh. THF (20 ml) was added. The reaction mixture was stirred at RT overnight and it was hydrolyzed with 2 M HCl (50 ml). The mixture was extracted with Et_2O several times and the combined organic layers were concentrated under reduced pressure. The residue was taken up in toluene (100 ml) and ethylene glycol (20 ml, excess) was added. The mixture was heated to reflux overnight and was then concentrated in *vacuo*. A black powder (1.52 g, 50 %) was obtained after recrystallization from toluene.

1H -NMR (400 MHz, $CDCl_3$, FID BRO002#10): δ = 7.55 (d, J = 3.6 Hz, 2H), 7.32 (d, J = 3.6 Hz, 2H), 4.39 (s, 8H) ppm.

E References

- [1] M. Göppert-Mayer, *Annalen der Physik* **1931**, *401*, 273-294.
- [2] W. Kaiser, C. G. B. Garrett, *Physical Review Letters* **1961**, *7*, 229-231.
- [3] W. Denk, J. Strickler, W. Webb, *Science* **1990**, *248*, 73-76.
- [4] M. Pawlicki, H. A. Collins, R. G. Denning, H. L. Anderson, *Angewandte Chemie International Edition* **2009**, *48*, 3244-3266.
- [5] S. R. Marder, *Chemical Communications* **2006**, 131-134.
- [6] M. Rumi, J. W. Perry, *Advances in Optics and Photonics* **2010**, *2*, 451-518.
- [7] M. Albota, D. Beljonne, J.-L. Brédas, J. E. Ehrlich, J.-Y. Fu, A. A. Heikal, S. E. Hess, T. Kogej, M. D. Levin, S. R. Marder, D. McCord-Maughon, J. W. Perry, H. Röckel, M. Rumi, G. Subramaniam, W. Webb, X.-L. Wu, C. Xu, *Science* **1998**, *281*, 1653-1656.
- [8] B. H. Cumpston, S. P. Ananthavel, S. Barlow, D. L. Dyer, J. E. Ehrlich, L. L. Erskine, A. A. Heikal, S. M. Kuebler, I. Y. S. Lee, D. McCord-Maughon, J. Qin, H. Röckel, M. Rumi, X.-L. Wu, S. R. Marder, J. W. Perry, *Nature* **1999**, *398*, 51-54.
- [9] M. A. Salem, M. Gedik, A. Brown, in *Handbook of Computational Chemistry* (Eds.: J. Leszczynski, A. Kaczmarek-Kedziera, T. Puzyn, M. G. Papadopoulos, H. Reis, M. K. Shukla), Springer International Publishing, Cham, **2017**, pp. 1875-1893.
- [10] C. D. Andrade, C. O. Yanez, L. Rodriguez, K. D. Belfield, *The Journal of Organic Chemistry* **2010**, *75*, 3975-3982.
- [11] M. Lunzer, *Master Thesis, TU Wien* **2014**.
- [12] G. Bort, T. Gallavardin, D. Ogden, P. I. Dalko, *Angewandte Chemie International Edition* **2013**, *52*, 4526-4537.
- [13] C. N. LaFratta, J. T. Fourkas, T. Baldacchini, R. A. Farrer, *Angewandte Chemie International Edition* **2007**, *46*, 6238-6258.
- [14] S. Kawata, Y. Kawata, *Chemical Reviews* **2000**, *100*, 1777-1788.
- [15] W. R. Zipfel, R. M. Williams, W. W. Webb, *Nature Biotechnology* **2003**, *21*, 1369-1377.
- [16] C. W. Spangler, *Journal of Materials Chemistry* **1999**, *9*, 2013-2020.
- [17] T.-C. Lin, S.-J. Chung, K.-S. Kim, X. Wang, G. S. He, J. Swiatkiewicz, H. E. Pudavar, P. N. Prasad, in *Polymers for Photonics Applications II: Nonlinear Optical, Photorefractive and Two-Photon Absorption Polymers* (Ed.: K.-S. Lee), Springer Berlin Heidelberg, Berlin, Heidelberg, **2003**, pp. 157-193.
- [18] W. G. Fisher, W. P. Partridge Jr., C. Dees, E. A. Wachter, *Photochemistry and Photobiology* **1997**, *66*, 141-155.
- [19] G. C. R. Ellis-Davies, *Nature Methods* **2007**, *4*, 619-628.
- [20] M. Rumi, S. Barlow, J. Wang, J. W. Perry, S. R. Marder, in *Photoresponsive Polymers I* (Eds.: S. R. Marder, K.-S. Lee), Springer Berlin Heidelberg, Berlin, Heidelberg, **2008**, pp. 1-95.
- [21] G. S. He, L.-S. Tan, Q. Zheng, P. N. Prasad, *Chemical Reviews* **2008**, *108*, 1245-1330.
- [22] A. Ajami, W. Husinsky, R. Liska, N. Pucher, *Journal of the Optical Society of America B* **2010**, *27*, 2290-2297.
- [23] H. Myung Kim, B. Rae Cho, *Chemical Communications* **2009**, 153-164.
- [24] F. Terenziani, C. Katan, E. Badaeva, S. Tretiak, M. Blanchard-Desce, *Advanced Materials* **2008**, *20*, 4641-4678.
- [25] E. Collini, *Physical Chemistry Chemical Physics* **2012**, *14*, 3725-3736.
- [26] X.-B. Zhang, J.-K. Feng, A.-M. Ren, C.-C. Sun, *The Journal of Physical Chemistry A* **2006**, *110*, 12222-12230.
- [27] M. Kaur, A. K. Srivastava, *Journal of Macromolecular Science, Part C* **2002**, *42*, 481-512.
- [28] B. Jia, J. Li, M. Gu, *Australian Journal of Chemistry* **2007**, *60*, 484-495.
- [29] L. H. Nguyen, M. Straub, M. Gu, *Advanced Functional Materials* **2005**, *15*, 209-216.
- [30] M. Tromayer, *Master Thesis, TU Wien* **2014**.
- [31] Y. Lu, F. Hasegawa, Y. Kawazu, K. Totani, T. Yamashita, W. Toshiyuki, *Sen'i Gakkaishi* **2004**, *60*, 165-172.

- [32] X. Zhou, Y. Hou, J. Lin, *AIP Advances* **2015**, *5*, 030701.
- [33] J. Serbin, A. Egbert, A. Ostendorf, B. N. Chichkov, R. Houbertz, G. Domann, J. Schulz, C. Cronauer, L. Fröhlich, M. Popall, *Optics Letters* **2003**, *28*, 301-303.
- [34] K. Kaneko, H.-B. Sun, X.-M. Duan, S. Kawata, *Applied Physics Letters* **2003**, *83*, 2091-2093.
- [35] D. Wu, Q.-D. Chen, L.-G. Niu, J.-N. Wang, J. Wang, R. Wang, H. Xia, H.-B. Sun, *Lab on a Chip* **2009**, *9*, 2391-2394.
- [36] C. Schizas, V. Melissinaki, A. Gaidukeviciute, C. Reinhardt, C. Ohrt, V. Dedoussis, B. N. Chichkov, C. Fotakis, M. Farsari, D. Karalekas, *The International Journal of Advanced Manufacturing Technology* **2010**, *48*, 435-441.
- [37] R. Guo, S. Xiao, X. Zhai, J. Li, A. Xia, W. Huang, *Optics Express* **2006**, *14*, 810-816.
- [38] M. Malinauskas, H. Gilbergs, A. Žukauskas, V. Purlys, D. Paipulas, R. Gadonas, *Journal of Optics* **2010**, *12*, 035204.
- [39] A. Ovsianikov, B. Chichkov, P. Mente, N. A. Monteiro-Riviere, A. Doraiswamy, R. J. Narayan, *International Journal of Applied Ceramic Technology* **2007**, *4*, 22-29.
- [40] S. J. Jhaveri, J. D. McMullen, R. Sijbesma, L.-S. Tan, W. Zipfel, C. K. Ober, *Chemistry of Materials* **2009**, *21*, 2003-2006.
- [41] A. Ovsianikov, S. Schlie, A. Ngezahayo, A. Haverich, B. N. Chichkov, *Journal of tissue engineering and regenerative medicine* **2007**, *1*, 443-449.
- [42] E. D. Lemma, B. Spagnolo, M. De Vittorio, F. Pisanello, *Trends in Biotechnology* **2019**, *37*, 358-372.
- [43] W. Zhou, S. M. Kuebler, K. L. Braun, T. Yu, J. K. Cammack, C. K. Ober, J. W. Perry, S. R. Marder, *Science* **2002**, *296*, 1106-1109.
- [44] M. Malinauskas, M. Farsari, A. Piskarskas, S. Juodkasis, *Physics Reports* **2013**, *533*, 1-31.
- [45] J. T. Fourkas, in *Three-Dimensional Microfabrication Using Two-Photon Polymerization (Second Edition)* (Ed.: T. Baldacchini), William Andrew Publishing, **2020**, pp. 57-76.
- [46] M. Tromayer, A. Dobos, P. Gruber, A. Ajami, R. Dedic, A. Ovsianikov, R. Liska, *Polymer Chemistry* **2018**, *9*, 3108-3117.
- [47] J. Torgersen, *PhD Thesis, TU Wien* **2013**.
- [48] K. D. Belfield, X. Ren, E. W. Van Stryland, D. J. Hagan, V. Dubikovsky, E. J. Miesak, *Journal of the American Chemical Society* **2000**, *122*, 1217-1218.
- [49] J. S. Beckwith, A. Rosspeintner, G. Licari, M. Lunzer, B. Holzer, J. Fröhlich, E. Vauthey, *The Journal of Physical Chemistry Letters* **2017**, *8*, 5878-5883.
- [50] B. Holzer, M. Lunzer, A. Rosspeintner, G. Licari, M. Tromayer, S. Naumov, D. Lumpi, E. Horkel, C. Hametner, A. Ovsianikov, R. Liska, E. Vauthey, J. Fröhlich, *Molecular Systems Design & Engineering* **2019**, *4*, 437-448.
- [51] P. Soman, J. A. Kelber, J. W. Lee, T. N. Wright, K. S. Vecchio, R. L. Klemke, S. Chen, *Biomaterials* **2012**, *33*, 7064-7070.
- [52] J. L. Young, A. W. Holle, J. P. Spatz, *Experimental Cell Research* **2016**, *343*, 3-6.
- [53] C. Barner-Kowollik, M. Bastmeyer, E. Blasco, G. Delaittre, P. Müller, B. Richter, M. Wegener, *Angewandte Chemie International Edition* **2017**, *56*, 15828-15845.
- [54] A. Accardo, M.-C. Blatché, R. Courson, I. Loubinoux, C. Vieu, L. Malaquin, *Biomedical Physics & Engineering Express* **2018**, *4*, 027009.
- [55] G. Justin, S. Finley, A. R. Abdur Rahman, A. Guiseppi-Elie, *Biomedical Microdevices* **2009**, *11*, 103-115.
- [56] A. Ovsianikov, V. Mironov, J. Stampfl, R. Liska, *Expert Review of Medical Devices* **2012**, *9*, 613-633.
- [57] Z. Li, J. Torgersen, A. Ajami, S. Mühleder, X. Qin, W. Husinsky, W. Holthoner, A. Ovsianikov, J. Stampfl, R. Liska, *RSC Advances* **2013**, *3*, 15939-15946.
- [58] A. Aryasomayajula, P. Bayat, P. Rezai, P. R. Selvaganapathy, in *Springer Handbook of Nanotechnology* (Ed.: B. Bhushan), Springer Berlin Heidelberg, Berlin, Heidelberg, **2017**, pp. 487-536.

- [59] D. Mandt, P. Gruber, M. Markovic, M. Tromayer, M. Rothbauer, S. R. A. Krayz, F. Ali, J. van Hoorick, W. Holnthoner, S. Mühleder, P. Dubrueel, S. Van Vlierberghe, P. Ertl, R. Liska, A. Ovsianikov, *International Journal of Bioprinting* **2018**, *4*, 144.
- [60] A. L. Antaris, H. Chen, K. Cheng, Y. Sun, G. Hong, C. Qu, S. Diao, Z. Deng, X. Hu, B. Zhang, X. Zhang, O. K. Yaghi, Z. R. Alamparambil, X. Hong, Z. Cheng, H. Dai, *Nature Materials* **2016**, *15*, 235-242.
- [61] H. Zhu, W. Li, Y. Wu, B. Liu, S. Zhu, X. Li, H. Ågren, W. Zhu, *ACS Sustainable Chemistry & Engineering* **2014**, *2*, 1026-1034.
- [62] B. Wang, G. Feng, M. Seifrid, M. Wang, B. Liu, G. C. Bazan, *Angewandte Chemie International Edition* **2017**, *56*, 16063-16066.
- [63] V. H. K. Fell, N. J. Findlay, B. Breig, C. Forbes, A. R. Inigo, J. Cameron, A. L. Kanibolotsky, P. J. Skabara, *Journal of Materials Chemistry C* **2019**, *7*, 3934-3944.
- [64] L. Zalewski, M. Wykes, S. Brovelli, M. Bonini, T. Breiner, M. Kastler, F. Dötz, D. Beljonne, H. L. Anderson, F. Cacialli, P. Samorì, *Chemistry – A European Journal* **2010**, *16*, 3933-3941.
- [65] B. Holzer, *Diploma Thesis, TU Wien* **2010**.
- [66] D. Lumpi, *Diploma Thesis, TU Wien* **2009**.
- [67] J. Bintinger, *Diploma Thesis, TU Wien* **2011**.
- [68] J. Xing, J. Liu, T. Zhang, L. Zhang, M. Zheng, X. Duan, *Journal of Materials Chemistry B* **2014**, *2*, 4318-4323.
- [69] S. C. Drayss-Orth, *Dissertation, Universität Basel* **2016**.
- [70] K. Willinger, *Journal of Materials Chemistry* **2009**, 5364-5376.
- [71] H. B. Goodbrand, N.-X. Hu, *The Journal of Organic Chemistry* **1999**, *64*, 670-674.
- [72] M. M. Tatsuo Ishiyama, Norio Miyaoura, *The Journal of Organic Chemistry* **1995**, *60*, 7508-7510.
- [73] L. J. L. Richard Hooper, Marie K. Mapes, Douglas Schumacher, David A. Moline, Robert West, *Macromolecules* **2001**, *34*, 931-936.
- [74] R. Heathcote, J. A. S. Howell, N. Jennings, D. Cartlidge, L. Cobden, S. Coles, M. Hursthouse, *Dalton Transactions* **2007**, 1309-1315.
- [75] L. Han, Y. Zhang, W. Chen, X. Cheng, K. Ye, J. Zhang, Y. Wang, *Chemical Communications* **2015**, *51*, 4477-4480.
- [76] Y. L. Thomas Cardolaccia, Kirk S. Schanze, *Journal of the American Chemical Society* **2008**, *130*, 2535-2545.
- [77] J. Liang, J. Zhang, L. Zhu, A. Duarandin, V. G. Young, N. Geacintov, J. W. Canary, *Inorganic Chemistry* **2009**, *48*, 11196-11208.
- [78] I. Lee, J. E. Kwon, Y. Kang, K. C. Kim, B.-G. Kim, *ACS Sensors* **2018**, *3*, 1831-1837.
- [79] Y. L. Taifeng Liu, Yongli Yan, Yuliang Li, Yanwen Yu, Nan Chen, Songhua Chen, Chao Liu, Yongsheng Zhao, Huibiao Liu, *The Journal of Physical Chemistry C* **2012**, *116*, 14134-14138.
- [80] G. M. Kumares Ghosh, Asoke P. Chattopadhyay, *European Journal of Organic Chemistry* **2009**, 4515-4524.
- [81] C. J. Wood, K. C. D. Robson, P. I. P. Elliott, C. P. Berlinguette, E. A. Gibson, *RSC Advances* **2014**, *4*, 5782-5791.
- [82] A. Vilsmeier, A. Haack, *Berichte der deutschen chemischen Gesellschaft (A and B Series)* **1927**, *60*, 119-122.
- [83] J. Zhang, *Chemical Communications* **2018**, *54*, 8178-8181.
- [84] F. S. Mancilha, *European Journal of Organic Chemistry* **2006**, *21*, 4924-4933.
- [85] O. Hassan Omar, S. la Gatta, R. R. Tangorra, F. Milano, R. Ragni, A. Operamolla, R. Argazzi, C. Chiorboli, A. Agostiano, M. Trotta, G. M. Farinola, *Bioconjugate Chemistry* **2016**, *27*, 1614-1623.
- [86] T. S. Y. Tsubata, Y. Yamashita, T. Mukai, T. Miyashi, *Heterocyclic Compounds* **1992**, *23*.
- [87] M. G. Murali, *RSC Advances* **2014**, *4*, 44902-44910.
- [88] K. Ono, S. Tanaka, Y. Yamashita, *Angewandte Chemie International Edition in English* **1994**, *33*, 1977-1979.
- [89] S.-i. Kato, *Chemical Communications* **2004**, 2342-2343.

- [90] A. Biffis, P. Centomo, A. Del Zotto, M. Zecca, *Chemical Reviews* **2018**, *118*, 2249-2295.
- [91] N. Marion, O. Navarro, J. Mei, E. D. Stevens, N. M. Scott, S. P. Nolan, *Journal of the American Chemical Society* **2006**, *128*, 4101-4111.
- [92] N. E. Ustyuzhanina, P. A. Fomitskaya, A. G. Gerbst, A. S. Dmitrenok, N. E. Nifantiev, *Marine Drugs* **2015**, *13*, 770-787.
- [93] K. Sakamoto, Y. Takashima, H. Yamaguchi, A. Harada, *The Journal of Organic Chemistry* **2007**, *72*, 459-465.
- [94] R. Anémian, D. C. Cupertino, P. R. Mackie, S. G. Yeates, *Tetrahedron Letters* **2005**, *46*, 6717-6721.
- [95] A. Leliège, P. Blanchard, T. Rousseau, J. Roncali, *Organic Letters* **2011**, *13*, 3098-3101.
- [96] M. M. Cieslinski, P. J. Steel, S. F. Lincoln, C. J. Easton, *Supramolecular Chemistry* **2006**, *18*, 529-536.
- [97] D. Nishimura, T. Oshikiri, Y. Takashima, A. Hashidzume, H. Yamaguchi, A. Harada, *The Journal of Organic Chemistry* **2008**, *73*, 2496-2502.
- [98] H. Onagi, B. Carrozzini, G. L. Cascarano, C. J. Easton, A. J. Edwards, S. F. Lincoln, A. D. Rae, *Chemistry – A European Journal* **2003**, *9*, 5971-5977.
- [99] A. Hedges, in *Starch (Third Edition)* (Eds.: J. BeMiller, R. Whistler), Academic Press, San Diego, **2009**, pp. 833-851.
- [100] N. Marion, S. P. Nolan, *Accounts of Chemical Research* **2008**, *41*, 1440-1449.